

Design of Prestressed Concrete Girders Without End Blocks

WA-RD 81.1

Final Report
February 1986



Washington State Department of Transportation
Planning, Research and Public Transportation Division
In Cooperation With
United States Department of Transportation
Federal Highway Administration

624.1834
ITANI
1986
c.2

Washington State Department of Transportation

Duane Berentson, Secretary
A.D. Andreas, Deputy Secretary
James P. Toohey, Assistant Secretary for Planning, Research and Public Transportation

Washington State Transportation Commission Research Committee

Richard Odabashian, Commissioner
Jerry Overton, Commissioner
Leo B. Sweeney, Commissioner

WSDOT Research Executive Committee

A.D. Andreas, Chair, Deputy Secretary for Transportation

E.W. Ferguson, Administrator, District 4
Robert C. Schuster, Assistant Secretary for Highways
James Sainsbury, Acting Assistant Secretary for Marine Transportation
James P. Toohey, Assist. Sec. for Plan'g, Research & Public Transp.

WSDOT Research Technical Committees

Highway Operations and Development

Roland Cook, Chairman, District 2 Administrator

John Aaspas, District 4 Project Engineer
William P. Carr, Associate Research Director
Rich Darnell, District 3 Maint. & Operations Engineer
C. Stewart Gloyd, Bridge/Structures Engineer
Wayne Gruen, State Traffic Engineer
Kern Jacobson, District 1 Public Transportation and Planning Engineer
Stan Moon, Location/Design Engineer
Ed Schlect, Construction Engineer - Paving
Don Senn, District 2 Location/Construction Engineer
Dick Shroll, District 6 Maintenance Superintendent
John Stanton, Assistant Professor, University of Washington
Ken Thomas, Operations Engineer, Bellingham Public Works Dept.

Materials and Product Development

Del Vandehey, Chairman, State Construction Engineer

Keith W. Anderson, Research Specialist
Bill Beeman, District 5 Administrator
Jerry Higgins, Assistant Professor, Washington State University
Newton Jackson, Pavement/Soils Engineer
Alan King, Public Works Director, Okanogan County
Bob Krier, Bridge Operations Engineer
Art Peter, Materials Engineer
Bob Spratt, District 2 Maintenance Engineer
John Strada, Construction Engineer - Grading

Planning and Multimodal

George Smith, Chairman, Manager, Public Transportation Office

Ron Anderson, Manager, District 6 Management Services
Ken Casavant, Professor, Washington State University
King Cushman, Director, Pierce County Transit Development
John Doyle, Manager, Economy Branch
Kris Gupta, Manager, Transportation Data
Jerry Lenzi, Multimodal Transportation
Don Trantum, District 6 Administrator

WSDOT Research Implementation Committee

Stan Moon, Chairman, Location/Design Engineer

Kern Jacobson, District 1 Public Transportation and Planning Engineer
Bob Krier, Bridge Operations Engineer
Dennis Ingham, Highway Maintenance Engineer
Stan Moon, Location/Design Engineer
Art Peters, Materials Engineer
James Sainsbury, Acting Assistant Secretary, Marine Transportation
Ed Schlect, Construction Engineer
Gerald Smith, District 1 Project Engineer
Bob Spratt, District 2 Maintenance Engineer

WSDOT Research Office

G. Scott Rutherford, Director
William P. Carr, Associate Director

Keith W. Anderson, Federal Program Manager
George D. Crommes, Technology Transfer Manager
Kim Jennen, Clerk
Julie Leverson, Planning Technician
Ellen Loyer, Clerk Typist
Carl Toney, Research Administrator

Transportation Research Council

Jerry Overton, Chair

Federal Highway Administration

Paul C. Gregson, Division Administrator

Private Sector

Neal Degerstrom, President, N.A. Degerstrom, Inc.
Milton "Bud" Egbers, President, Skagit Valley Trucking
Richard Ford, Preston, Thorgrimson, Ellis, Holman
William Francis, Vice President, Burlington Northern R.R.
Sam Guess, Senator, The State Senate
Lawrence Houk, Vice President, Lockhead Shipbuilding
Charles H. Knight, President, Concrete Technology
Michael Murphy, President, Central Pre-Mix Concrete
Richard S. Page, President, Washington Roundtable
James D. Ray, Senior Manager, IBM Company

Universities

C.J. Nyman, Associate Provost for Research, Wash. State Univ.
Gene L. Woodruff, Vice Provost for Research, Univ. of Washington

Washington State Department of Transportation

Duane Berentson, Secretary

A.D. Andreas, Deputy Secretary
R.E. Bockstruck, District 1 Administrator
C.W. Beeman, District 5 Administrator
J.L. Clemen, Assistant Secretary for Mngt Services
R.C. Cook, District 2 Administrator
E.W. Ferguson, District 4 Administrator
W.H. Hamilton, Assistant Secretary for Aeronautics
J. Sainsbury, Acting Assistant Secretary, Marine Transportation
R.C. Schuster, Assistant Secretary for Highways
G.L. Smith, Manager, Public Transportation Office
D. Trantum, District 6 Administrator
D.J. Vandehey, State Construction Engineer
J.D. Zirkle, District 3 Administrator

Washington State Transportation Commission

Bernice Stern, Chair

Vaughn Hubbard, Vice Chair
Richard Odabashian, Commissioner
Jerry Overton, Commissioner
Albert Rosellini, Commissioner
Leo B. Sweeney, Commissioner
Pat Wanamaker, Commissioner

WSDOT Research District Liaisons

District 1 - Kern Jacobson, Public Transp. and Plan'g Engr
District 2 - Don Senn, Location/Construction Engineer
District 3 - Bob George, Assistant Location Engineer
District 4 - R.N. Coffman, Maintenance Engineer
District 5 - Robert MacNeil, Design Engineer
District 6 - Richard Larson, Design and Planning Engineer

Federal Highway Administration

M. Eldon Green, Regional Administrator
Ernest J. Valach, Director, Planning and Program Development
Otis C. Hazelton, Research and T2 Engineer

Paul C. Gregson, Division Administrator
Charles W. Chappell, Division Transportation Planner
Charles E. Howard, Assistant Transportation Planner

Washington State Transportation Center (UW and WSU)

G. Scott Rutherford, Director
Ken Casavant, Associate Director, WSU
Joe P. Mahoney, Associate Director, UW

Khosrow Babael, Research Engineer
Rhonda Brooks, Research Aide
Lisa Christopherson, Secretary
Mark Hallenbeck, Research Engineer
Michelle Illy, Secretary
Ed McCormack, Research Engineer
Amy O'Brien, Coordinator
Bev Odegaard, Program Assistant
Ron Porter, Word Processing Technician
Sheryl Sannes, Research Aide
Cy Ulberg, Research Engineer
Duane Wright, Research Aide



3 3166 0000 0919 1

TECHNICAL REPORT STANDARD TITLE PAGE

1. Report No. WA-RD 81.1	2. Government Accession No.	3. Recipient's Catalog No.	
4. Title and Subtitle Design of Prestressed Concrete Girders Without End Blocks		5. Report Date February 1986	
		6. Performing Organization Code	
7. Author(s) Rafik Y. Itani and Ronald L. Galbraith		8. Performing Organization Report No.	
9. Performing Organization Name and Address Structural Engineering Section Dept. of Civil & Environmental Engineering Washington State University Pullman, WA 99164-2914		10. Work Unit No.	
		11. Contract or Grant No. Y 2811 Task 14	
		13. Type of Report and Period Covered Final Report 7/85 - 2/86	
12. Sponsoring Agency Name and Address Washington State Department of Transportation		14. Sponsoring Agency Code	
15. Supplementary Notes Conducted in cooperation with the U.S. Dept. of Transportation, Federal Highway Administration			
16. Abstract <p>This report investigates the feasibility of removing end blocks from the Washington State series 10 and 14 simply supported prestressed girders. These girders are characterized by their 5" webs and are pretensioned using both harped and straight 1/2" grade 27 strands.</p> <p>A series 14 girder, 48 ft. long, is manufactured without end blocks and destructively tested. Based on the results of this test, a 100 ft, series 10 girder was manufactured without end blocks and monitored in a bridge under actual service conditions.</p> <p>Results from these tests show that the modified ends performed effectively under both prestress transfer and service loads. Accordingly, a recommendation is made to remove end blocks from such girders.</p>			
17. Key Words Concrete, girders, beams, prestressed, pretensioned, end blocks, stresses		18. Distribution Statement	
19. Security Classif. (of this report) Unclassified	20. Security Classif. (of this page)	21. No. of Pages 119	22. Price

WASHINGTON STATE LIBRARY
OLYMPIA, WASHINGTON

C1

DESIGN OF PRESTRESSED CONCRETE
GIRDERS WITHOUT END BLOCKS

By

Rafik Y. Itani, Ph.D. and Ronald L. Galbraith

Washington State Transportation Center

Structural Engineering Section
Dept. of Civil & Environmental Engineering
Washington State University
Pullman, WA 99164-2914

Final Report

Research Project Y-2811
Task 14

Prepared for

Washington State Transportation Commission
Department of Transportation
and in cooperation with
U.S. Department of Transportation
Federal Highway Administration

February, 1986

The contents of this report reflect the views of the authors who are responsible for the facts and the accuracy of the data presented herein. The contents do not necessarily reflect the official views or policies of the Washington State Department of Highways or the Federal Highway Administration. This report does not constitute a standard, specification, or regulation.

TABLE OF CONTENTS

	Page
LIST OF TABLES	iv
LIST OF ILLUSTRATIONS	v
ACKNOWLEDGMENTS	vii
ABSTRACT	viii
Chapter	
1 INTRODUCTION	1
2 LITERATURE REVIEW	4
3 TEST OF GIRDER UNDER CONTROLLED CONDITIONS	18
3.1 Girder Design	18
3.1a Unmarked End	21
3.1b Marked End	21
3.2 Instrumentation	24
3.3 Prestress Transfer	26
3.4 Cylinder Samples	28
3.5 Shear Test Set-Up	30
3.5a Unmarked End Test	30
3.5b Marked End Test	37
3.6 Experimental Stress Analysis	37
3.7 Steel Stress	42
3.8 Concrete Stresses	47
3.9 Theoretical Comparison	58
3.10 Conclusion	59

	Page
Chapter	
4 TEST OF ACTUAL HIGHWAY GIRDER WITHOUT END BLOCKS	61
4.1 Girder Design	61
4.2 Girder Details	62
4.3 Instrumentation	62
4.4 Girder Construction	69
4.5 Prestress Transfer	71
4.6 Stress Analysis of Prestress Transfer	73
4.7 Addition of Concrete Slab	85
4.8 Stresses Due to Addition of Concrete Slab	85
4.9 Superposition of Prestress Transfer and Slab Stresses	87
4.10 Live Loading of Girder	91
4.11 Stresses Due to Live Loading	93
4.12 Theoretical Comparison	97
4.13 Conclusion	99
5 CONCLUSIONS AND RECOMMENDATIONS	100
REFERENCES	105
APPENDIX A	107

LIST OF TABLES

		Page
Table		
3.1	Loads and Comments for Unmarked End Test	35
3.2	Loads and Comments for Marked End Test	39
3.3	Stresses in Stirrups, Unmarked End	48
3.4a-c	Stresses in Stirrups, Marked End	50

LIST OF ILLUSTRATIONS

	Page
Figure	
3.1a	Cross Section of WSDOT Series 14 Girder 19
3.1b	Cross Section of WSDOT Series 10 Girder 20
3.2a	Steel Reinforcement at the Ends of the Test Girder 22
3.2b	Construction of Girder Showing Steel Reinforcement 23
3.3	Locations of Strain Gages and Rosettes 25
3.4	Cracking of Unmarked End Due to Prestress Transfer 27
3.5	Uniaxial Compressive Strength Versus Age of Concrete . . . 29
3.6	Uniaxial Compressive Stress-Strain Curves 31
3.7	Method of Support for Test Girder 32
3.8	Loading Used for Shear Tests 33
3.9	Diagonal Cracking Due to Shear 36
3.10	Locations of Supports and Loads for Shear Test of Marked End 38
3.11a-d	Steel Tensile Stress Distributions 43
3.12	Locations of Strain Gages on Stirrups 49
3.13a-d	Principal Stresses in Concrete 54
3.14	Transverse Stress Distributions for Series 14 Girder . . . 60
4.1	Cross Section of WSDOT Series 10 Pretensioned Concrete Girder 63
4.2	Details of Steel Reinforcement 64
4.3	Shear Capacity Diagram 65
4.4a	Locations of Gages on Stirrups 67
4.4b	Locations of Rosettes on Concrete 67
4.4c	Stirrup Instrumented with Strain Gages 68

Figure

4.5	Mounting of Strain Rosettes	70
4.6	Girder after Prestress Transfer with Slight Upwards Deflection at Midspan	72
4.7	Girder on Storage Supports with Crack	74
4.8a-h	Steel Tensile Stress Distributions	75
4.9	Principal Stresses Due to Prestress Transfer	84
4.10	Girder in Place at Bridge Site	86
4.11	Principal Stresses in Concrete	88
4.12a-b	Principal Stresses in Concrete	89
4.13	Dimensions of Truck Used in Live Load Test	92
4.14	Direct Concentrated Loads on Girders for Live Load Test (kips)	92
4.15	Locations of Rear Axle for Live Loading	94
4.16a-b	Principal Stresses in Concrete	95
4.17	Transverse Stress Distributions for Series 10 Girder . . .	98
5.1a-b	Cracks in Girders with End Blocks	102
5.1c-d	More Cracks	103

ACKNOWLEDGMENTS

We wish to express our gratitude and appreciation to the following organizations for making this research possible.

The Washington State Department of Transportation and its engineers, Mr. Stew Gloyd and Mr. Umesh Vashishth, who showed sincere interest in this project and contributed their technical assistance. Appreciation also goes to Nancy Mortimer, engineer from WSDOT District 6, who assisted in scheduling the on-site test of the Sullivan Road overpass.

Acknowledgment is also due to Mr. Rick Anderson and Concrete Technology Corporation of Tacoma for manufacturing and testing a series 14 girder. Mr. Anderson's technical assistance and comments were extremely valuable in data collection and reduction.

Appreciation is extended to Mr. Chuck Prussack and Central Pre-Mix of Spokane for their assistance in manufacturing the series 10 girder for use on the Sullivan Road overpass.

Special gratitude is due to Washington State Transportation Center (TRAC) for its support of this research. A thanks is extended to Mr. Bill Carr and Mr. Scott Rutherford for their interest in this project. Appreciation is also due to FHWA for their support of the research program under which this project has been conducted.

Finally, the efforts and help of Mr. Ron Galbraith, a WSU graduate student, are greatly acknowledged. Mr. Galbraith worked on this project as a research assistant in pursuit of his master's degree. Others whose help is appreciated include Dr. Fumio Kamiya of the Forestry and Forest Products Institution of Tsukuba, Japan, and Mr. Girish Hiremath, a graduate student at WSU.

ABSTRACT

This research investigates the feasibility of removing end blocks from pretensioned prestressed concrete bridge girders to improve their cost efficiency. The girders being studied are the pretensioned series used by the Washington State Department of Transportation. These girders are characterized by 5-inch thick webs, and are prestressed using both harped and straight, $\frac{1}{2}$ inch diameter, grade 270 strands. Presently, these girders are manufactured with end blocks and are used in both simple and continuous span bridges. This research deals solely with the simply supported case.

A series 14 girder 48 feet long is manufactured without end blocks and destructively tested to determine ultimate strength capabilities. In addition, a 100-foot long, series 10 girder is manufactured without an end block at one end, and is monitored in a bridge under actual loading conditions. Both girders have been instrumented with strain gages on the steel reinforcement and concrete of the end regions for analyzing the stresses induced. Strain readings are taken during the detensioning process as well as during various stages of loading.

The new design is based on a five-inch thick web which is kept constant throughout the girder while providing adequate shear and anchorage zone reinforcement in the ends. Results of the stress analyses indicate that the modified ends perform effectively under both prestress transfer and service loads. It is recommended that on simply supported spans end blocks be removed from the WSDOT series pretensioned girders, providing a uniform web width across the girder. This is expected to decrease both manufacturing costs and time, thereby benefiting Washington State and its taxpayers.

CHAPTER 1

INTRODUCTION

An end block is basically a short section at the end of a prestressed concrete girder of which the web has been thickened, or the whole section has been enlarged and made rectangular. End blocks were developed for post-tensioned girders to allow room for embedding the bulky anchorage hardware used for the prestressing strands. They also assist in the placement and compaction of the concrete in the end regions, as well as in the distribution of the prestressing force. The practice of providing end blocks for post-tensioning carried over into the design of pretensioned prestressed girders. However, the prestress force in pretensioned girders is transferred by bond between the concrete and prestressing strands over a distance known as the transfer length. No mechanical anchorage devices are needed, therefore the use of end blocks for pretensioned prestressed girders is questionable.

Although they are usually necessary for the post-tensioned case, the use of end blocks has several disadvantages. The construction of an end block requires special formwork which deviates from that of the regular cross section. This can add appreciably to the manufacturing cost. The end block contributes as much as five percent to the total weight of a girder. This increases both transportation and installation costs. In addition, girders with end blocks witness higher tensile stresses upon the detensioning (13) than girder without end blocks. Therefore, end blocks are both uneconomical and undesirable and should be omitted, if possible, from pretensioned girders.

The State of Washington currently uses many pretensioned prestressed girders in highway bridge construction. A significant number of these girders are of the series 10 or series 14 type. The basic cross section of this type of girder is a bulb-T with a five inch web, and a height of 58 inches for the series 10 and 73.5 inches for the series 14. These girders are prestressed using both straight and harped grade 270 strands, with the number of strands depending on the span length which ranges from 80 to 140 feet. The end blocks consist of a web width of 16 inches for the series 10 and 12 inches for the series 14 girder. The length ranges from 27 to 42 inches from the end followed by a 90-inch transition to the five inch web width.

Past research indicates that end blocks can be removed from pretensioned girders by substituting adequate stirrup reinforcement in their place. In fact, tensile stresses in steel reinforcement were found to be higher for girders with end blocks than those without (13). End blocks have been successfully removed from AASHTO Type IV, V and VI girders which have 8 inch webs, and other girders with 6 inch webs, but none that compare with the small web to depth ratio of the Washington series.

The objective of this research is to study the possibility of removing end blocks from WSDOT series 10 and 14 girders, while retaining the same cross section and a five inch web. In place of the end blocks, vertical stirrup reinforcement conforming to the AASHTO specifications for anchorage zones are provided.

In order to investigate the feasibility of removing end blocks, a test girder was designed with vertical stirrups in the end region instead of end blocks. The girder was instrumented with strain gages on both the stirrups and concrete of the end region. Then, the strains caused by

prestress transfer and loading were recorded so that a stress history of the girder could be determined, and the performance of the vertical reinforcement could be evaluated.

With the success of the test girder, the design was then implemented in an actual girder which again was instrumented with strain gages. This girder was monitored during prestress transfer and under actual service conditions.

The second chapter of this report contains a review of literature relevant to pretensioned prestressed girders. The stress analysis of the regions and the effect of end blocks on the stress distribution were the major focus of this review.

Chapter 3 describes the design, instrumentation and testing of the test girder which was performed at Concrete Technology Corporation. Results of this test are also presented in this chapter.

The set up and testing of the in service girder is described in Chapter 4 of this report, as well as presentation of results.

Chapter 5 presents the final conclusions and recommendations for the removal of end blocks from WDOT series 10 and 14 pretensioned prestressed concrete girders.

CHAPTER 2

LITERATURE REVIEW

There have been many studies dealing with prestressed concrete girders. The ones of concern for this research involve the stresses in the end regions of these girders. Most of the experiments and analyses have involved post-tensioned girders, while the series used by the Washington State Department of Transportation are pretensioned. The results of post-tensioned beam experiments are of little value for pretensioned beam research because the two methods of stressing have different effects on the related end zones of the beams. Instead of being concentrated on the bearing area of the end anchorages, the prestress force of a pretensioned beam is transferred to the concrete over the transmission length at the end of the strands. Therefore, this literature review will be focused primarily on studies involving pretensioned prestressed concrete beams.

Probably the most important investigation in relation to this research was performed by W.T. Marshall and Alan H. Mattock (10) and reported in October of 1962. Marshall and Mattock were the first investigators whose primary goal was to measure the stresses which cause horizontal cracking in the ends of pretensioned prestressed girders.

According to their paper, two series of girders were tested. The first series had the same I-shaped cross section, while the second series used two cross sections and also included vertical stirrup reinforcement. Other variables in the tests included: web thickness, arrangement of prestressing strands, surface condition of the strands, size of vertical stirrups and magnitude of prestressing force.

The tests consisted of transferring the prestress force to the girders and measuring the strains produced. The prestress force was transferred by torch-cutting seven days after casting. Strain gage readings were taken before transfer, and after each group of strands was cut. From the results of the tests, a strain distribution was found for each girder.

Marshall and Mattock also looked at a survey of prestressed concrete highway bridges of which 25 out of 41 contained pretensioned prestressed girders with horizontal cracking in the end zones. From the results of the field survey and their experiments, Marshall and Mattock concluded that end blocks are not necessary in pretensioned prestressed girders. They found that end blocks do not ensure the absence of horizontal cracking and cannot restrict the growth of a horizontal end crack once it has started. Instead of end blocks, Marshall and Mattock suggest that vertical stirrup reinforcement should be provided close to the end face of a pretensioned prestressed concrete girder. They developed the following expression for the necessary cross sectional area of stirrups:

$$A_t = 0.021 \frac{T}{f_s} \cdot \frac{h}{l_t} \quad \text{Equation 2.1}$$

where, A_t = cross sectional area of stirrups in square inches

T = total prestressing force

h = beam depth

f_s = maximum allowable working stress of steel

l_t = the transfer length (may be assumed to be 50 times the strand diameter)

The stirrups should be distributed uniformly over a distance equal to one fifth of the girder depth, with the first stirrup as close to the end face as possible. Marshall and Mattock pointed out that the vertical

stirrup reinforcement will ensure satisfactory performance of the end zone, and any horizontal cracks which occur will be fine and short and will not affect the service performance of the girder.

In July of 1963, Peter Gergely, Mete A. Sozen and Chester P. Siess (3) concluded their findings of a study on the effect of reinforcement on anchorage zone cracks. They were interested in developing a direct method of designing transverse reinforcement by assuming the initiation of a crack. Both an experimental and an analytical investigation were undertaken with the following reported.

Gergely, Sozen and Siess found that for an eccentric load, the spalling stresses would be larger for a rectangular end-block than for an I-shaped one.

They also proposed a set of design specifications which can be applied to the anchorage zone of pretensioned concrete members.

1) Transverse reinforcement shall be provided within a distance $\frac{h}{2}$ from the end of the beam to carry the total force:

$$F_t = \frac{M_m}{h-z} \quad \text{Equation 2.2}$$

and the stress in the transverse reinforcement shall be limited by

$$f_s \leq 10^5 \left(\frac{w}{A_s} \right)^{\frac{1}{2}} \quad \text{Equation 2.3}$$

but not greater than 30,000 psi, where:

A_s = area of one stirrup

F_t = total stirrup force

h = height of beam

z = distance between the end of the beam and the centroid of the areas of the stirrups that are within $h/2$ from the end.

w = permissible nominal crack width (in.)

M_m = the maximum unbalanced moment caused by forces acting on a free body bounded by a transverse section and a longitudinal section within the member.

For draped pretensioned strands, the point of action of the resultant prestressing force shall be taken at 25 diameters along the strands from the end.

2) Closed stirrups extending from the top to the bottom of the section shall be used. The spacing within a distance h shall not be greater than $h/5$ and shall not be less than minimum required for shear, with the first stirrup as close to the end of the beam as permitted.

In June of 1965, P.D. Arthur and S. Ganguli (1) published an article investigating the distribution of stress in the end-zones of pretensioned concrete I beams. Two series of tests on a total of 23 beams were carried out with the following factors being studied: transmission length, distribution of vertical strain, and web cracking. Two different arrangements of prestressing wires were used in the testing, as well as three different web widths. The results of the testing showed that the maximum vertical strain on the end face of the end block increased linearly with the applied prestressing force.

The article also looked at applying the theories of post-tensioned beams to pretensioned beams in the design of the end zones. The theories of Magnel, Marshall (an adaptation of Bleich-Sievers theory), and Guyon were looked at in their prediction of the vertical tensile stresses in the end zone at transfer. Arthur and Ganguli proposed a modification of Magnel's theory so that it can be applied to pretensioned beams. Two expressions were developed for determining the maximum tensile stress on the end face of the beam. The first equation assumes that the end block length $a = l_t$:

$$f_y = \frac{20M}{b_w l_t^2} \quad \text{Equation 2.4}$$

where, b_w = width of the web of the I beam at the centroid axis

l_t = transmission length of the wires

M = moment of the prestressing forces and the prestress in the beam about a horizontal plane through the end block.

Or, when the end block length is equal to the depth of the beam d :

$$f_y = \frac{20M}{b_w d^2} \quad \text{Equation 2.5}$$

The modified Magnel approach came closest to Arthur and Ganguli's experimental values (± 30 percent in the prediction of peak stress on the end face).

While investigating cracking in beams, Arthur and Ganguli found that cracking is likely to occur at a strain on the end face of the beam of about 40×10^{-5} , or at a peak tensile stress on the end face of 0.3 times the cube strength of the concrete at the time of transfer.

S. Ganguli (2), in January 1966, published a paper discussing the investigations performed by Hoyer, Evans, Ganguli, Janney and Base on the transmission length in pretensioned prestressed concrete. From these investigations, he formed some interesting conclusions about the transmission length:

- 1) Compaction of concrete at the ends of the unit is of great importance, therefore vibrators should be used.
- 2) A large concentration of prestressing wires in I or inverted T-sections can cause horizontal shear cracks to form.
- 3) Wires near the top of a girder may have greater transmission lengths than wires near the bottom, therefore tension cracks may form near the end.
- 4) Sudden transfer by flame-cutting increases the transmission length greatly.

- 5) When strands are used, extra reinforcement might be needed to prevent bursting cracks in the concrete.
- 6) 80 percent of the maximum prestress is developed over one-half of the transmission length.

In April of 1966, W.T. Marshall (11) proposed a modification to a method developed by H. Sievers for determining the maximum tensile stress in the web of a post-tensioned beam, so that it could be applied to a pretensioned one. The modified expression for the maximum tensile stress becomes:

$$\sigma_y = \frac{K[P(e - h/4)]}{Bh^2} \quad \text{Equation 2.6}$$

where, e = eccentricity of applied load, P
 B = beam width
 h = height of beam
 K = coefficient

The value of K depends on the transfer length and the depth of the beam, and was found to range from 5.47 to 12.3.

In October of 1966, Hawkins (5) reported his findings on end-block analysis from an investigation in which he evaluated past theoretical and experimental analysis and behavior of both post-tensioned and pretensioned concrete girders.

Hawkins' major conclusions are:

- 1) End blocks be designed by treating the problem as an equilibrium of free bodies produced by the cracks. The important variables would be the width and length of the cracks and the placement of reinforcement steel.
- 2) Bursting zone cracks are more dangerous than spalling zone cracks.
- 3) Stirrups for controlling spalling zone cracks should be placed as close to the end of the beam as possible.

- 4) Guyon's method of partitioning should be used to predict cracks in the bursting zone.
- 5) Two-dimensional analysis underestimates the maximum transverse strains for a three-dimensional problem.
- 6) Rectangular end blocks should not be used for I-beams.

P. Gergely and M. Sozen (4), in April 1967, presented an article introducing a method for designing the vertical reinforcement to restrain longitudinal cracks in the end zones of prestressed concrete girders. This proposed method is backed up by a series of experimental results which agree closely with the theoretical values.

The method of analysis used by Gergely and Sozen assumes the presence of a longitudinal crack and is concerned with the equilibrium of the two girder sections, above and below the crack. The analysis uses the following parameters: applied prestressing force, stirrup force, the length and width of the crack, and the dimensions of the end block. Gergely and Sozen developed equations for estimating the location of the crack and the magnitude of the unbalanced moment which creates the tension forces in the transverse steel. From this information, the stirrup forces can be calculated and the reinforcement is selected to confine the crack.

This analysis was found to work best for prestressed girders whose anchorage zones contain loads of high eccentricity. For the case of pretensioned strands, the total force transferred is divided up and concentrated at a finite number of points along the anchorage length of the strands.

Gergely and Sozen conducted experiments to confirm their assumptions. Tests were conducted on 10 reinforced beams and 25 transversely reinforced beams with the following being varied: the cross

section (rectangular and I-shapes), the amount of reinforcement and the applied load. The results showed that both the position of the crack and the forces in the stirrups agreed with the analytical results.

In March of 1970, D. Krishnamurthy (7) reported the results of tests performed on thirty-two pretensioned prestressed concrete I-beams. The main objectives of the tests were to study the effect of sudden transfer on the transmission length of 0.2 inch diameter indented wires, and the effect of sudden transfer on the vertical tensile stresses on the end face centroid of the beams. All the beams were prestressed with the same force, with the variables in the tests being cross sectional dimensions and the rate of transfer of the prestressing force to the concrete.

The results of the tests showed that sudden transfer increases the vertical tensile stresses on the end face of the beam, which increases the tendency to crack. The sudden transfer was also found to increase the transmission length, which does not agree with the views of Marshall and Mattock or Arthur and Ganguli. Finally, Krishnamurthy recommended that to reduce the magnitude of the vertical tensile stresses in the end zones, and to reduce the transmission lengths of the prestressing wires, gradual transfer should be used in the production of the pretensioned beams.

E.G. Nawy and J.C. Potyondy (12), in May 1971, reported their findings from their experiment involving the testing to failure of 22 pretensioned I- and T-beams. From the results of the tests, Nawy and Potyondy concluded:

- 1) Confining reinforcement has no influence on the magnitude of the load at first cracking.
- 2) T-sections cracked at a lower load than I-sections.

- 3) Cracks in T-beams stabilized at about 80 percent of the ultimate moment, while I-beams cracked gradually up to the ultimate load.

An equation was developed for controlling the permissible crack width under overload.

Krishnamurthy (8) published another article in July 1971 discussing the results of over sixty tests performed on short I-beams (4 feet 6 inches long). All the beams were subjected to the same prestressing force, with the following being varied: concrete strength, method of transfer, cross sectional dimensions and the arrangement of prestressing wires. From the measured strains, the stress distribution within the end zones were plotted. Using these results, expressions were developed for obtaining the maximum tensile stress on the end face of the beam, and the stress distribution in the end region:

$$\sigma_{zend} = \frac{10M}{bdl_t} \quad \text{Equation 2.7}$$

$$\sigma_z = \frac{10M}{bdl_t} \left(1 - \frac{x}{l_t}\right) e^{\frac{-3.5x}{l_t}} \quad \text{Equation 2.8}$$

where, M = resulting bending moment between the prestressing force and the internal prestress developed in concrete on the centroidal axis

b = web width

d = depth of the beam

l_t = transmission length of the tendon

This equation was used to predict the maximum tensile stresses on the end faces of the beams used in the tests of Marshall and Mattock, and those of Arthur and Ganguli. These values were compared to the experimental results and the values predicting using Marshall's method and the modified Magnel's method. There was good comparison with the

experimental values and Marshall's method was found to overestimate in some cases. However, the modified Magnel's method was found to be inconsistent and unreliable in the estimation of stresses.

Krishnamurthy also developed an equation for estimating the load at which the concrete would crack.

$$P_c = \frac{f_{ct} P_e}{\sigma_{zend}} \quad \text{Equation 2.9}$$

where, P_c = cracking load
 f_{ct} = splitting or cracking tensile stress of concrete
 P_e = effective prestressing force at transfer

He recommended that end reinforcement be provided when the calculated tensile stress on the end face exceeds the effective tensile stress.

In October 1971, P. Zia and T. Mostafa (16) published an article in which they introduce an equation for determining the transfer length of prestressing strands. By analyzing the results of several tests performed by different researchers, Zia and Mostafa propose the following expression:

$$l_t = 1.5 \frac{f_{si}}{f_{ci}} d_b - 4.6 \text{ (inches)} \quad \text{Equation 2.10}$$

where, f_{si} = initial stress in prestressing strand, before losses, ksi
 f_{ci} = compressive strength of concrete at time of initial prestress, ksi
 d_b = nominal diameter of prestressing strand, in.

This equation takes into account the strand size, the initial prestress and the concrete strength at transfer. The equation can be

used for a range of concrete strength from 2000 to 8000 psi. When compared with ACI requirements, the results agree for small size strands and is conservative for low strength concrete at transfer.

In October 1976, a study by P. Kalyanasundaram, C.S. Krishnamoorthy and P. Srinivasa Rao (6) was published. This article examined the application of the finite element method to the end-zones of pretensioned prestressed concrete girders to determine the stress distribution. Both two-dimensional and three-dimensional finite element analysis were applied to a few specific cases in which the end-zone stresses had been determined experimentally. The finite element results were compared to both experimental values and values predicted by the formulae proposed by the various researchers: Krishnamurthy, Arthur and Ganuli, and Plahn and Kroll. The close agreement between results indicates that this method is effective in the determination of the stress distribution.

The two-dimensional finite element analysis with a fine mesh was found to give as good results as the three-dimensional analysis with a coarse mesh. Therefore, it was assumed that the two-dimensional analysis should be the better choice since it is cheaper. Advantages of the finite element analysis over other methods are that it gives a complete picture of the stress distribution, and also makes it possible to study the influence of changing the section parameters or bond characteristics on the stress distribution in the end-zone.

In September of 1984, B.G. Rabbat and H.G. Russel (14) presented a paper at The Second Bridge Engineering Conference on the structural efficiency and cost effectiveness of bridges built with precast pretensioned I-section and T-section girders with cast-in-place decks. In their study, Rabbat and Russell compared Bulb-T, Colorado and

Washington girders with AASHTO-PCI girders. This included a survey of highway agencies and producers throughout the United States on the advantages and disadvantages of the specified cross sections, as well as a parametric study using a computer program which they developed. The parameters studied include: girder spacing, span length, cross section, concrete and strand characteristics, and costs of materials.

The Washington series, as well as others, were found to be more structurally efficient than AASHTO-PCI girders. However, the survey found that there was concern about possible difficulties in the manufacture and transportation of girders with five inch thick webs. Therefore, a study was also performed in which all of the cross sections were modified with six inch thick webs. Increasing the web thickness for the girders with five inch webs also included eliminating the end blocks. Again, the Washington series were more efficient than AASHTO-PCI girders.

Rabbat and Russell concluded that the Washington series are the second most cost-effective sections following the Bulb-T's. They recommended that Bulb-T girders with a 6 inch thick web be used as the national standard precast, prestressed concrete bridge girder. They also suggested that use of girders with end blocks and five inch thick webs would be beneficial where experience has demonstrated the thickness to be satisfactory.

Finally, in December of 1984, Daniel A. Sarles and Rafik Y. Itani (15) presented a paper investigating the anchorage zone stresses in prestressed concrete girders. A finite element analysis of the transfer of prestress was performed for both post-tensioned and pretensioned I-beams, with and without end blocks. Of special interest to this

research is the analysis of the stress distributions in the anchorage zones of WSDOT Series 10 and 14 girders.

Sarles and Itani found that the maximum total tensile force occurred along a horizontal section 21.57 inches above the base for Series 10, and 28.33 inches above the base for Series 14. It was also found that the total transverse tensile force increased sharply by the provision of an end block for both sections. However, the transverse tensile stress decreased, for both cases, when the end block was present.

Sarles and Itani concluded that for WSDOT Series 10 and 14 girders, end blocks only serve to reduce the congestion of transverse vertical reinforcement. They recommended that end blocks be required only if required by quality control. Finally, if they are to be used, it is recommended that the width be kept to a minimum, and that the transition length not exceed the length of the end block.

Also of importance to this research are the AASHTO specifications regarding the design of the anchorage zones for pretensioned beams. According to section 1.6.15, "where all tendons are pretensioned wires or 7-wire strand, the use of end blocks will not be required." Instead, vertical reinforcement shall be provided as required by the specifications: "In pretensioned beams, vertical stirrups acting at a unit stress of 20,000 psi to resist at least 4 percent of the total prestressing force shall be placed within the distance of $d/4$ of the end of the beam, the end stirrups to be as close to the end of the beam as practicable. For at least the distance d from the end of the beam, nominal reinforcement shall be placed to enclose the prestressing steel in the bottom flange."

A look at current practice in the state of Texas provided some interesting information on the elimination of end blocks. The Texas Highway Department began using beams without end blocks 14 years ago, and paid particular attention to the ends of the beams. Cracking had occurred occasionally when end blocks were used, and continued to occur after they were eliminated. However, the cracks were very small and it was predicted that they would "close up" when future loads were imposed. Experiments with wrapped strand patterns proved effective at relieving the cracking problem. Now, Texas requires the wrapped pattern to be used if cracking is observed in the first beams cast of a given design.

CHAPTER 3

TEST OF GIRDER UNDER CONTROLLED CONDITIONS

In order to prove the feasibility of removing end blocks from WSDOT series 10 and 14 pretensioned girders, it was necessary to test the ultimate load capacity of the revised end region under controlled laboratory conditions. It was also necessary to monitor the performance of the end region during prestress transfer and during different stages of loading to determine the effectiveness of the design. For this stage of the research, a series 14 girder was manufactured and tested at Concrete Technology Corporation (CTC) of Tacoma.

3.1 Girder Design

The girder used for this test was of series 14 type (see Fig. 3.1a). This cross section was selected because it has the smallest web to depth ratio of the Washington series and is therefore the most critical. A full length girder was simulated by using a strand pattern similar to that used for 110 foot long girders.

A 48 foot girder was constructed with 28 straight and 10 harped, $\frac{1}{2}$ inch grade 270 prestressing strands. The harped strands followed the same angle as those for a 110 foot girder, up to 30 inches on either side of the centerline. A web thickness of five inches was kept constant throughout the length of the test girder.

The girder was designed with two different amounts of shear reinforcement in the end regions so that two separate tests could be performed. One end contained light reinforcement in an attempt to force

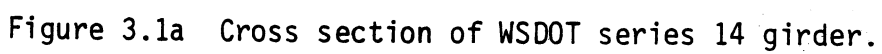


Figure 3.1a Cross section of WSDOT series 14 girder.

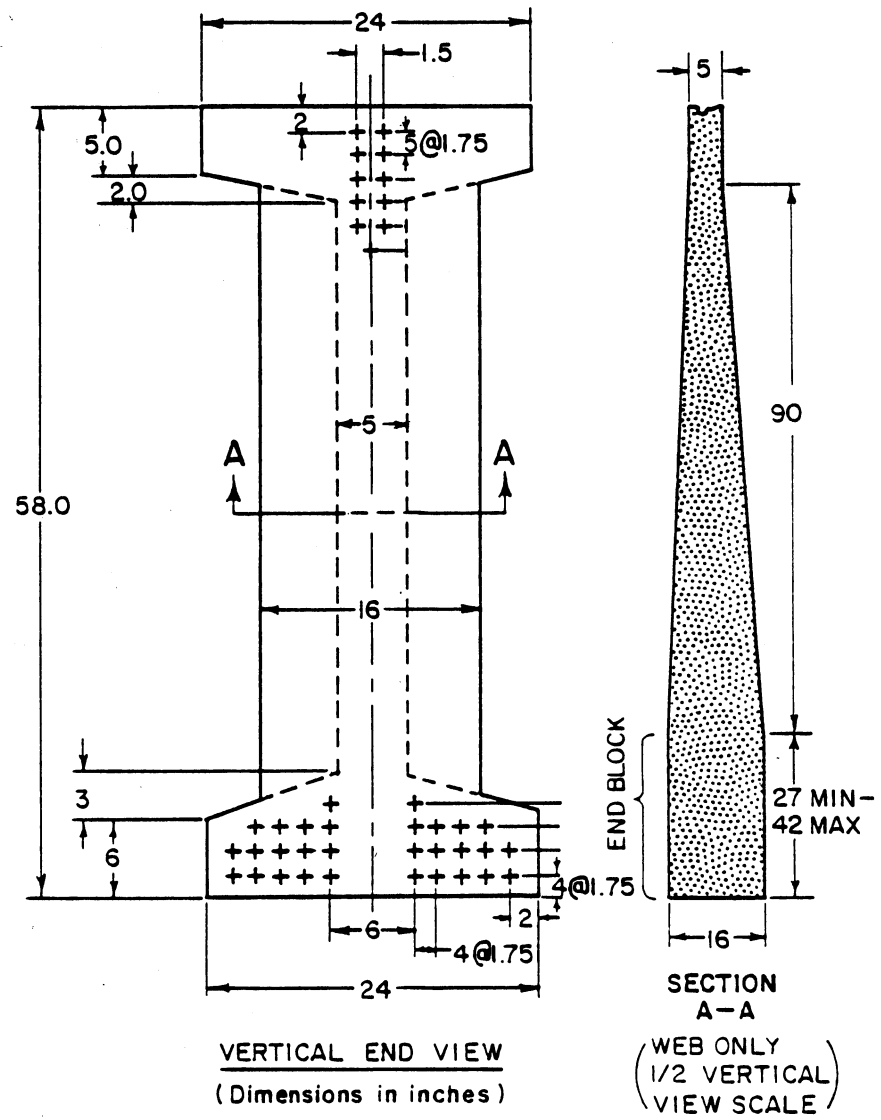


Figure 3.1b Cross section of WSDOT series 10 girder.

shear failure to occur in the end region. The other end was more heavily reinforced with an ultimate shear capacity of 400 kips.

3.1a Unmarked End

The lightly reinforced end, known as the unmarked end, contained 4 pairs of #4 grade 60 stirrups at 4 inch spacing starting 2 inches from the end of the girder (see Fig. 3.2a). After this, the spacing was increased to a maximum of 16 inches. In addition to the vertical stirrups, ties were provided around the straight prestressing strands to contain the bursting stresses induced at the time of detensioning. Three ties were spaced at 8 inches starting 2 inches from the end, and 3 more were spaced at 16 inches. Longitudinal reinforcement for the unmarked end consisted of 4 pairs of #3 bars spaced at 16 inches in the web region of the girder.

3.1b Marked End

The vertical reinforcement for the marked end of the girder consisted of the AASHTO shear requirements for a nominal shear of 400 kips. In addition, the anchorage zone requirement of: "... vertical stirrups acting at a unit stress of 20,000 psi to resist at least 4 percent of the total prestressing force shall be placed within a distance of $d/4$ of the end of the beam, the end stirrups to be as close to the end of the beam as practicable" was provided. Satisfying these requirements, as well as providing proper clearance between the stirrups and transitional spacing, produced the following stirrup spacing for the marked end of the girder. The first pair of stirrups was located $1\frac{1}{2}$ inches from the end of the girder followed by 6 spaced at 2 inches, 6

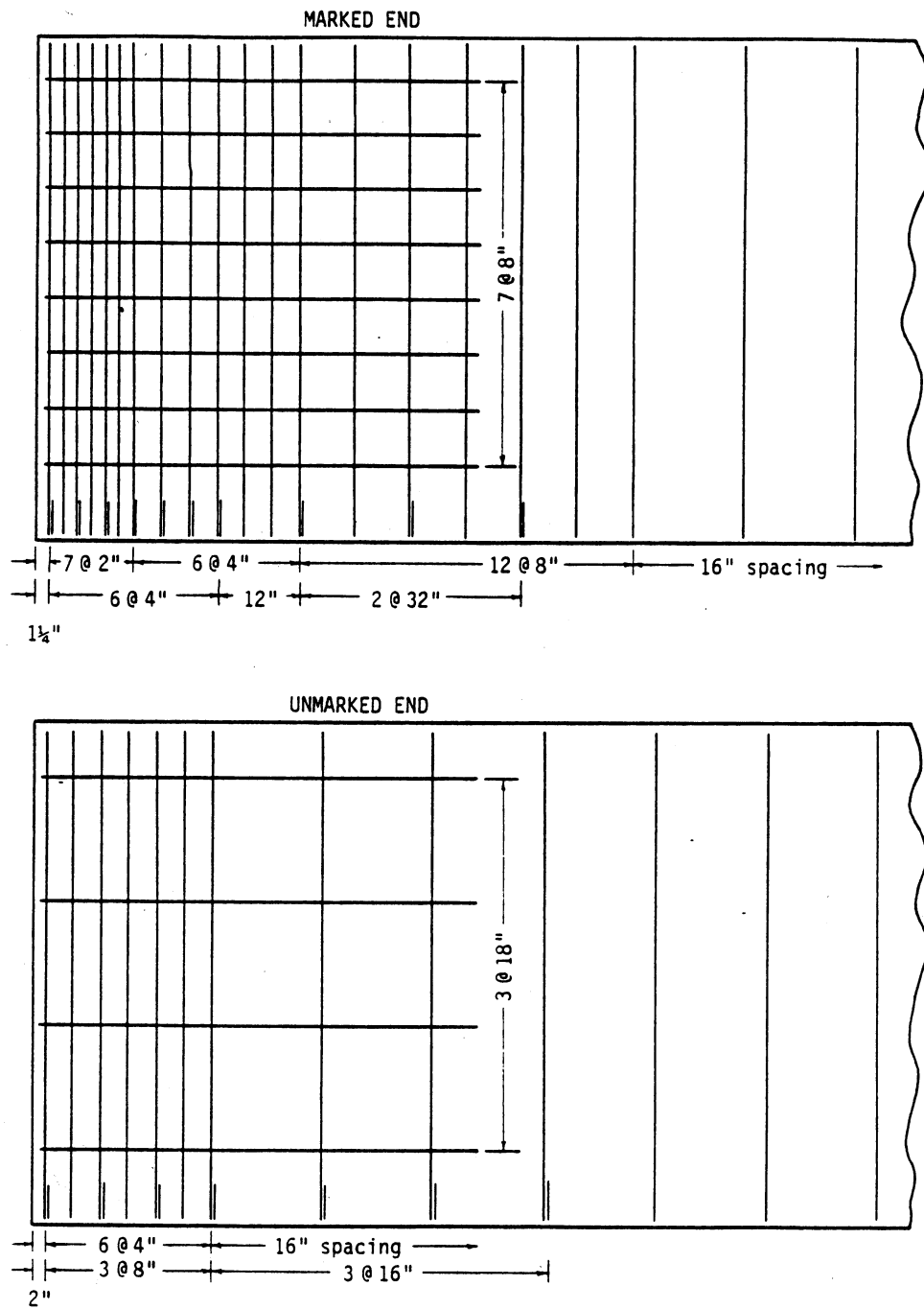
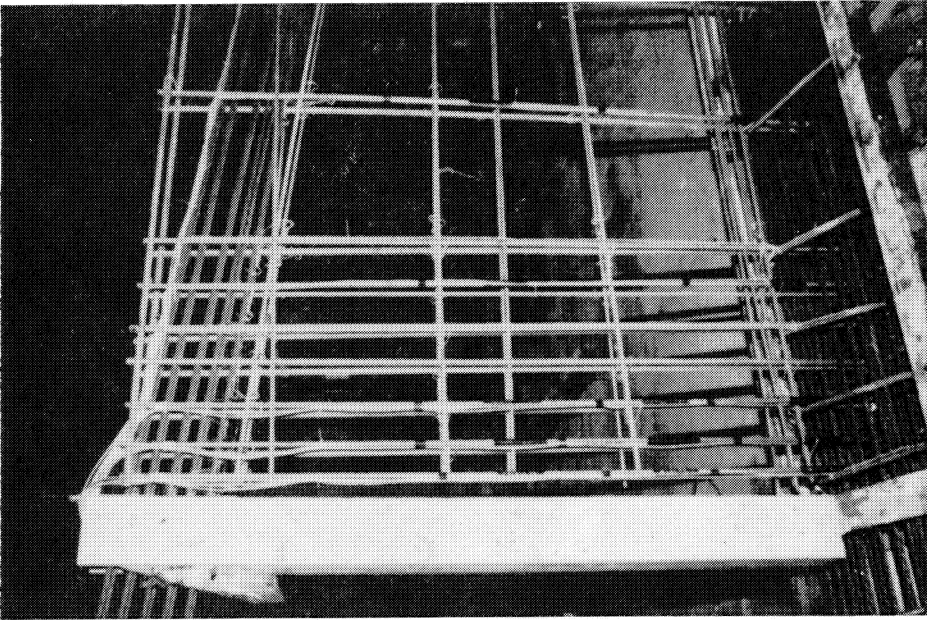
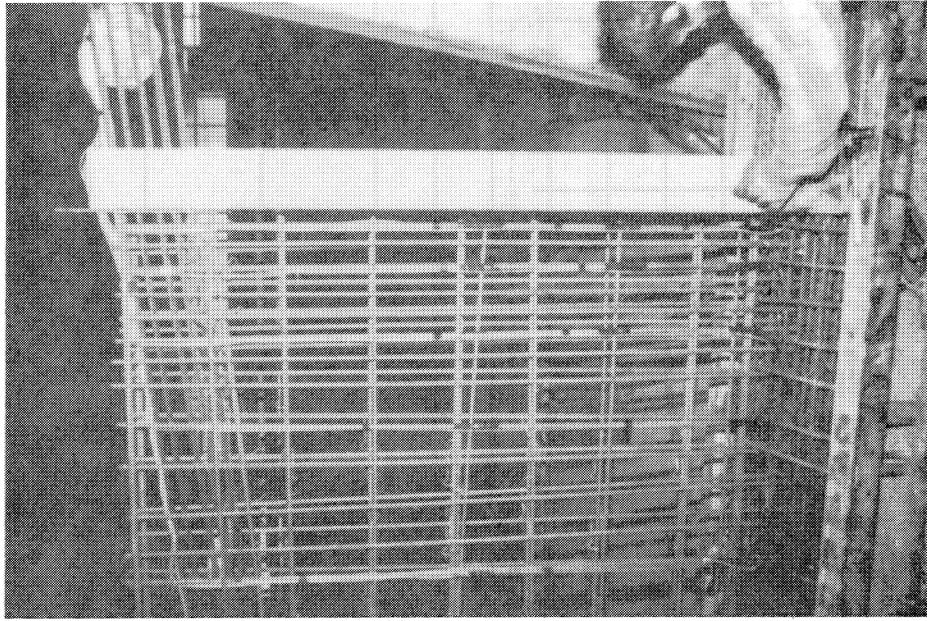


Figure 3.2a Steel reinforcement at the ends of the test girder.



(unmarked end)



(marked end)

Figure 3.2b Construction of girder showing steel reinforcement in end regions.

spaced at 4 inches, 12 spaced at 8 inches and the remainder at 16 inch spacing (see Fig 3.2a). The ties were spaced, starting at $1\frac{1}{2}$ inches from the end, 6 #4 ties at 4 inches spacing followed by 3 ties at 16 inch spacing. Eight pairs of #3 bars were spaced 8 inches on center for the longitudinal reinforcement.

3.2 Instrumentation

Instrumentation of the girder consisted of both strain rosettes located on the concrete surface, and strain gages on stirrups and ties within the concrete. The placement of the gages was chosen so that the stress distribution from both prestress transfer and loading could be determined.

Seventeen SR-4 10mm gages were placed on seven stirrups at each end of the test girder (see Fig. 3.3). The gages were located at points where maximum stresses in the steel stirrups were expected. For the first 3 stirrups from the ends, the gages were placed at 8, 22 and 36 inches from the bottom of the girder. The remainder of the instrumented stirrups contained only 2 gages each, at 8 and 36 inches from the bottom. For the marked end, the instrumented stirrups were placed at $1\frac{1}{2}$, 6, 12, 22, 38, 70 and 102 inches from the end. The instrumented stirrups for the unmarked end were placed at 2, 6, 10, 22, 42, 74 and 106 inches. Six 10mm gages were also mounted on ties confining the straight prestressing strands. Three instrumented ties in the marked end were located at 2, 10 and 18 inches from the end, while in the unmarked end they were placed at 2, 18 and 42 inches.

Because of cost limitations, only the unmarked end of the girder was instrumented with concrete strain rosettes. Twelve rectangular rosettes

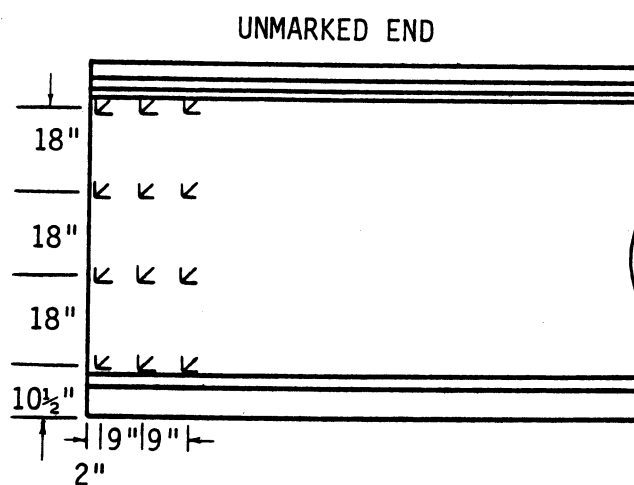
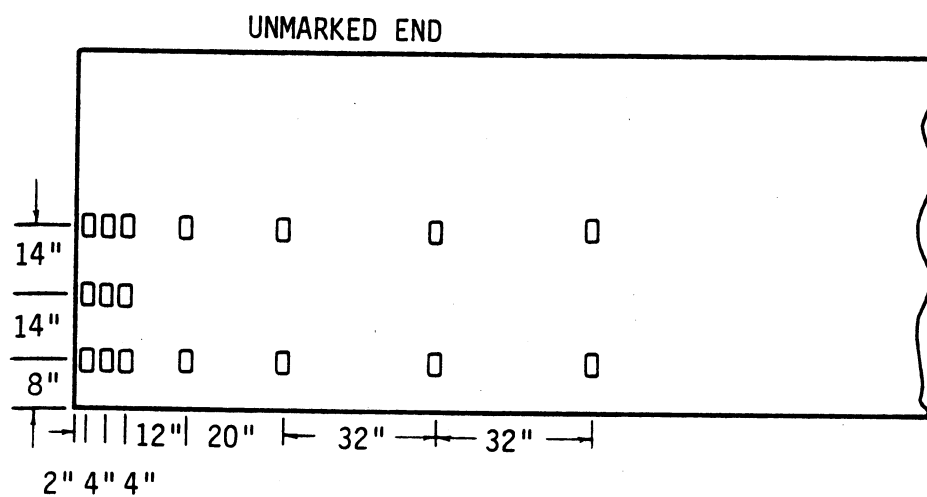
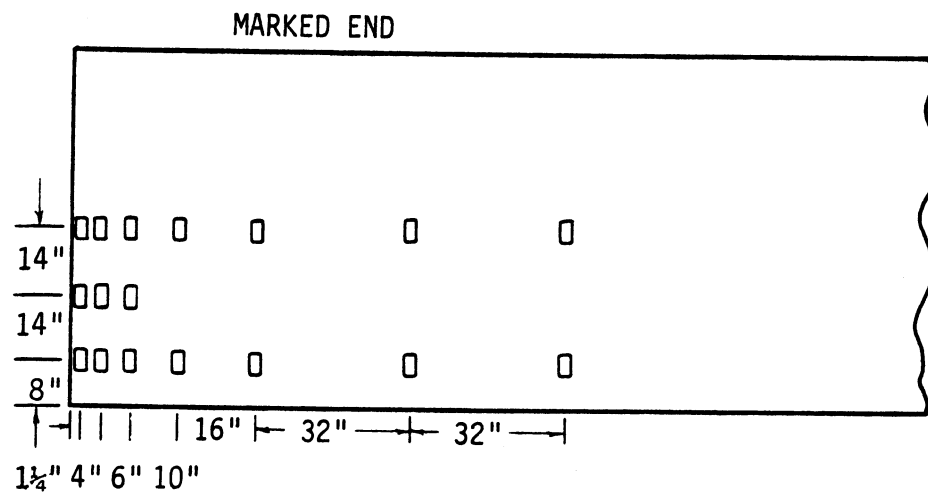


Figure 3.3 Locations of strain gages and rosettes.

were placed in 3 rows of 4, at distances of 2, 11 and 20 inches from the end of the girder. The rosettes were all located on the web region of the girder at 10.5, 28.5, 46.5 and 64.5 inches from the bottom, forming a grid-like pattern.

3.3 Prestress Transfer

Casting of the girder was completed on November 20th, 1984 at 3:40 PM. High early strength concrete was used, as well as hot air curing to cure the concrete quickly. At 10:30 the next morning, compressive cylinder tests indicated that the concrete had reached a compressive strength of over 5000 psi, therefore prestress transfer could begin.

The 38 prestressing strands were initially tensioned to a stress of 189 ksi. This stress was transferred to the girder in four stages, with strain readings taken after the completion of each stage. The first stage began at 11:43 AM by releasing 50 percent of the load on the harped strands and cutting five of the strands at the dead end (nonjacking end). At 11:47, the remaining load on the harped strands was released and the other five strands at the dead end were cut. At 11:54, the load on the 28 straight strands was released and the strands were cut. Finally, at 12:07 the girder lifted to break any residual bond with the form. For the next 5 days, the strains were monitored at intervals of 90 and 99 minutes until the girder was placed in storage.

The only visible results from the transfer of prestress test were two horizontal cracks in the unmarked end of the girder, located near the centroid and midway between the centroid and the bottom flange (see Fig. 3.4). These cracks were spalling or splitting cracks caused by tensile stresses resulting from the distribution of the concentrated compressive

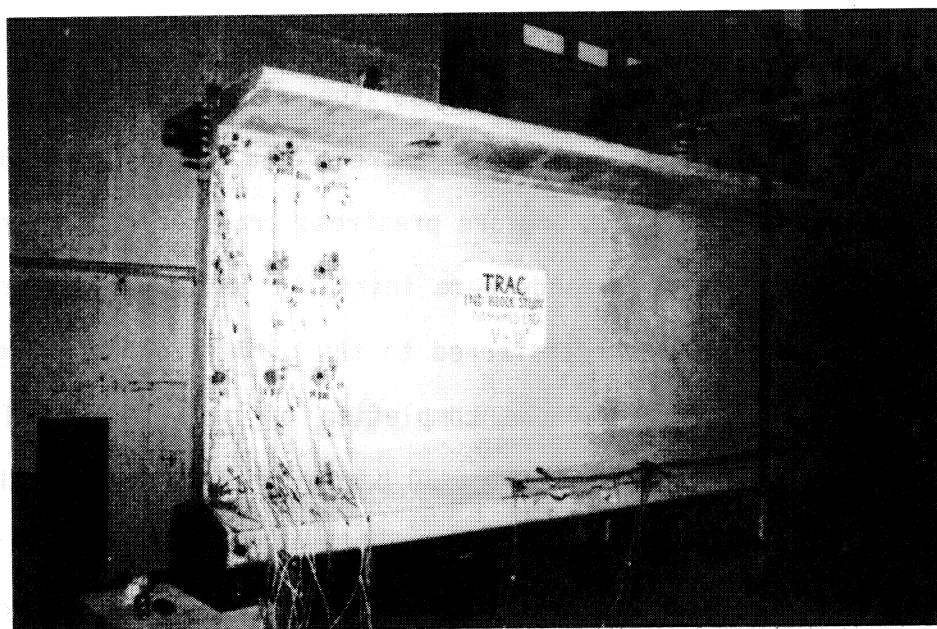


Figure 3.4 Cracking of unmarked end due to prestress transfer (cracks are outlined with black ink).

stresses at the end of the girder. The width of the cracks were 0.1 and 0.06 millimeters (0.004 and 0.0024 inches) and the lengths were around 10 to 15 inches. Since the width and length of these cracks were not very large, they were not expected to affect the performance of the girder under loading conditions, and in fact did close up. The results of the strain analysis during prestress transfer will be presented later in this chapter.

3.4 Cylinder Samples

At the time of casting, cylinder samples of the concrete were taken for compressive strength, density and elastic modulus determination. Ten samples were taken from each of the two batches used for the girder construction. Six of the cylinders from each batch were 4x8, while the other four were 6x12 inch cylinders. The cylinders were cured under the same conditions as the girder until they were removed to be tested. Concrete Tech. performed compressive strength tests on the 4x8 inch cylinders at ages of 19 hours, 7 and 24 days, using 2 cylinders from each batch for each test. The compressive strength increased from an initial value of 5415 psi to a maximum of 8670 psi (see Fig. 3.5). Density tests of the 24 day old cylinders indicated an average concrete density of 156.1 pcf.

The 6x12 inch cylinders were used to determine the elastic modulus and Poisson's ratio at the time of prestress transfer and 27 day strength. For these tests, horizontal and vertical dial gages were attached to the specimens and compressive loads were applied in increments of 10 and 20 kips. Deflections were obtained from the dial gages and converted to strains by dividing by the length. From this

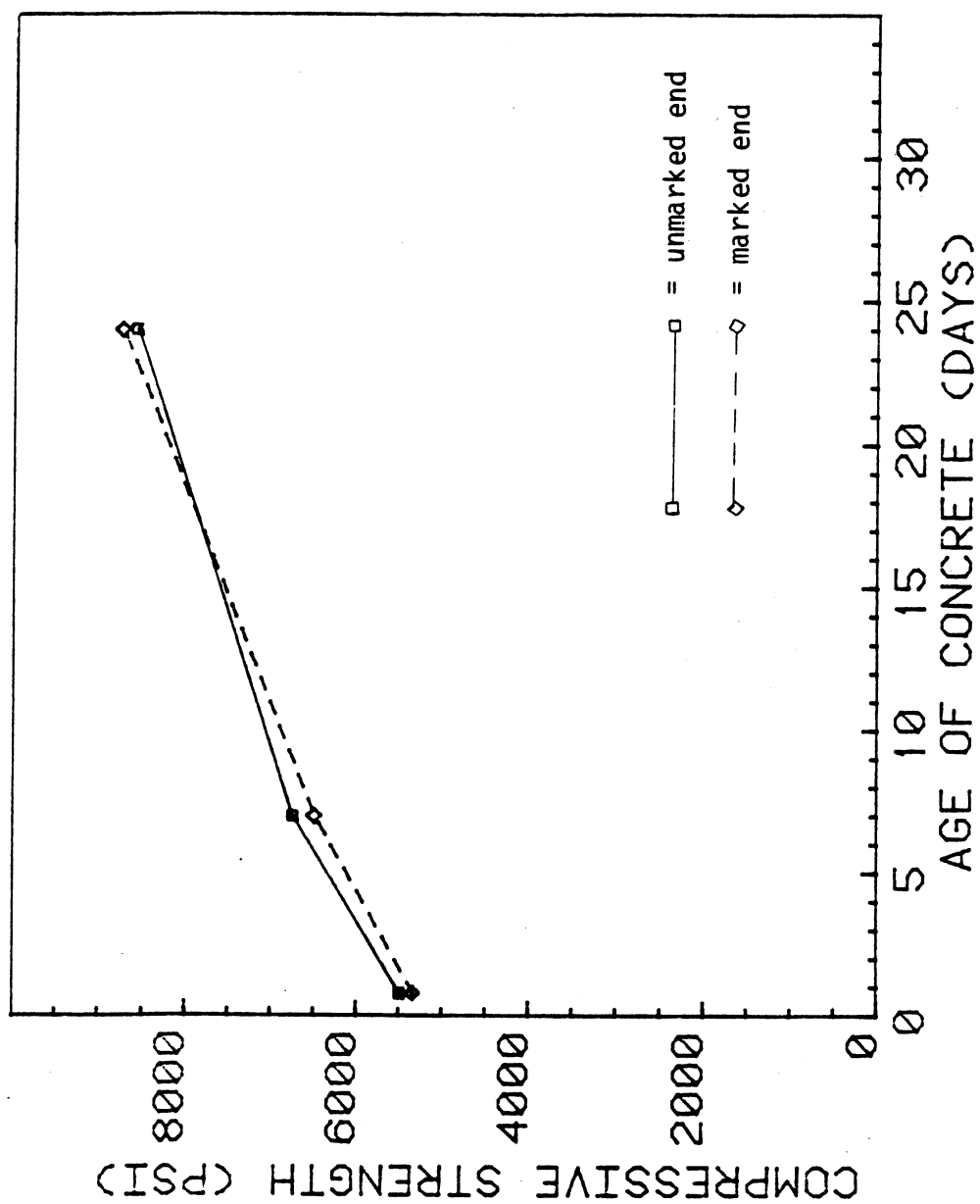


Figure 3.5 Uniaxial compressive strength versus age of concrete.

data, stress-strain diagrams were developed (See Fig. 3.6) for determining the elastic modulus, and Poisson's ratio was found by dividing the horizontal strain by the vertical strain. The 21 hour elastic modulus was found to be around 4000 ksi and it increased to 6000 ksi at 27 days of age. Poisson's ratio increased from approximately 0.22 to 0.45 over the 27 day period. These values were important for strain analysis when determining the principal stresses in the concrete.

3.5 Shear Test Set-Up

For conducting the shear tests, the girder was placed on reinforced concrete blocks topped with pin supports. On top of the support at the unmarked end was a 6 inch x $\frac{1}{4}$ inch x 20 inch Fabreeka pad, while a frictionless Teflon pad was on the other support causing it to behave like a roller (see Fig. 3.7). Therefore, the beam was simply supported.

The loading was induced by five hydraulic jacks which could be controlled manually to achieve specified end shears. The jacks, 3-100 ton rams and 2-30 ton rams, were placed on top of the girder with their upward movement constrained by short W-sections connected to the 3 foot thick concrete floor of the testing facility (see Fig. 3.8). The jacks were located closer to the end of the girder being tested to keep from failing the other end, and were also aligned symmetrically to prevent transverse bending or torsional stresses.

3.5a Unmarked End Test

On December 14, 24 days after casting, the shear test of the unmarked end was performed. The 6 inch support was flush with the end of the girder, and the first 100 ton ram was located 10 feet from the end.

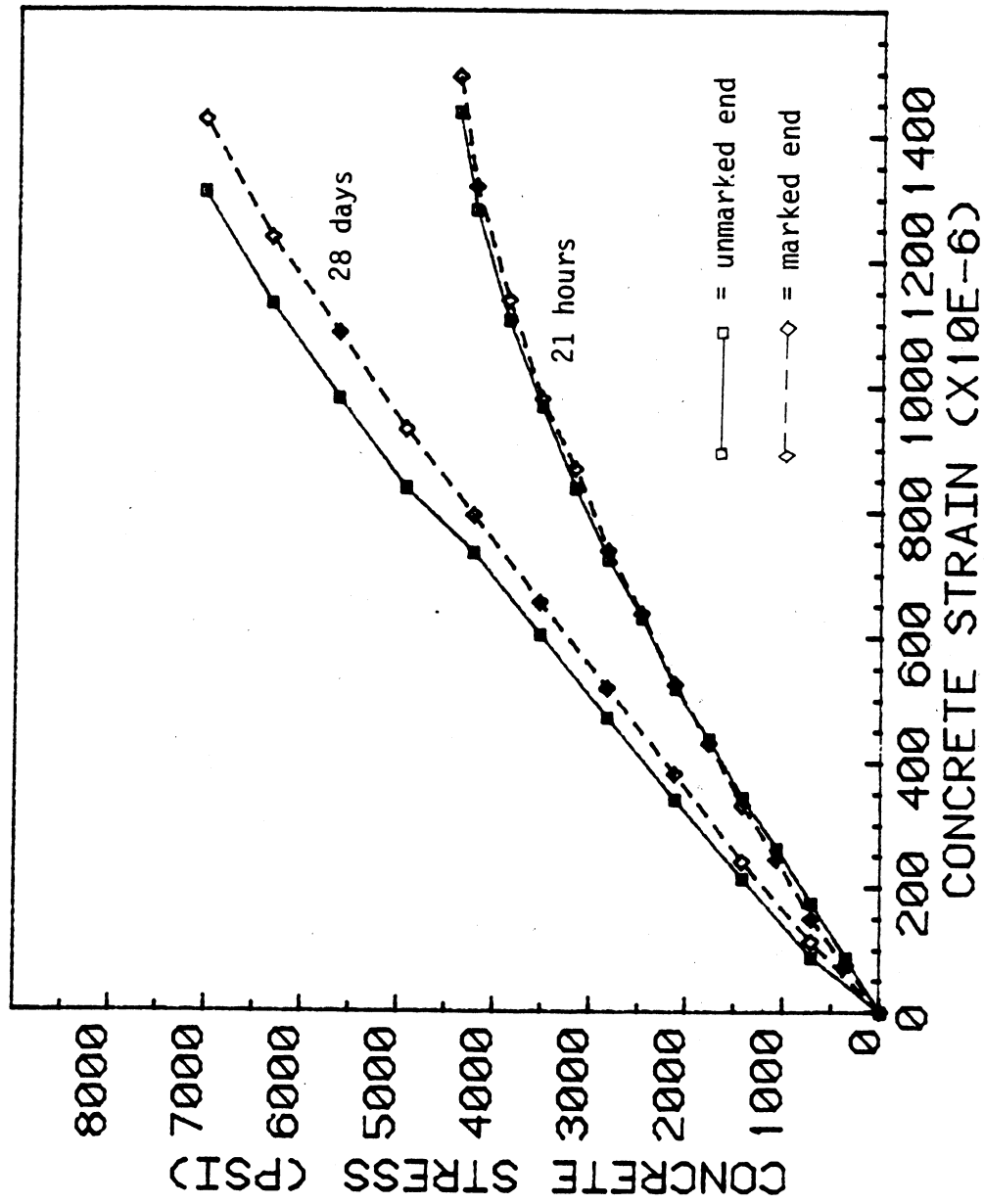


Figure 3.6 Uniaxial compressive stress-strain curves.

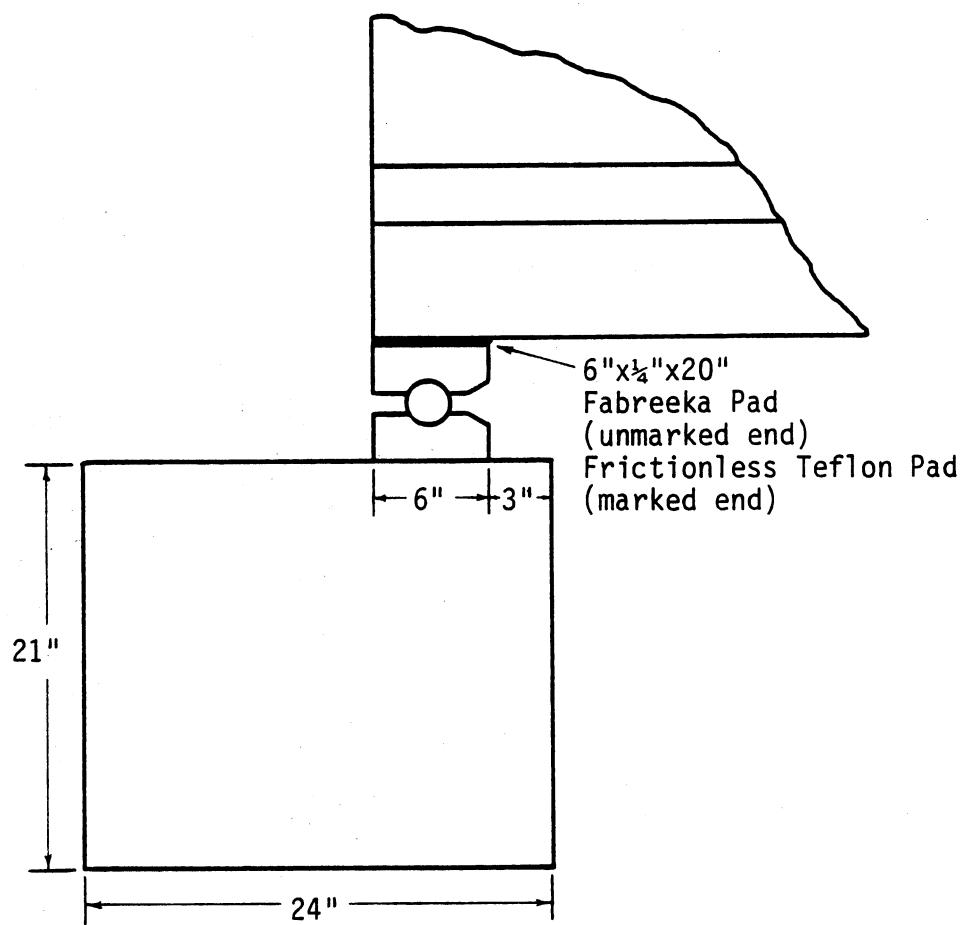


Figure 3.7 Method of support for test girder.

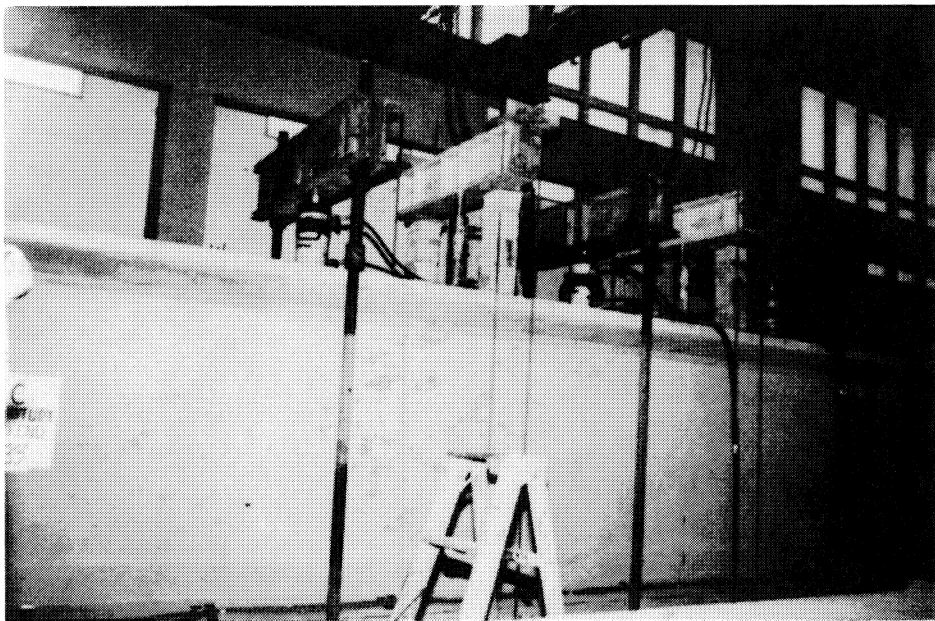


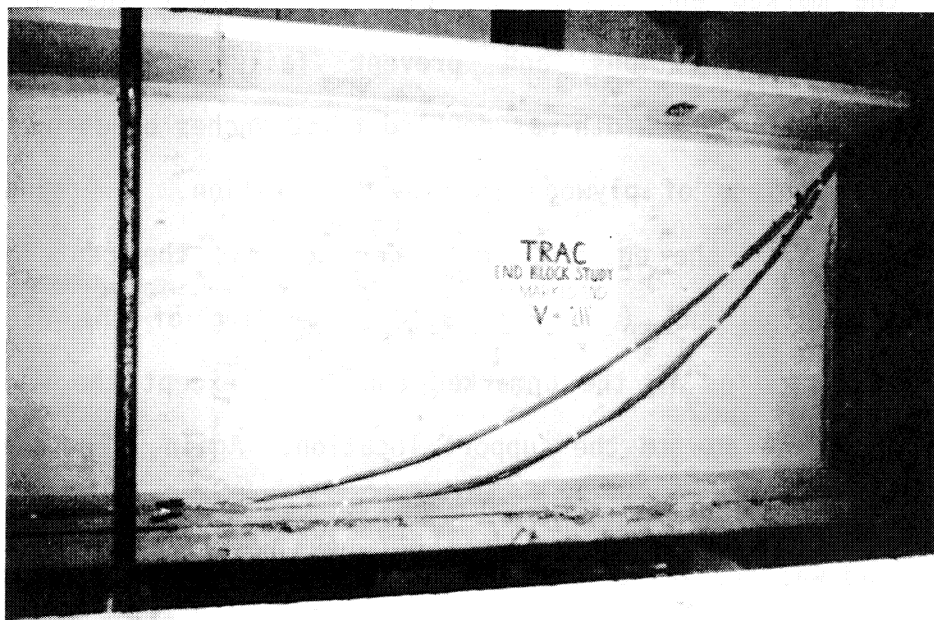
Figure 3.8 Loading used for shear tests.

The rest of the rams were spaced at 3 foot intervals, alternating between 30 ton and 100 ton. An initial load of 0.1 kips was applied to each of the jacks, which combined with the dead weight of the girder to cause an initial end shear of 18.1 kips. The load was increased in stages with strain readings taken between each loading (see Table 3.1). At end shears of 44.7, 72.7, 101.0 and 128.5 kips, there were no visible changes except that the splitting cracks caused by prestress transfer began to decrease in width. The girder sustained the approximate service load of 156.1 kips without any problems.

The first sign of cracking occurred at an end shear of 183.9 kips when a diagonal crack appeared at the intersection of the web and bottom flange near the support. At this point, the shear stress is high because of the abrupt reduction in width of the cross section, and the longitudinal compression is reduced by the effect of the applied loads. Therefore, maximum principal tensile stresses are produced causing an inclined crack to form. As the load was increased to 212.0 kips, the diagonal crack extended through the web up to a distance of about $h/2$ (see Fig. 3.9). At 239.3 kips, the first crack continued to grow and a second crack formed parallel to the first one. As the load was being increased to an end shear of 263.1 kips, the girder collapsed onto the floor of the testing facility. Although the girder was designed with a nominal shear of 300 kips, a maximum shear of only 260 kips was reached. However, the failure was not caused by shear but rather crushing of the concrete between the web and bottom flange where the bearing area was not enough to carry the high compressive force.

Table 3.1
LOADS AND COMMENTS FOR UNMARKED END TEST

Load Stage	Applied Loads (kips)					Unmarked End Shear (kips)	Comments
	P ₁	P ₂	P ₃	P ₄	P ₅		
0	0.1	0.1	0.1	0.1	0.1	18.1	Splitting crack widths 0.10 mm & 0.06 mm (0.004 in & 0.0024 in)
1	10.0	5.2	10.0	5.1	10.0	44.7	No visible change
2	20.4	10.3	20.4	10.7	20.4	72.7	Splitting crack widths 0.05 mm & 0.05 mm (0.002 in & 0.002 in)
3	30.8	15.7	30.8	16.4	30.8	101.0	No visible change
4	41.2	20.6	41.2	21.5	41.2	128.5	Splitting crack widths less than 0.05 mm (0.002 in)
5	51.6	25.6	51.6	26.6	51.6	156.1	Approximate service load No visible change
6	62.0	30.8	62.0	31.8	62.0	183.9	Splitting cracks closed Diagonal crack appeared in bottom flange
7	72.3	36.0	72.3	37.9	72.3	212.0	Diagonal crack spread through web to approximately H/2
8	82.6	41.5	82.6	42.2	82.6	239.3	Diagonal crack grew in length and width New crack formed parallel to first one
9	90.9	47.0	90.9	47.4	90.9	263.1	Girder failed in bearing/compression



(marked end)



(unmarked end)

Figure 3.9 End shears of 211 kips with diagonal cracking of unmarked end.

3.5b Marked End Test

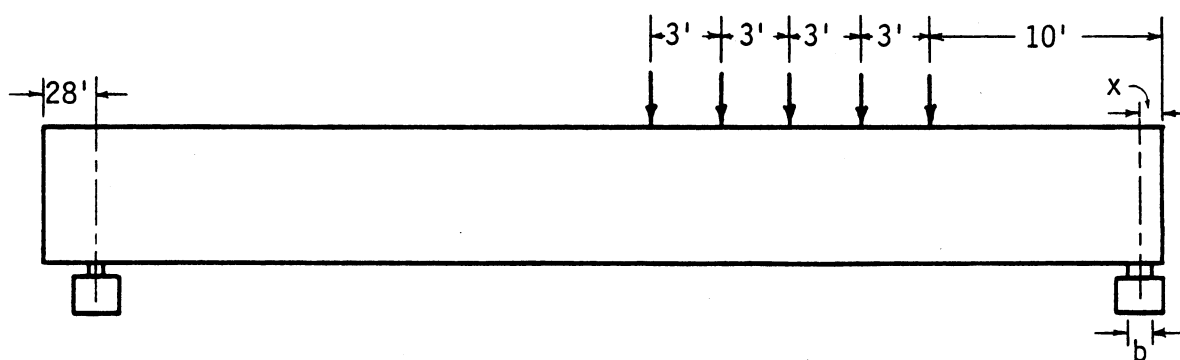
For the marked end test, the method of support was changed to simulate actual conditions and prevent failure due to bearing compression. The support width was doubled to 12 inches by using 2 6-inch supports and a piece of plywood to provide rotation. The support was also moved in from the end of the girder so that the centerline was 12 inches from the end. (see Fig. 3.10). Loading of the girder was performed the same as in the unmarked end test, except the end shears were slightly less due to the support location. Again, strain readings were taken after each stage of the loading.

The load was increased from an initial end shear of 17.1 kips up to 264.4 kips (see Table 3.2) without any cracks or other problems. However, at an end shear of 291.7 kips, the reaction floor of the testing facility began to fail so the loading was discontinued. Two more tests were conducted using a six inch support width and distances of $8\frac{1}{2}$ inches and 3 inches from the centerline of the support to the end of the girder. The second test was loaded up to end end shear of 235.6 kips with no cracking, and the third was loaded to 245.3 kips with only a slight diagonal crack forming at an end shear of 179.5 kips.

3.6 Experimental Stress Analysis

Strains were monitored for both steel and concrete and converted to stresses. The stresses present in the reinforcing steel were calculated by multiplying the strains by the modulus of elasticity of the steel (29×10^6 psi).

For analyzing the stresses in concrete, several assumptions were made. It was assumed that both steel and concrete were stressed within



Test	x	b
3.1	12"	12"
3.2	8½"	6"
3.3	3"	6"

Figure 3.10 Locations of supports and loads for shear test of marked end.

Table 3.2
LOADS AND COMMENTS FOR MARKED END TEST

Load Stage	P ₁	Applied Loads P ₂	Applied Loads P ₃	Applied Loads P ₄	Applied Loads P ₅	Marked End Shear (kips)	Comments
0	0.1	0.1	0.1	0.1	0.1	17.1	Begin test 3.1
1	10.0	5.2	10.0	5.1	10.0	43.5	No new cracks
2	20.4	10.3	20.4	10.7	20.4	71.3	No new cracks
3	30.8	16.4	30.8	15.7	30.8	99.5	No new cracks
4	41.2	21.5	41.2	20.6	41.2	126.7	No new cracks
5	51.6	26.6	51.6	25.6	51.6	154.3	No new cracks
6	62.0	31.8	62.0	30.8	62.0	181.9	No new cracks
7	72.3	36.9	72.3	36.0	72.3	209.3	No new cracks
8	82.6	42.2	82.6	41.5	82.6	237.0	No new cracks
9	93.0	47.0	93.0	47.4	93.0	264.8	No new cracks
10	103.3	52.0	103.3	52.1	103.3	291.7	Loading discontinued due to hold-down failure
0	0.1	0.1	0.1	0.1	0.1	17.2	Begin test 3.2
11	51.6	26.6	51.6	25.6	51.6	153.5	No new cracks
12	62.0	31.8	62.0	30.8	62.0	181.0	No new cracks
13	72.3	36.9	72.3	36.0	72.3	208.0	No new cracks
14	82.6	42.2	82.6	41.5	82.6	235.6	Loading discontinued
0	0.1	0.1	0.1	0.1	0.1	17.3	Begin test 3.3
15	51.6	26.6	51.6	25.6	51.6	152.3	No new cracks
16	62.0	31.8	62.0	30.8	62.0	179.5	Hairline diagonal crack
17	72.3	36.9	72.3	36.0	72.3	206.4	No new cracks
18	82.6	42.2	82.6	41.5	82.6	233.6	No new cracks
19	86.8	44.8	86.8	44.2	86.8	245.3	No new cracks
0	0.1	0.1	0.1	0.1	0.1	17.3	Cracks closed up

their elastic ranges, and that the concrete remained uncracked. It was also assumed that the concrete behaved as an isotropic and homogeneous material. Since the strains were measured on an unstressed surface of the girder, a condition of plane stress exists. Combining this fact with the assumption that deformations are small makes the condition of plane strain also valid. These assumptions provide the basis for analyzing the concrete stresses using the equations of mechanics associated with linear elastic behavior, plane stress and strain, and Hooke's law.

First the shearing strain γ_{xy} is computed using the relation

$$\gamma_{xy} = 2\epsilon_{45} - \epsilon_0 - \epsilon_{90} \quad \text{Equation 3.1}$$

where the strains ϵ_0 , ϵ_{45} and ϵ_{90} correspond to strains at 0° , 45° and 90° which were obtained directly from the strain rosette data. Then, using $\epsilon_x = \epsilon_0$, $\epsilon_y = \epsilon_{90}$ and γ_{xy} from above, Mohr's circle of strain can be plotted. The vertical axis corresponds to $\gamma/2$ and horizontal axis to ϵ , with positive values located to the right of the vertical and above the horizontal. For Mohr's circle construction, shearing strains which cause clockwise rotation will be considered positive and counterclockwise rotation negative.

From Mohr's circle, the principal strains ϵ_{p1} and ϵ_{p2} can be determined using the relation:

$$\epsilon_{p1}, \epsilon_{p2} = \frac{\epsilon_x + \epsilon_y}{2} \pm \sqrt{\left(\frac{\epsilon_x - \epsilon_y}{2}\right)^2 + \left(\frac{\gamma_{xy}}{2}\right)^2} \quad \text{Equation 3.2}$$

The orientation of the principal planes is given by:

$$\theta = \frac{1}{2} \tan^{-1} \left[\frac{\gamma_{xy}}{\epsilon_x - \epsilon_y} \right] \quad \text{Equation 3.3}$$

where positive θ corresponds to counterclockwise rotation.

Finally, the principal stresses were calculated using the equations:

$$\sigma_{p_1} = \frac{E}{1-\nu^2} (\epsilon_{p_1} + \nu \epsilon_{p_2}) \quad \text{Equation 3.4}$$

$$\sigma_{p_2} = \frac{E}{1-\nu^2} (\epsilon_{p_2} + \nu \epsilon_{p_1}) \quad \text{Equation 3.5}$$

where E is Young's modulus and ν is Poisson's ratio.

Although the strains were monitored over a period of five days after prestress transfer, only the readings during the first few hours are reliable. Beyond this, the readings are significantly distorted by creep of the concrete and drift of the strain gages and measuring equipment.

Before performing the shear tests, new initial strain readings were taken upon which all strains induced by loading were based. Therefore, the stresses calculated for the shear tests are not the actual stresses present in the girder. In order to get a better idea of the actual stresses, both those induced by prestress transfer and shear loading were combined. It was not possible to just superimpose the strains and then calculate the principal stresses, because the elastic modulus changed from the time of prestress transfer to the time of loading. Therefore, it was necessary to calculate the normal and shearing stresses for the two different cases, superimpose them, and then determine the principal stresses and orientations for the combined case.

The normal and shearing stresses were calculated using the following expressions derived from Hooke's law:

$$\sigma_x = \frac{E}{1-\nu^2} (\epsilon_x + \nu \epsilon_y) \quad \text{Equation 3.6}$$

$$\sigma_y = \frac{E}{1-\nu^2} (\epsilon_y + \nu \epsilon_x) \quad \text{Equation 3.7}$$

$$\tau_{xy} = \frac{E}{2(1+\nu)} \gamma_{xy} \quad \text{Equation 3.8}$$

where the strains ϵ_x and ϵ_y were obtained from the measured data and γ_{xy} was computed as before. To determine the principal stresses, Mohr's circle of stress was used. The horizontal axis corresponds to normal stresses with tensile stresses plotted to the right of the origin. The vertical axis corresponds to shearing stress, with those causing clockwise rotation plotted above the horizontal axis and those causing counterclockwise rotation plotted below.

From Mohr's circle, the principal stresses can be determined using the expression

$$\sigma_{p1}, \sigma_{p2} = \frac{\sigma_x + \sigma_y}{2} \pm \sqrt{\left(\frac{\sigma_x - \sigma_y}{2}\right)^2 + \tau_{xy}^2} \quad \text{Equation 3.9}$$

and the corresponding rotation to the principal planes given by

$$\theta = \frac{1}{2} \tan^{-1} \left[\frac{2\tau_{xy}}{\sigma_x - \sigma_y} \right] \quad \text{Equation 3.10}$$

with positive θ corresponding to counterclockwise rotation.

The results of the stress analysis are presented in two sections: steel stresses and concrete stresses.

3.7 Steel Stresses

For analyzing stresses in the stirrup reinforcement during prestress transfer, the maximum tensile stress was plotted versus distance from the end of the girder (see Figs. 3.11a-d). To do so, the maximum tensile strain reading was found for each instrumented stirrup and converted to stress. The plot for the unmarked end shows a maximum stress of around 22,000 psi at the end which decreases to zero at the approximate transfer

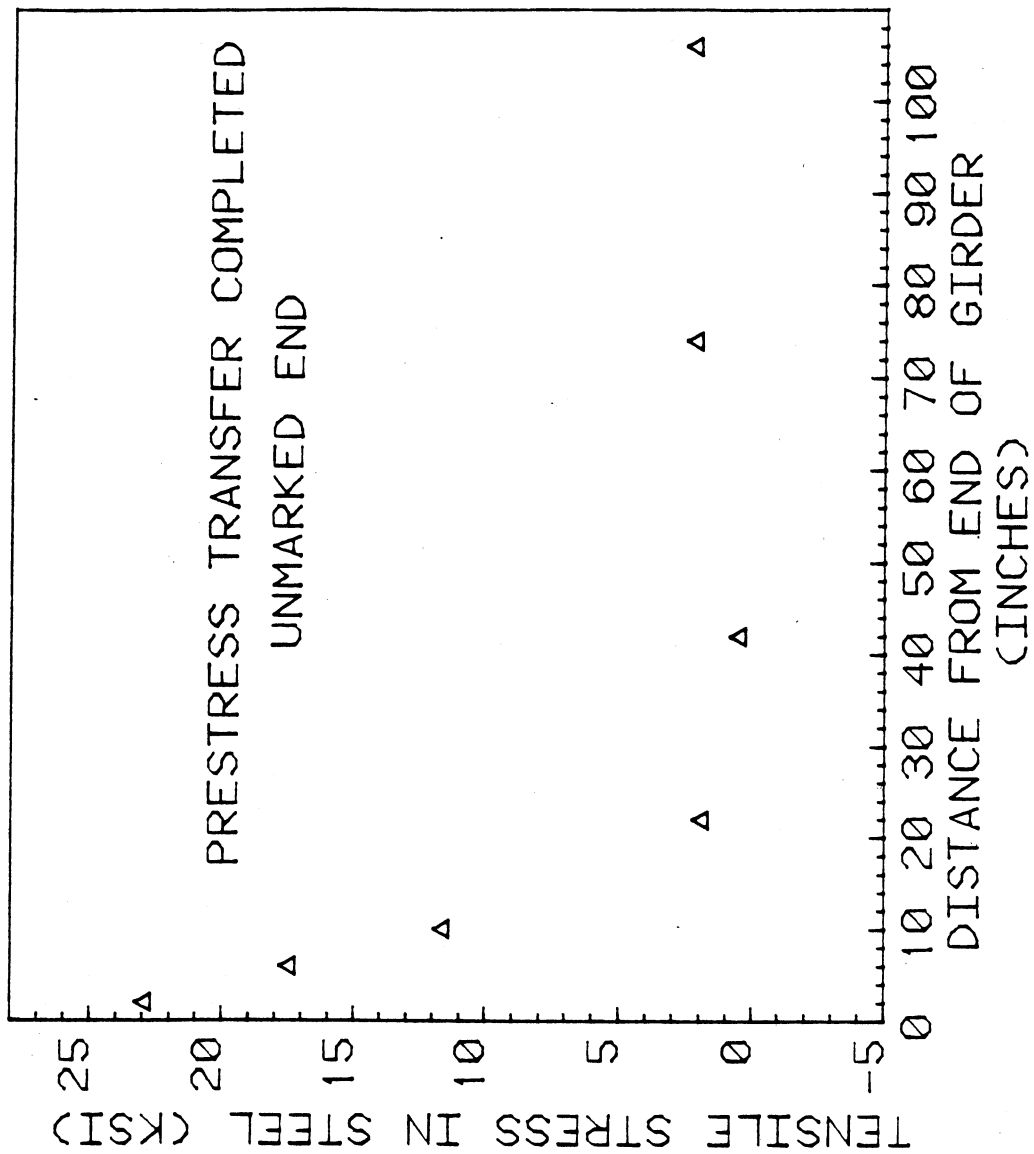


Figure 3.11a

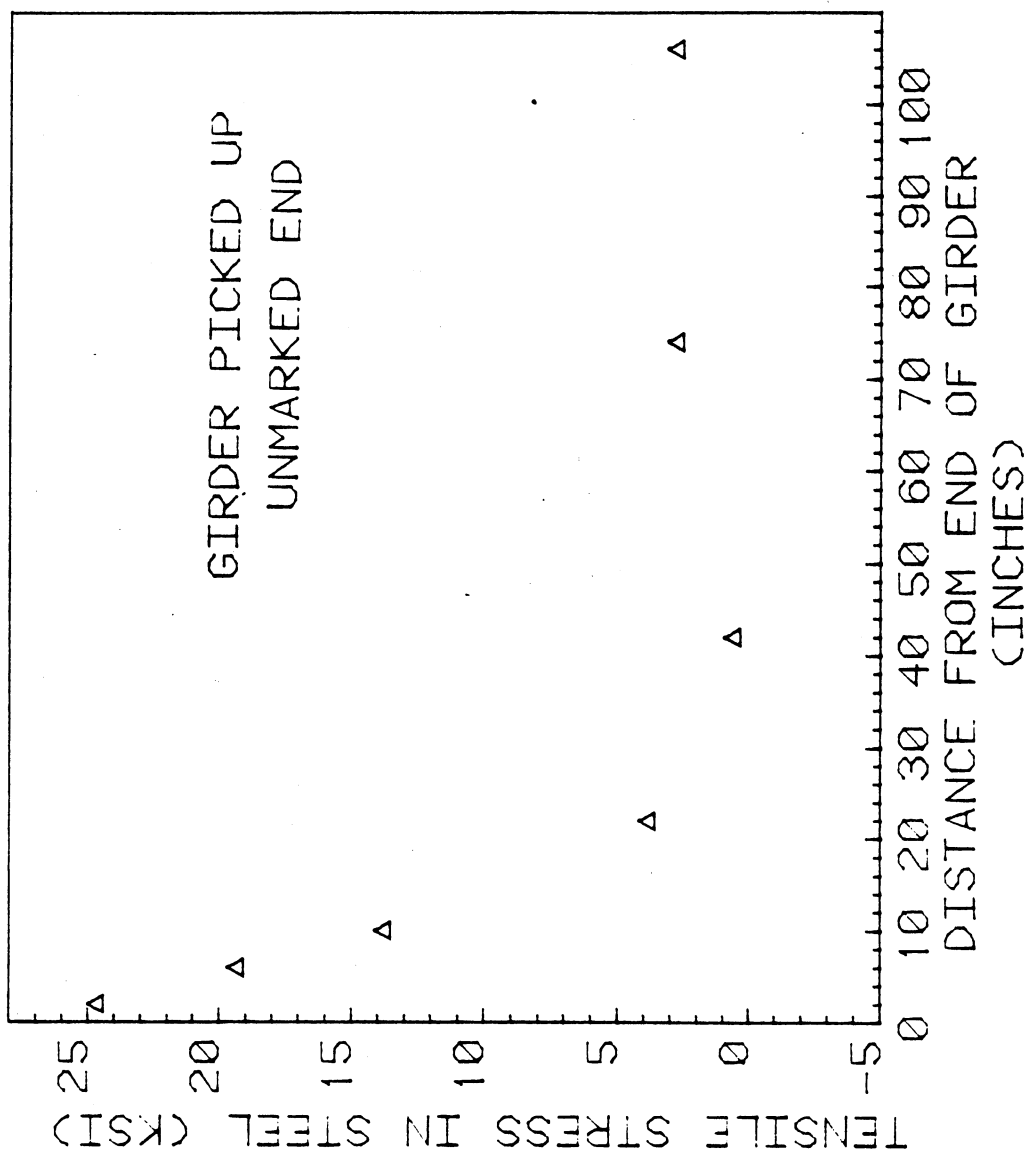


Figure 3.11b

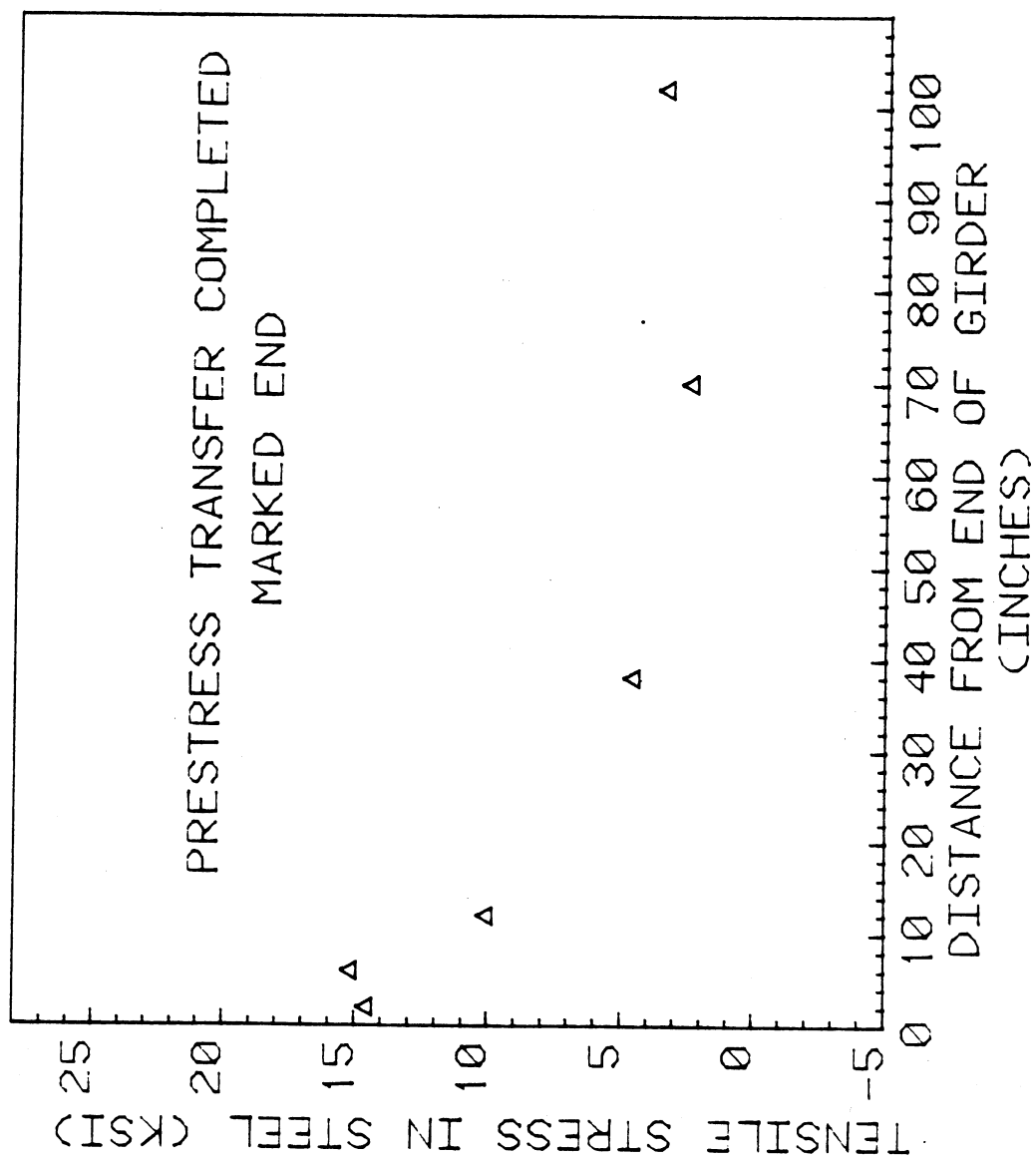


Figure 3.11c

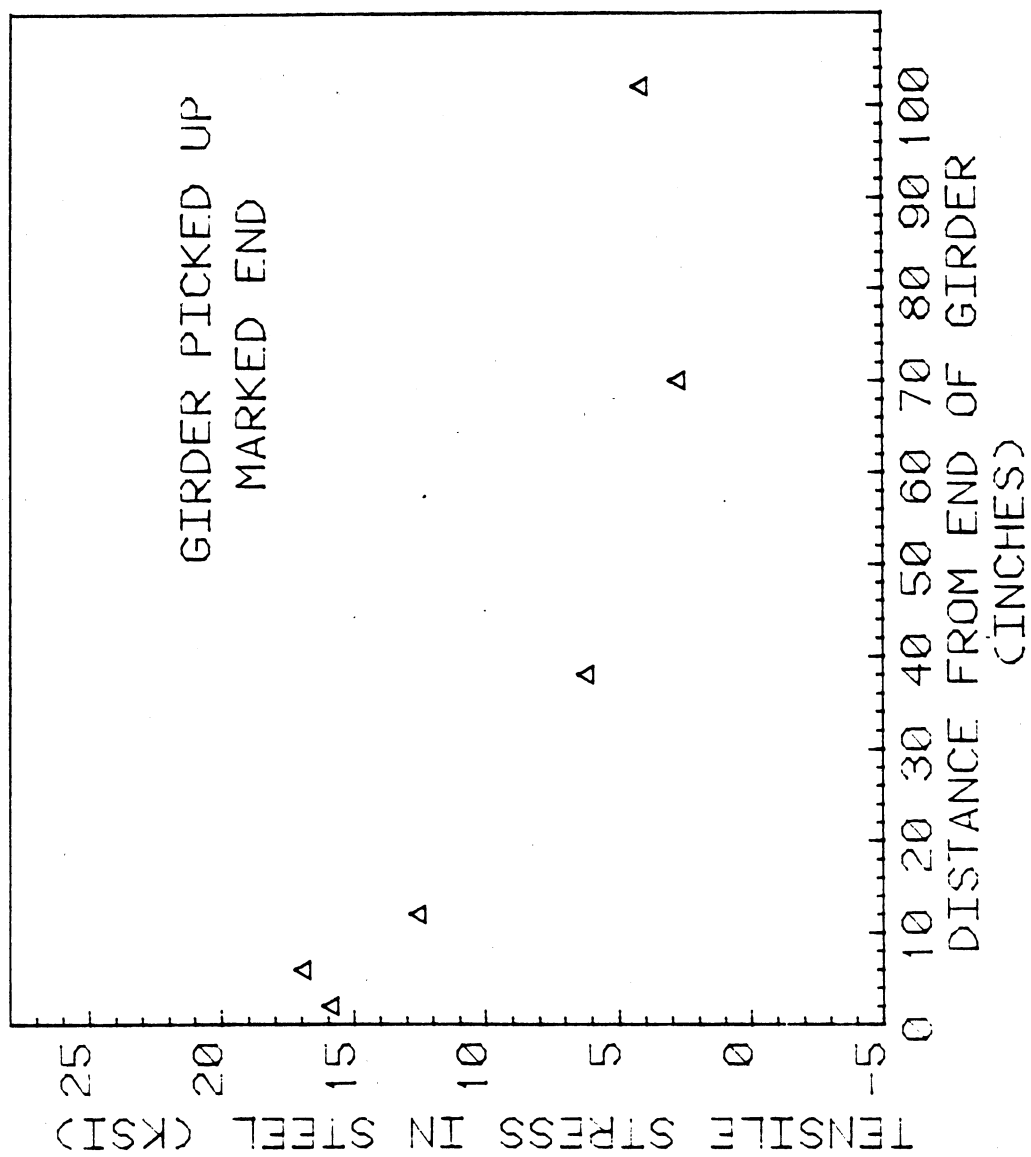


Figure 3.11d

length. This corresponds well with past theoretical and experimental data. The plot of the marked end indicates that the tensile stress is much less at the end of the girder, and is around 15,000 psi. However, it does not follow the same pattern as the unmarked end, which could be the result of the heavy vertical reinforcement.

Stresses induced in the stirrups during the shear test of the unmarked end are presented in tabular form (see Table 3.3 and Figure 3.12 for locations). This makes it easy to follow the stress development of a certain gage through each stage of the loading. At an end shear of 239.3 kips, the final reading before failure, high tensile stresses were recorded for gages 106, 109, 111 and 114. These agree well with the locations of the cracks that formed (see Fig. 3.12). A compressive stress of around 55 ksi was indicated by the gage located closest to the lower corner of the girder. This high stress confirms that failure of the unmarked end was caused by the crushing of the concrete at the support.

Shear test of the marked end did not produce any critical stresses in the end region of the girder (see Table 3.4a-c). Only gage No. 121 measured tensile stresses. These stresses were well within the allowable tensile stress for service load design of 24,000 psi for Grade 60 reinforcement. The rest of the gages measured compressive stresses which were maximum above the support, but not of critical magnitude.

3.8 Concrete Stresses

The principal stresses in the concrete are orientated on diagrams of the end of the girder for three conditions: prestress transfer, final loading before failure and a combination of prestress transfer and

Table 3.3
STRESSES IN STIRRUPS (psi)
UNMARKED END TEST

GAGE	END SHEAR (kips)									
	18.1	44.7	72.7	101.0	128.5	156.1	183.9	212.0	239.3	
100	0	-3538	-7308	-11165	-15254	-19720	-30305	-40339	-54549	
101	29	-3161	-7540	-10556	-13311	-15660	-19720	-22707	-25781	
102				-----NOT FUNCTIONING-----						
103	87	-2552	-5278	-7946	-10614	-12644	-16530	-20445	-25230	
104	0	-3538	-7482	-10005	-12122	-13978	-17225	-19633	-22069	
105	58	-2813	-6612	-9715	-12093	-14065	-17110	-18966	-20735	
106	29	-1624	-2929	-3886	-4524	-3248	5394	10266	10382	
107	29	-2233	-4872	-6554	-8149	-9454	-11745	-13137	-14442	
108	29	-1798	-4524	-6873	-8584	-9860	-11890	-13311	-14442	
109	0	-2610	1305	-4350	-1305	435	11774	27492	55419	
110	87	-841	-1914	-2958	-3451	-3799	-4031	-3712	-3393	
111	0	-203	-145	-145	-116	203	58	203	25143	
112	29	-203	-261	-522	-551	-174	-696	-464	696	
113	29	-261	-145	-377	-464	-406	-406	-406	-377	
114	29	-116	0	-87	-29	145	145	10034	35409	
115	928	783	6815	4582	4350	8249	2291	1537	5974	
116	58	-203	-116	-145	-203	-145	-464	-406	2958	

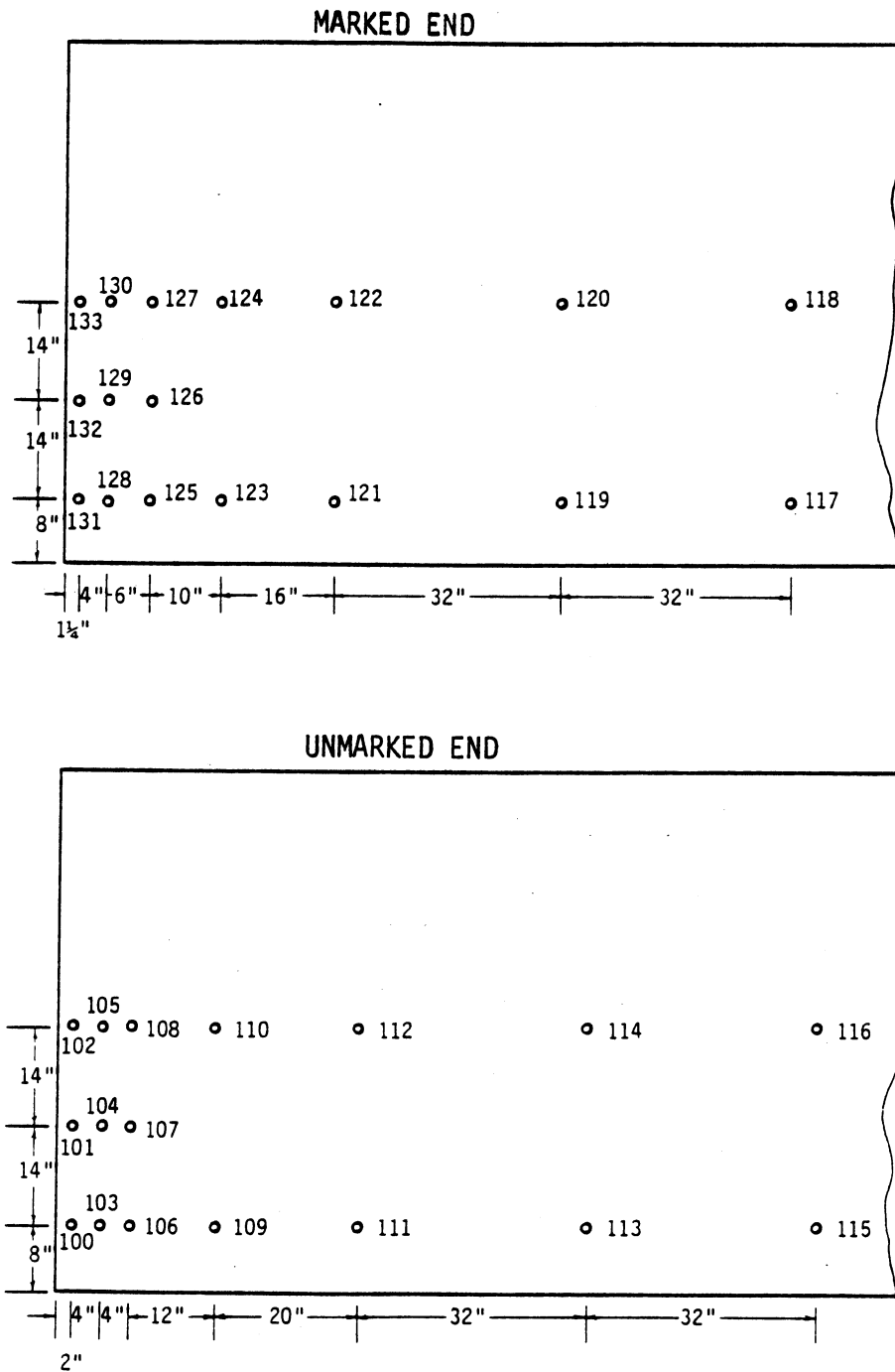


Figure 3.12 Locations of strain gages on stirrups.

Table 3.4a
STRESSES IN STIRRUPS (psi)
MARKED END TEST #1

GAGE	END SHEAR (kips)											
	17.1	43.5	71.3	99.5	126.7	154.3	181.9	209.3	237.0	264.8	291.7	
117	-58	-522	-638	-551	-725	-667	-812	-696	-580	-1160	-667	
118	29	0	0	0	-174	-145	-116	-145	-116	-261	-551	
119	0	0	-145	-203	-435	-522	-522	-638	-609	-5220	-580	
120	0	0	0	0	0	0	0	0	0	0	29	
121	0	174	0	0	-174	-116	0	145	290	377	725	
122	-58	0	-232	-435	-696	-783	-783	-986	-1044	-1131	-1131	
123	0	-580	-1769	-3074	-4727	-6003	-8207	-7859	-8671	-9570	-1044	
124												
125												
126	0	-1479	-3509	-5075	-6641	-7540	-8460	-9512	-10353	-11368	-12470	
127	-29	-406	-1044	-1769	-2668	-3219	-3886	-4437	-4959	-5597	-6380	
128	-29	-1769	-4321	-6090	-7917	-9077	-10498	-11774	-1305	-14297	-16240	
129	0	-1421	-3741	-5684	-7511	-8004	-9396	-10556	-11571	-12702	-14036	
130												
131	-58	-1856	-4437	-6119	-7424	-8625	-9280	-10237	-11049	-12064	-13311	
132	-29	-1450	-3828	-5771	-7453	-8613	-9918	-11136	-11716	-13166	-14500	
133	-116	-1102	-2552	-3915	-5452	-6264	-7395	-8352	-8961	-9918	-10904	

Table 3.4b
STRESSES IN STIRRUPS (psi)
MARKED END TEST #2

GAGE	END SHEAR (kips)				
	17.2	153.5	181.0	108.0	235.6
117	1160	348	348	435	261
118	-29	-319	-261	-319	-464
119	261	-348	-261	-435	-580
120	29	0	29	29	29
121	638	609	841	1015	1102
122	377	-580	-522	-667	-609
123	0	-4727	-5133	-5365	-5539
124	----NOT FUNCTIONING----				
125	----NOT FUNCTIONING----				
126	87	-8787	-9599	-10556	-11484
127	-87	-4031	-4669	-5220	-5887
128	-609	-1218	-13717	-15051	-16501
129	899	-9860	-11136	-12209	-13340
130	----NOT FUNCTIONING----				
131	-290	-10904	-12064	-12934	-14123
132	-203	-10614	-11977	-12818	-14210
133	783	-6960	-8033	-8874	-9889

Table 3.4c
STRESSES IN STIRRUPS (psi)
MARKED END TEST #3

GAGE	END SHEAR (kips)					
	17.3	152.3	179.5	206.4	233.6	245.3
117	1479	319	-145	-58	-145	-116
118	-87	-290	-145	-58	-232	-174
119	29	-406	145	-116	-203	-261
120	29	29	0	29	0	0
121	638	1102	58	145	377	609
122	-58	-58	-174	58	0	116
123	29	-348	145	348	1305	2784
124	----NOT FUNCTIONING----					
125	----NOT FUNCTIONING----					
126	-754	-8729	-116	-580	-1363	-1711
127	-609	-4553	-87	-406	-1102	-1305
128	-2407	-14094	-116	-1537	-3364	-4292
129	0	-12180	-58	-928	-2204	-2726
130	----NOT FUNCTIONING----					
131	-2146	-19343	-145	-1711	-3857	-4901
132	-1189	-13775	-29	-957	-2349	-2813
133	261	-8642	-29	-609	-1479	-1827

approximate service load (see Figures 3.13a-d). According to the AASHTO code, the allowable concrete stresses in pretensioned members before losses due to creep and shrinkage are $0.6 f'_{ci}$ for compression and $7.5 \sqrt{f'_{ci}}$ for tension where f'_{ci} is the compressive strength of concrete at the time of initial prestress. These correspond to calculated values of 3249 psi and 552 psi respectively. After losses have occurred, the allowable stresses due to service load are $0.4 f'_c$, or 3468 psi, for compression and $6 \sqrt{f'_c}$, or 559 psi, for tension. The modulus of rupture, or cracking stress, computed according to AASHTO specifications is $7.5 \sqrt{f'_c}$ or 698 psi.

At prestress transfer, maximum tensile and compressive principal stresses are located near the bottom flange and slightly in from the end of the girder. These stresses are probably the combined result of bursting stresses produced by the straight prestressing strands, and compressive stresses produced by the vertical reaction from the dead load of the girder. The magnitude of the compressive stress is well within the allowable limit; however, the tensile stress exceeds the allowable limit by almost 800 percent. At this point, a micro-crack has formed, and the bonded steel reinforcement is taking up the excess tensile stresses.

Principal stresses induced by the final stage of loading before failure of the test girder's unmarked end are shown in Figure 3.13b. Tensile and compressive stresses exceeding their allowable values are indicated by the two gages located near the bottom flange of the girder. The high principal compressive stress above the support again confirms that failure of the unmarked end was caused by the crushing of the concrete in this area.

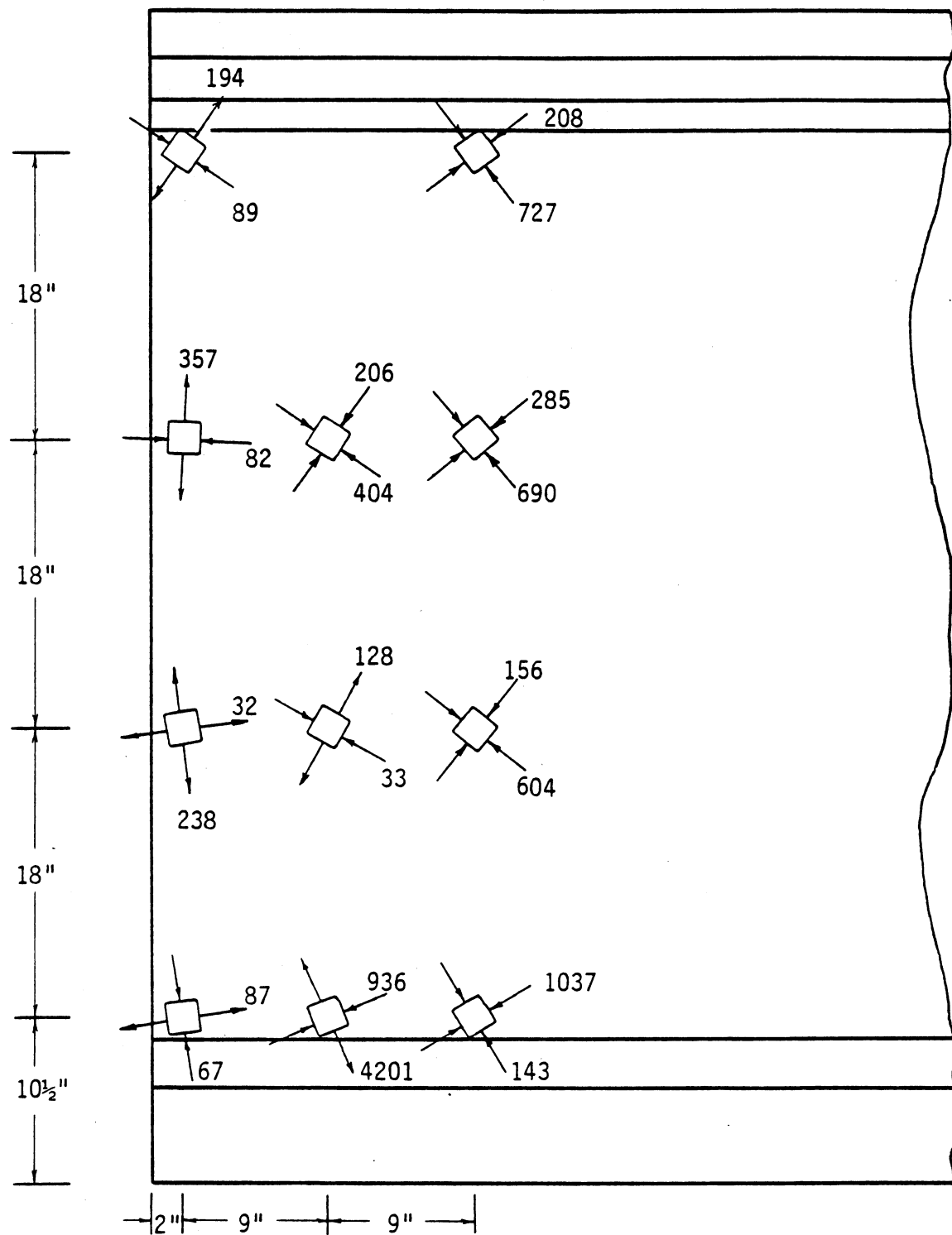


Figure 3.13a Principal stresses (psi) in concrete due to prestress transfer.

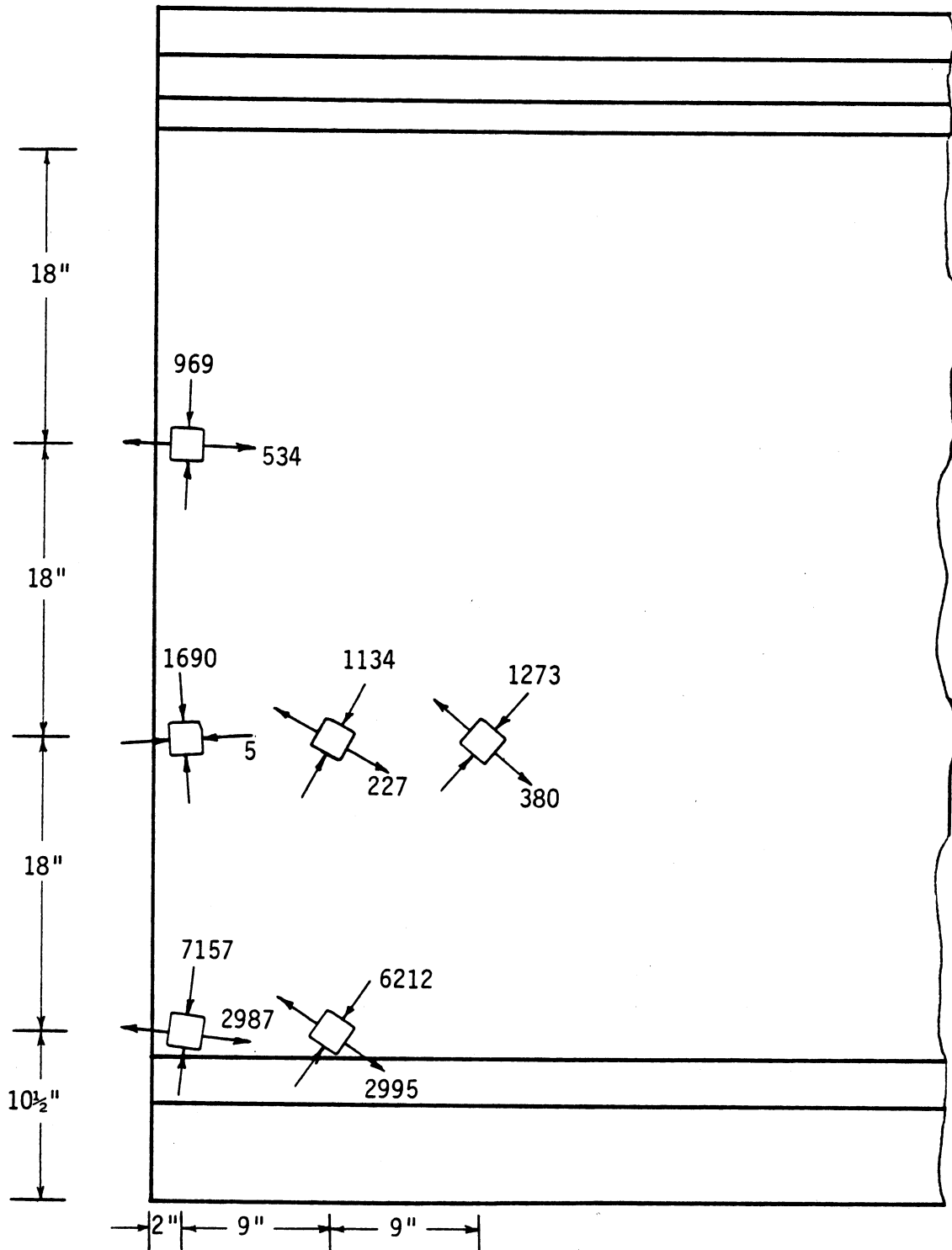


Figure 3.13b Principal stresses (psi) in concrete due to shear test.

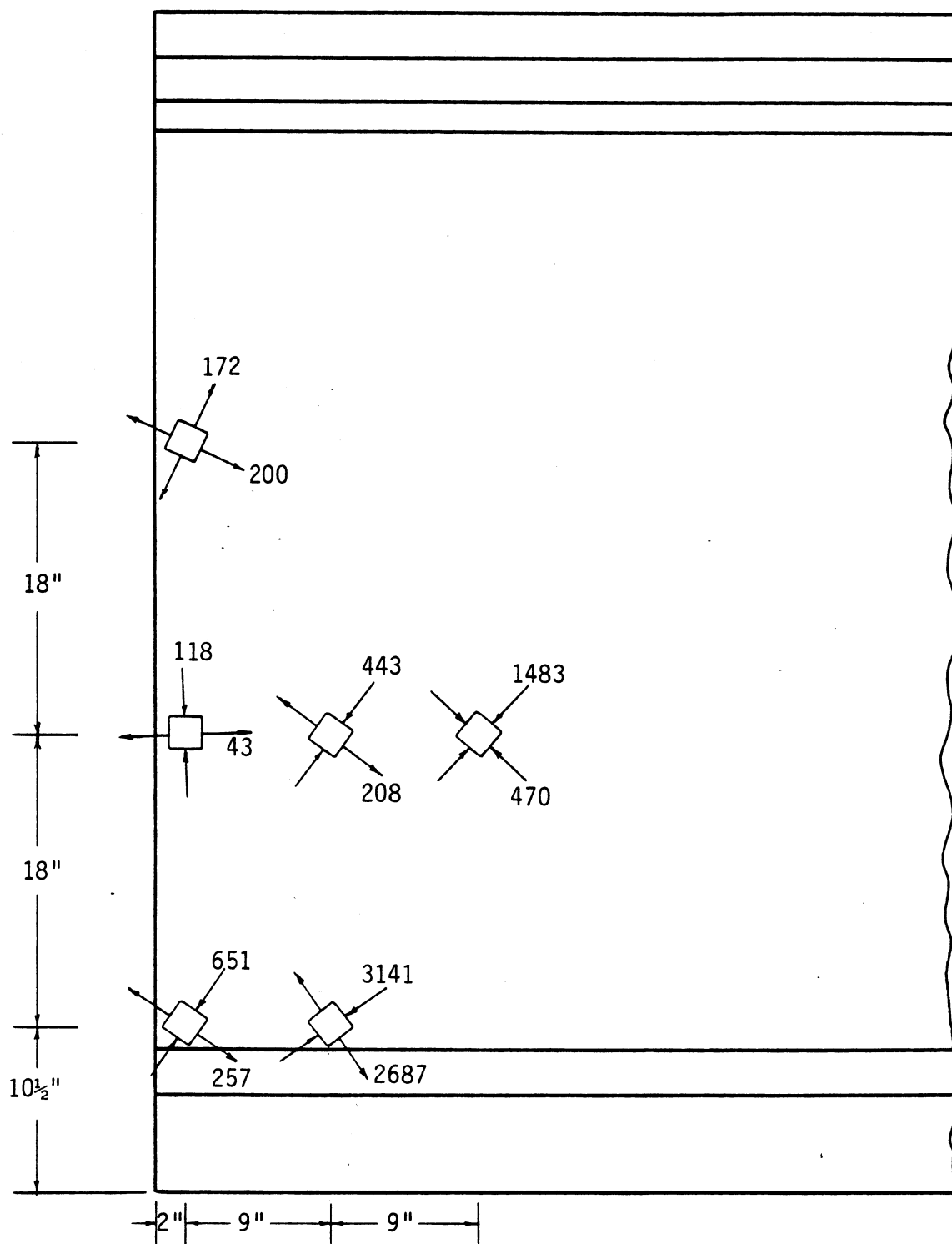


Figure 3.13c

Principal stresses (psi) in concrete due to combination of prestress transfer and service load.

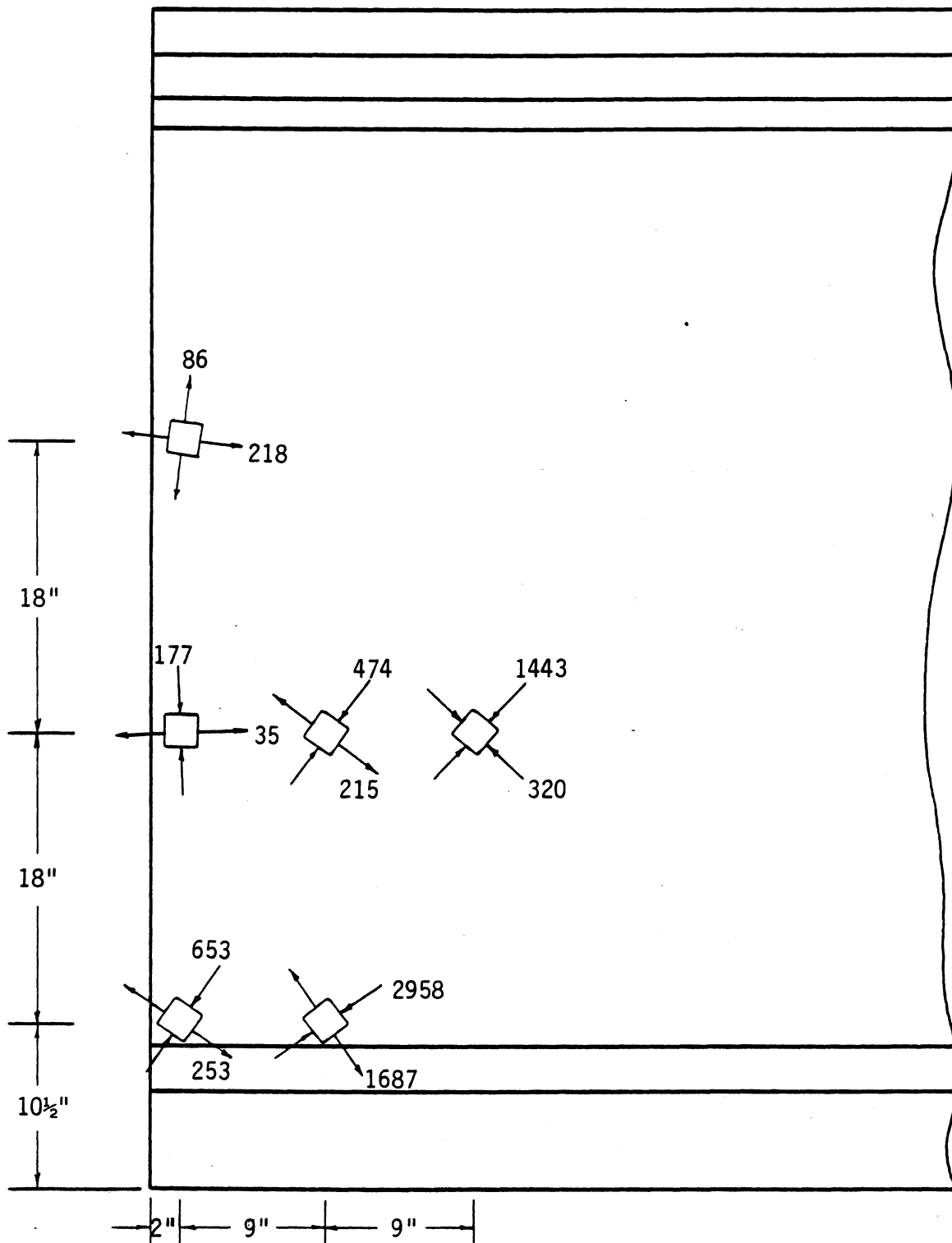


Figure 3.13d Principal stresses (psi) in concrete due to combination of prestress transfer and service load, with reduction for losses.

Finally, stresses caused by prestress transfer and the stresses at the simulated service load were combined to give the principal stresses shown in Figure 3.13c. The only principal stress to exceed the allowable value is the tensile stress of 2687 psi. However, this does not take into account losses due to creep and shrinkage of the concrete, or relaxation of the prestressing strands. Assuming the total losses to be 25 percent of the initial stresses, the horizontal, vertical and shearing stresses (σ_x , σ_y and τ_{xy}) at prestress transfer were reduced accordingly. These were again combined with the service load stresses to produce the principal stresses shown in Figure 3.13d. This caused the highest principal tensile stress to decrease to 1687 psi. Although it still exceeds the allowable value, this stress is greatly reduced from an initial value after detensioning of 4201 psi. Again, a tensile stress of this magnitude indicates that a crack has probably formed and that the bonded steel reinforcement is being stressed.

3.9 Theoretical Comparison

The theoretical method developed by D. Krishnamurthy (refer to Chapter 2) for determining the vertical stress distribution in the concrete of the end region of a pretensioned girder was used to compare with experimental results. Krishnamurthy's equation was developed for girders with prestressing strands located in both flanges, and it assumes that the section remains uncracked at the time of prestress transfer. Since cracks formed in the test girder, the stresses indicated by the concrete rosettes were not valid for comparison. Instead, the stresses in the steel stirrups were converted into equivalent concrete stresses by multiplying them by the modular ratio $n = 4/29$. Krishnamurthy's method

calculates vertical stresses at the centroid of the cross section, therefore the strain gages located 36 inches from the bottom of the girder were used in the comparison.

Figure 3.14 shows a plot of the vertical stress distributions for both marked and unmarked ends of the test girder, as well as that predicted using Krishnamurthy's equation. Although there are only three data points for the marked end, two of these compare well with the theoretical distribution. Conversely, the distribution of the unmarked end is much higher than the theoretical curve. This is probably due to the varying amounts of steel reinforcement in the end regions. Since the marked end is heavily reinforced, it tends to behave more elastically than the unmarked end, and therefore the distribution is better predicted by the theoretical method.

3.10 Conclusion

Results from the tests performed at Concrete Technology Corporation indicate that end blocks can be removed from WSDOT pretensioned concrete girders while retaining the five inch web width. The vertical stirrup reinforcement designed according to AASHTO shear and anchorage zone requirements is an effective replacement for end blocks, and there is no problem meeting the clear cover or spacing requirements. The tests also proved that concrete can be placed and compacted in the end region without problems of air pockets or honeycombing due to the congestion of the reinforcing steel. Therefore, it was recommended that this design be implemented in WSDOT girders.

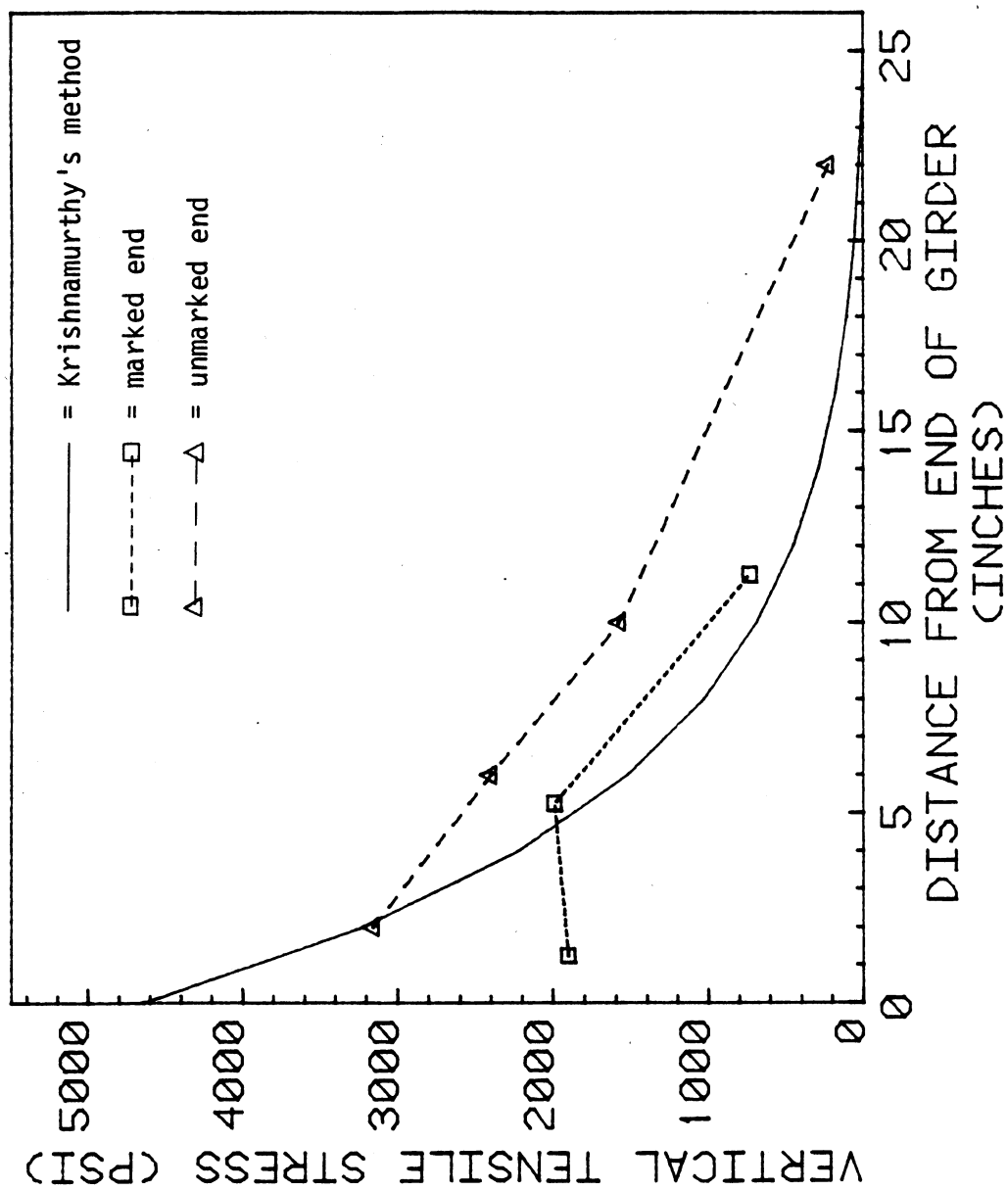


Figure 3.14 Transverse stress distribution.

CHAPTER 4

TEST OF ACTUAL HIGHWAY GIRDER WITHOUT END BLOCKS

The test of the series 14 pretensioned concrete girder at Concrete Technology Corporation proved that end blocks can be removed without affecting the girder's ultimate load capacity. With the completion of the CTC test, the research proceeded in implementing the design in a girder for use in an actual highway bridge. In order to monitor the performance of the girder during prestress transfer and under actual loading conditions both the concrete and the steel reinforcement of the end region were to be instrumented with strain gages.

A bridge using series 10 girders was selected for implementation. This bridge was located in Spokane, at the Sullivan Road Interchange of SR 90, for both timing and location conveniences. Construction of the girders was contracted to Central Pre Mix of Spokane. A revision of the contract called for the end of one of the interior girders to be constructed without an end block. The revision also provided the WSU team access to the girder for inspection, instrumentation and testing both during and after construction.

The strains induced in the steel and concrete were monitored and recorded during and after prestress transfer and also during construction and loading of the bridge. The resulting stresses were examined with the results and conclusions presented at the end of this chapter.

4.1 Girder Design

The series 10 pretensioned prestressed concrete girder incorporated into the Sullivan Road Interchange is designed for a span length of

103 feet and an HS-20 loading. It is one of the interior girders from a total of 14 spaced at 97.5 inches on center. The prestressing pattern consists of 41 bundled harped and straight $\frac{1}{2}$ inch diameter seven-wire, grade 270 strands (see Figure 4.1). Thirteen of the strands are harped at an angle of approximately 5.65° with harping points at a distance of 40.34 feet from either end. Between the harping points, the strands are bundled with a center of gravity 3.25 inches from the bottom of the girder. The remaining 28 strands are straight and located in the lower flange with a center of gravity $3 \frac{3}{8}$ inches from the bottom.

4.2 Girder Details

For the end of the girder without an end block, shear reinforcement is provided similar to that used in the Concrete Technology Corporation test. Pairs of #4 grade 60 stirrups are used with the first located $1\frac{1}{2}$ inches from the end. This is followed by 8 spaced at 2 inches, 4 spaced at 4 inches, 4 spaced at 10 inches and the remainder at 18 inches maximum spacing to the midspan of the girder (see Figure 4.2). Ties around the straight strands are located at $1\frac{1}{2}$ inches followed by 8 spaces at 4 inches. Finally, the longitudinal reinforcement in the form of #4 bars are located starting at $9\frac{1}{2}$ inches from the bottom followed by 4 spaces at $5\frac{1}{2}$ inches, one space at $7\frac{1}{2}$ inches and 2 bars at the top of the girder. The shear capacity diagram for the end region of this particular girder is shown in Figure 4.3.

4.3 Instrumentation

Instrumentation of the girder consisted of both strain gages mounted on stirrups and strain rosettes attached to the concrete. The pattern of

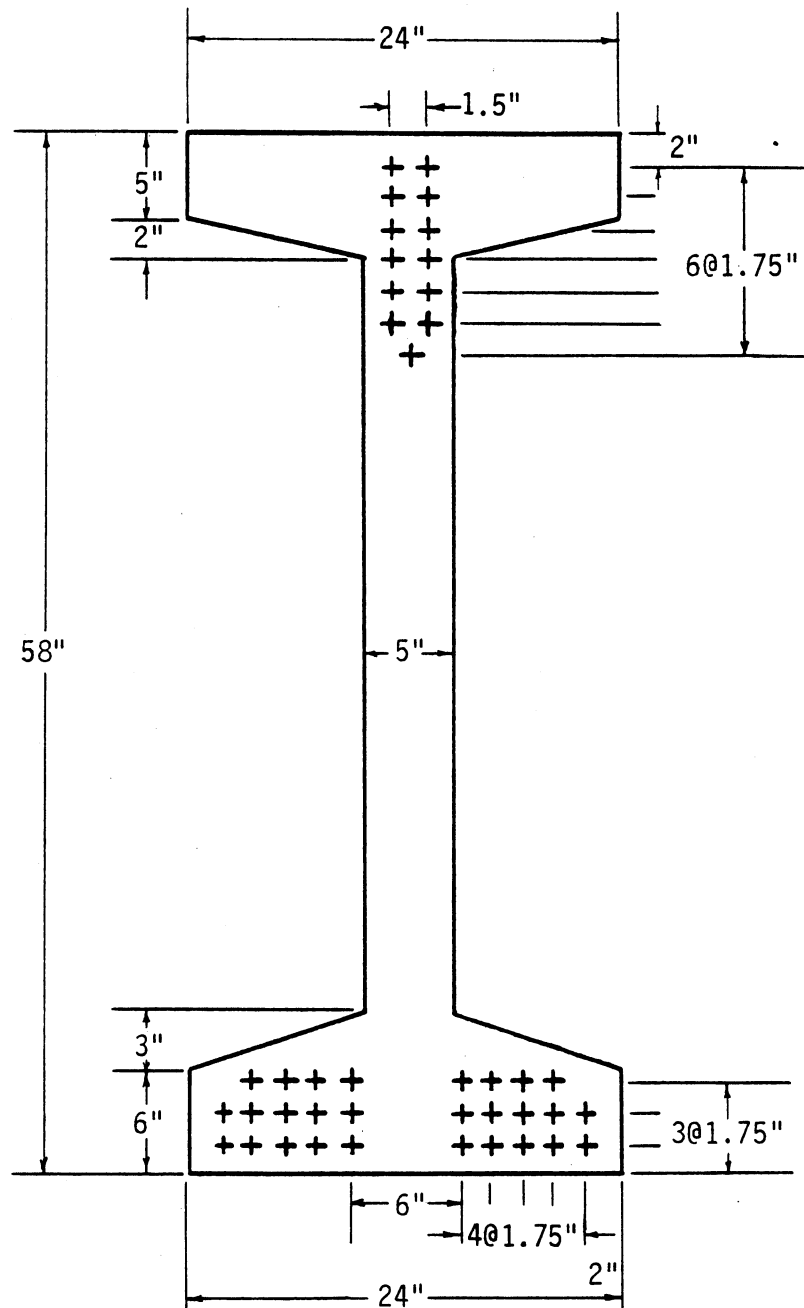


Figure 4.1 Cross section of WSDOT series 10 pretensioned concrete girder.

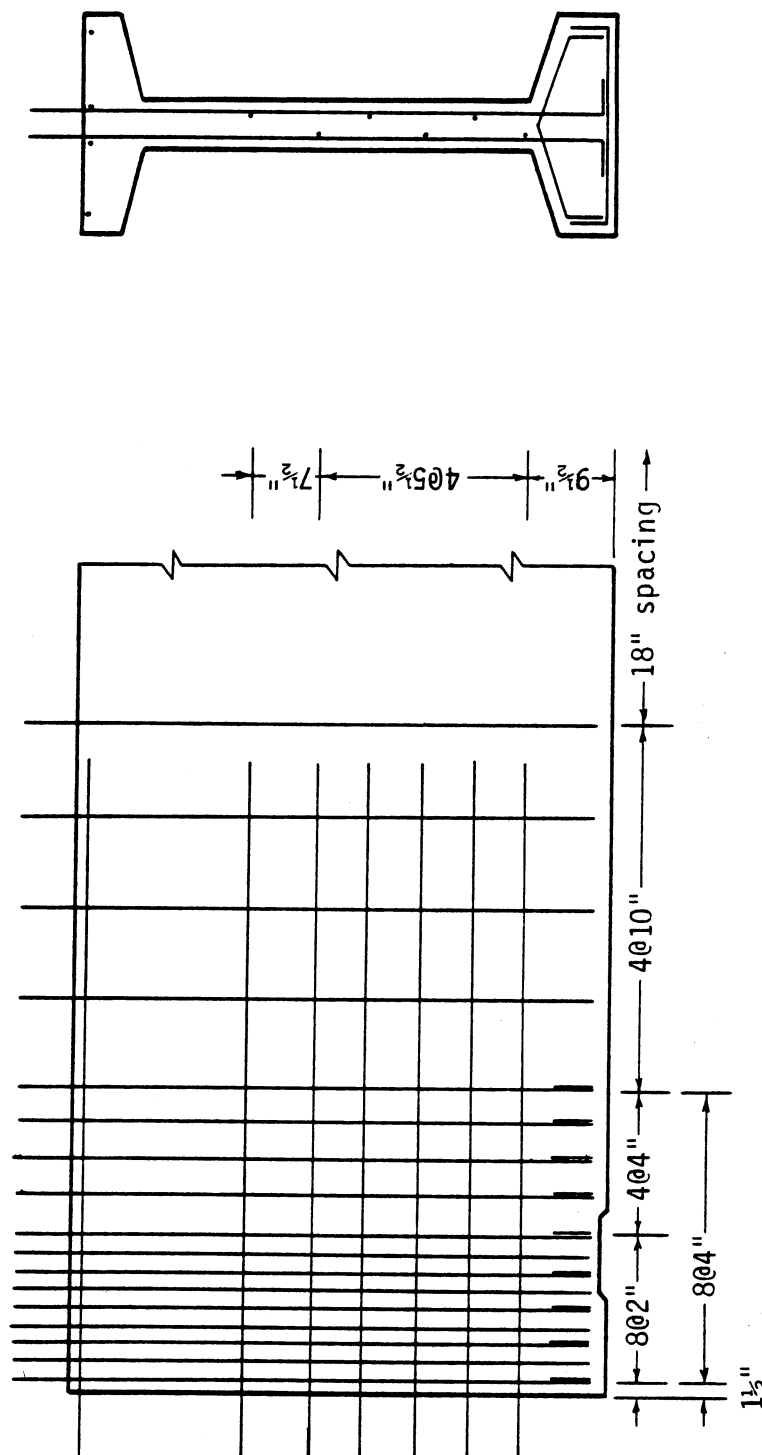


Figure 4.2 Details of steel reinforcement.

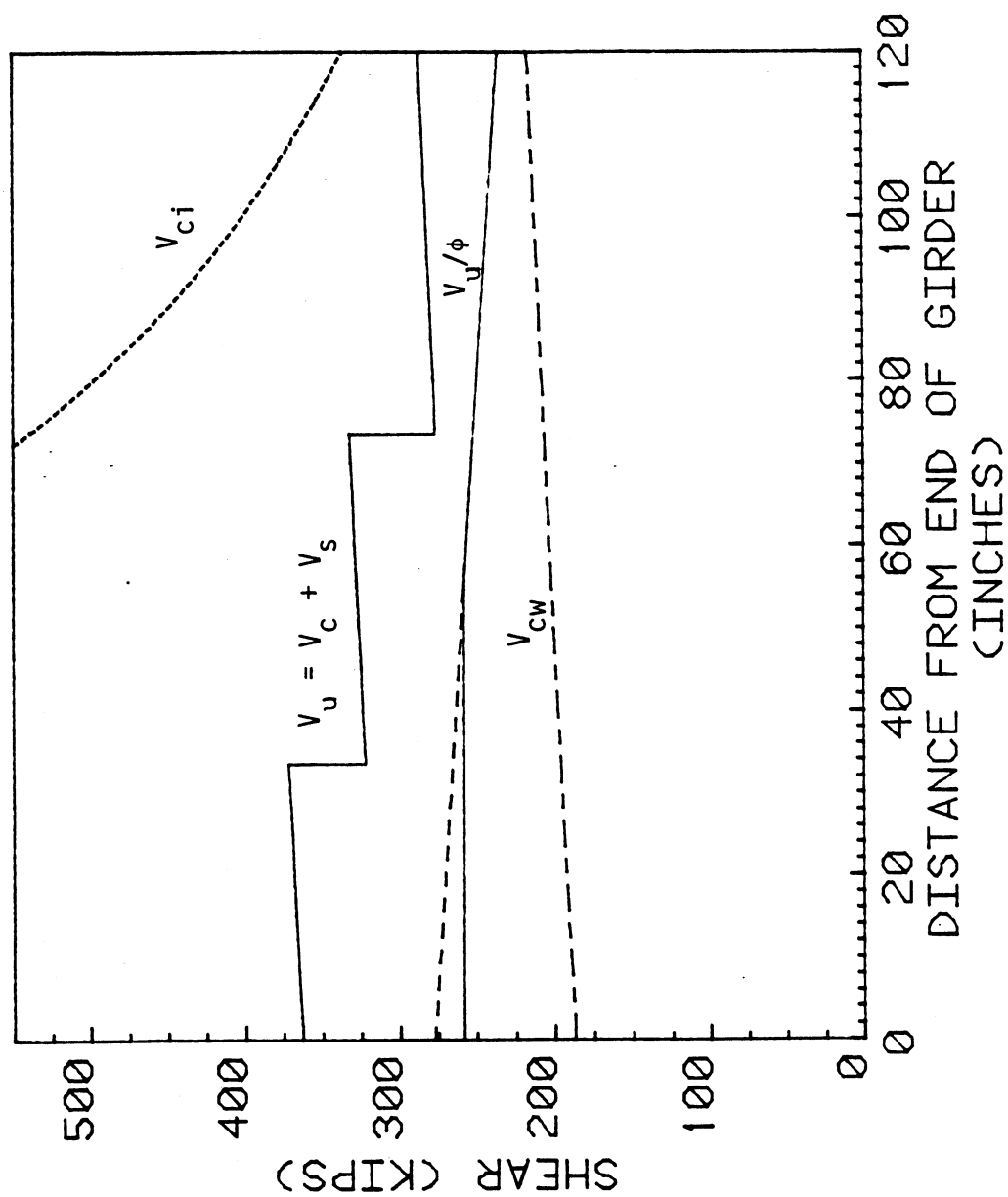


Figure 4.3 Shear capacity diagram.

the gages is similar to that used in the Concrete Tech test. Strain measuring equipment with a capacity of 60 channels made it possible to monitor 21 strain gages and 13 strain rosettes.

For instrumenting stirrups, TML type FLA-6-11 strain gages were chosen. These gages are 6mm in length and 2.4mm wide with a nominal resistance of 120 ohms and a gauge factor of approximately 2.1. The small size of the gages made them ideal because it minimized the amount of steel that needed to be removed to provide a smooth, flat surface. The gages were vertically aligned on the stirrups and attached with M-bond 200 adhesive. A three wire lead system was used for wiring the gages to eliminate the effect of temperature change on the lead wires.

After the gages were attached and wired, a coating of silicone rubber caulking was applied and allowed to cure. This provided protection from moisture as well as impact of concrete during placing and vibrating. A layer of electrical tape was also added as an extra precaution. The lead wires were surrounded by polyethylene plastic tubing which ran along the length of the stirrups and out the top of the girder.

A total of eight stirrups were instrumented, with the gages located at points where cracks were most likely to develop (see Figure 4.4a). The first two stirrups, $1\frac{1}{2}$ inches and $5\frac{1}{2}$ inches from the end, each carry 4 strain gages. The third at $9\frac{1}{2}$ inches has 3 gages while the remainder, located at $15\frac{1}{2}$, $43\frac{1}{2}$, $53\frac{1}{2}$, $63\frac{1}{2}$ and $91\frac{1}{2}$ inches each have 2 gages. The gages near the end are for determining the stresses induced by prestress transfer, while the gages starting at $43\frac{1}{2}$ inches from the end are mainly for monitoring the tensile stresses induced by shear.

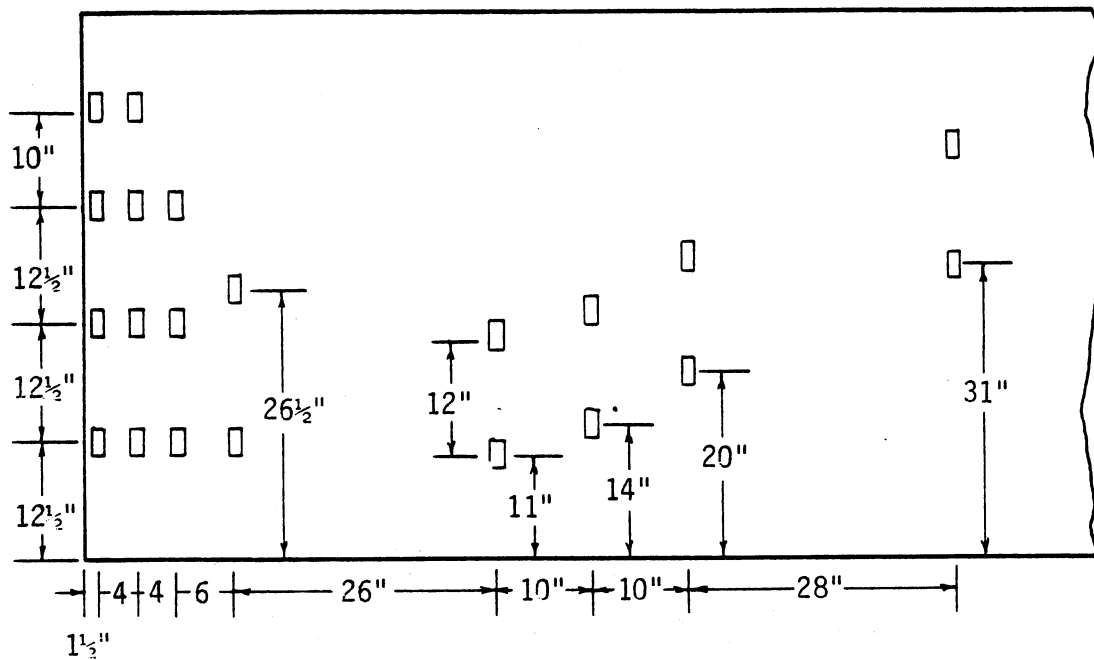


Figure 4.4a Locations of gages on stirrups.

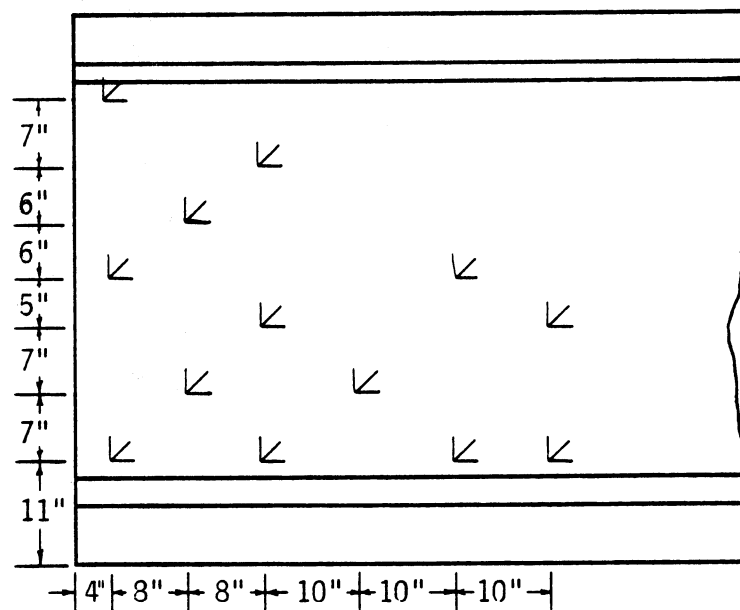


Figure 4.4b Locations of rosettes on concrete.



Figure 4.4c Example of stirrup instrumented with strain gages.

For monitoring the principal stresses in the concrete, TML type PR-5-11 rectangular rosettes were chosen. A plastic backing impregnated with a polyester resin makes them applicable to concrete.

Before mounting the rosettes on the concrete, a grid was drawn locating each of the gages (see Figure 4.5). The locations were sanded smooth and then cleaned using acetone. A base coat of RP-2 polyester adhesive only took about ten minutes to cure. The rosettes were mounted with another layer of the adhesive, and slight pressure was applied until the glue cured. Six terminals were also attached next to each rosette so that wires could be connected without the danger of pulling the rosettes off of the concrete. Again, the three wire lead system was used to eliminate temperature effects. Finally, the rosettes were numbered and covered with a thick layer of silicone rubber to protect them from the weather.

4.4 Girder Construction

Construction of the girder took place on March 8th. First, the 41 prestressing strands were placed and tensioned with a jacking force of 376 kips for the 13 harped strands and 810 kips for the 28 straight strands. This was followed by the placement of the steel reinforcement including stirrups, ties, transverse and longitudinal reinforcement. With everything properly located and inspected, the forms were brought into place. The forms had previously been altered by removing the tapered and widened end block sections at one end, and in their place continuing with the straight forms identical to the middle of the girder. This makes construction easier because the straight forms can be

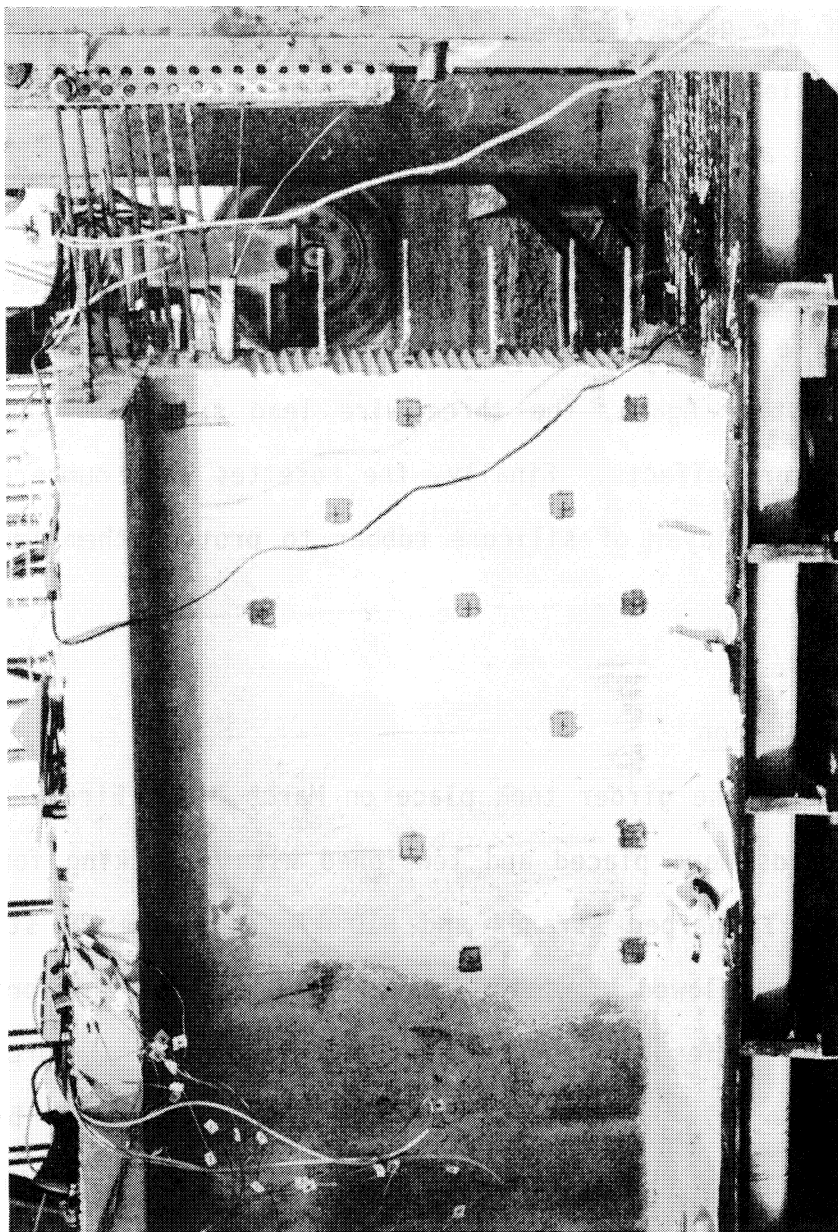


Figure 4.5 Mounting of strain rosettes.

continued beyond the end of the girder unlike end block forms which must be placed within a specified tolerance.

With the forms in place, vibration of the casting bed and placing of the concrete began. The concrete was placed in batches using high strength, early cure concrete. Cylinder samples were taken from each batch and vibrated along with the girder. The girder and cylinders were then steam cured for approximately 48 hours. The next morning, the forms at the end without end blocks were removed so that the rosettes could be mounted and equipment tested before detensioning the strands.

4.5 Prestress Transfer

On March 11th, the remaining forms were removed and cylinder tests indicated that the concrete had reached a compressive strength of 4500 psi, therefore prestress transfer could begin. The load was released in stages, with time allowed between each stage for taking strain readings. At 7:07 am the tie downs were cut and the load on the harped strands released, with six of the strands being cut at the dead end. Next, one quarter of the load on the straight strands, 202.5 kips, was released and seven were cut at the dead end. The remaining load was released in three increments of one quarter each time, with seven strands being cut at the dead end after each release, until prestress transfer was completed at 7:30. The only noticeable effect of prestress transfer at this time was a cambering upwards of the girder with a maximum deflection of around one inch at the midspan (see Figure 4.6).

At 7:41, the girder was picked up by crane and a strain reading was taken before disconnecting the wires. Then, the girder was transported to its storage site where it was placed on temporary supports of wooden



Figure 4.6 Girder after prestress transfer with slight upwards deflection at midspan.

blocks (see Figure 4.7). At this time, the equipment was reconnected and strain readings were taken at 10 and 15 minute intervals until 11:00 am when the intervals were set for 2 hours. On March 13th, the strain reading interval was set for twice a day until it was disconnected on March 25th.

Although strain readings were recorded for up to two weeks following prestress transfer, only the readings during the first couple of hours were reliable. Upon examining the data, it became evident that the magnitude of the strain readings were increasing rapidly with time, and almost all of the gages were indicating high positive (tensile) strains within ten hours from the completion of prestress transfer. This was attributed to the effects of creep and shrinkage of the concrete with time. Therefore, only the strain readings immediately following detensioning were examined, beyond this, the accuracy of the data is questionable.

4.6 Stress Analysis of Prestress Transfer

The only visible result from prestress transfer was the formation of a slight crack near the centroid of the girder (see Figure 4.7). With a length of only 13 cm (5 in) and width of 0.1 mm (0.004 in), the crack will not be detrimental to the service load capacity of the girder (13). The other results of prestress transfer can be seen by examining the induced stresses which have been computed from the recorded strain values.

The stresses in the steel stirrups were plotted with the maximum tensile stress versus distance from the end of the girder (see Figures 4.8a-h). The maximum stress was located in the stirrup closest to the

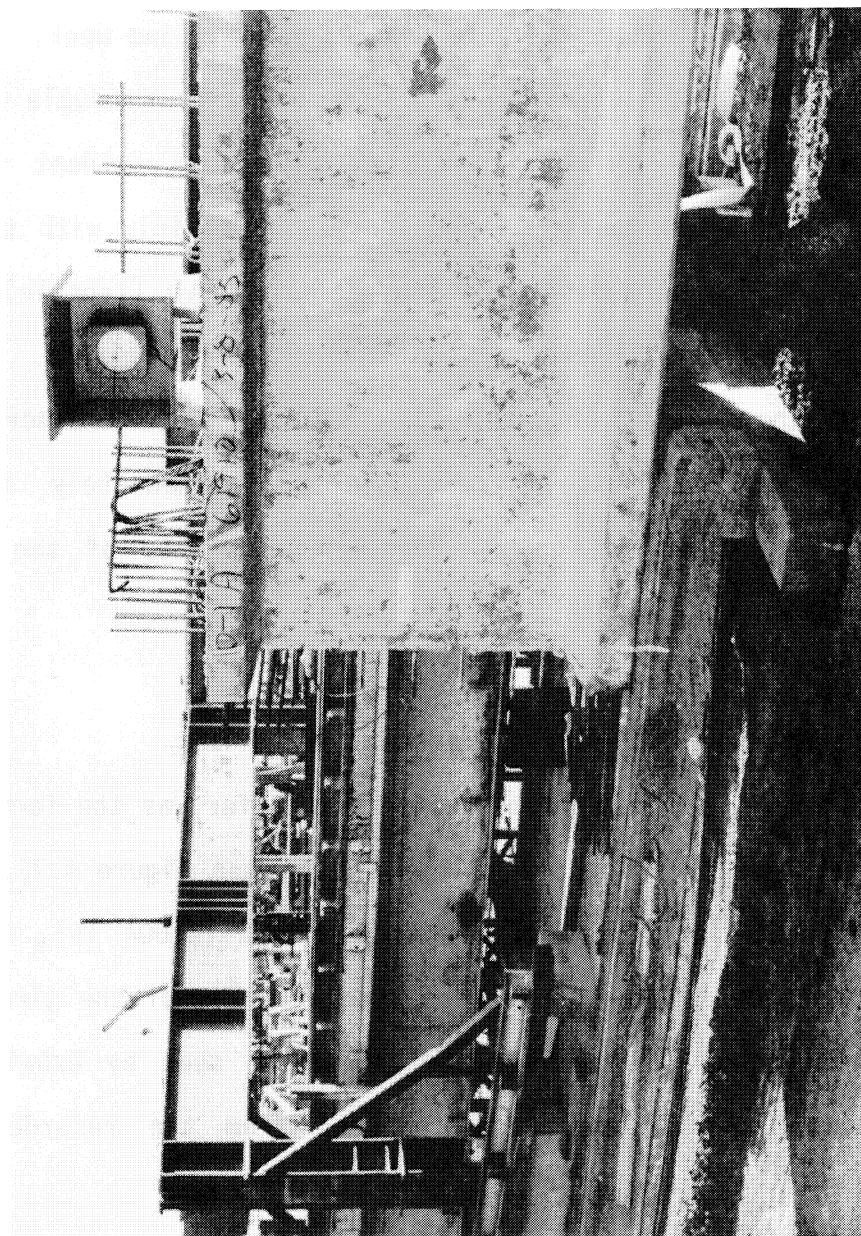


Figure 4.7 Girder on storage supports with crack from prestress transfer visible at the approximate centroid.

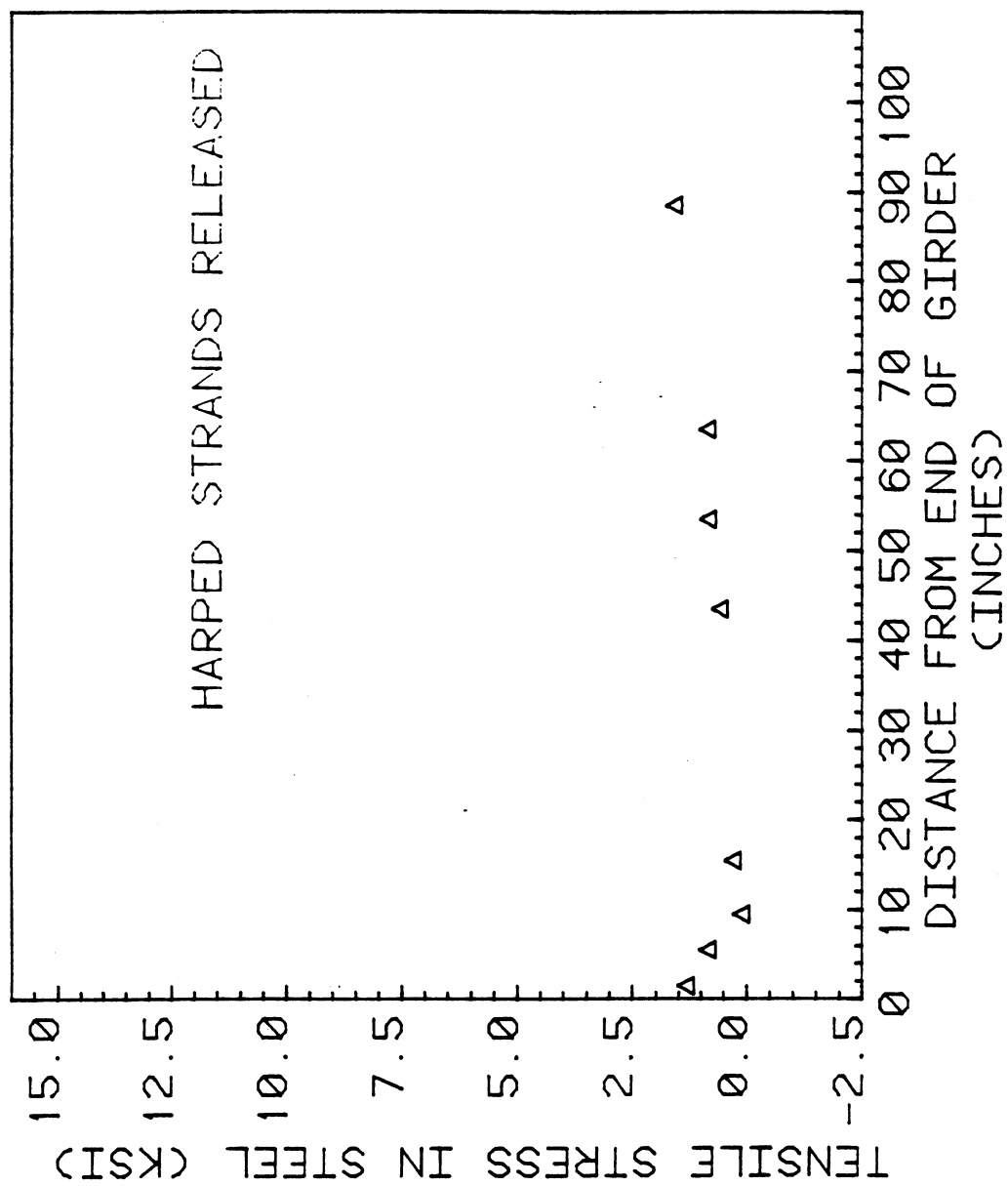


Figure 4.8a

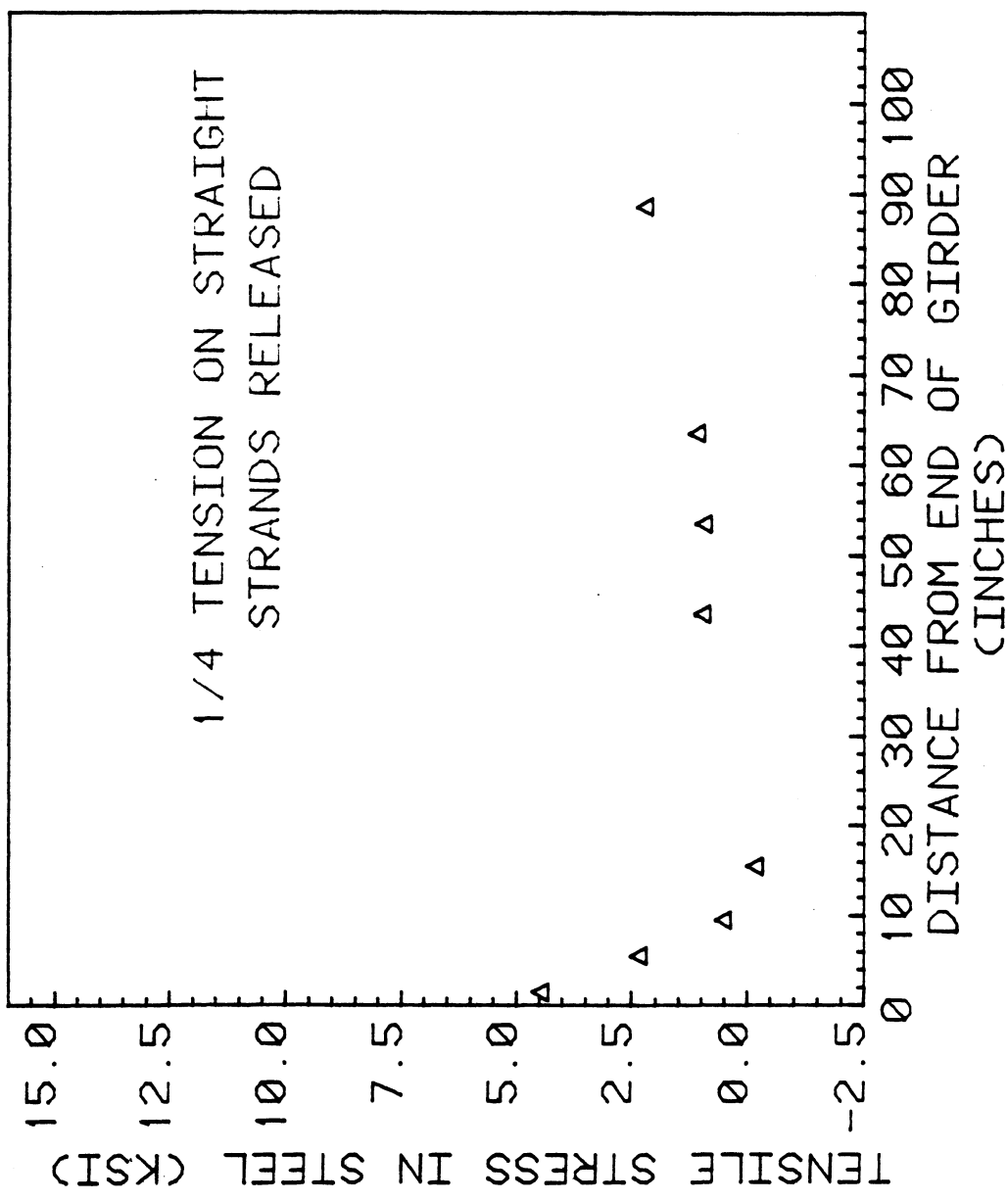


Figure 4.8b

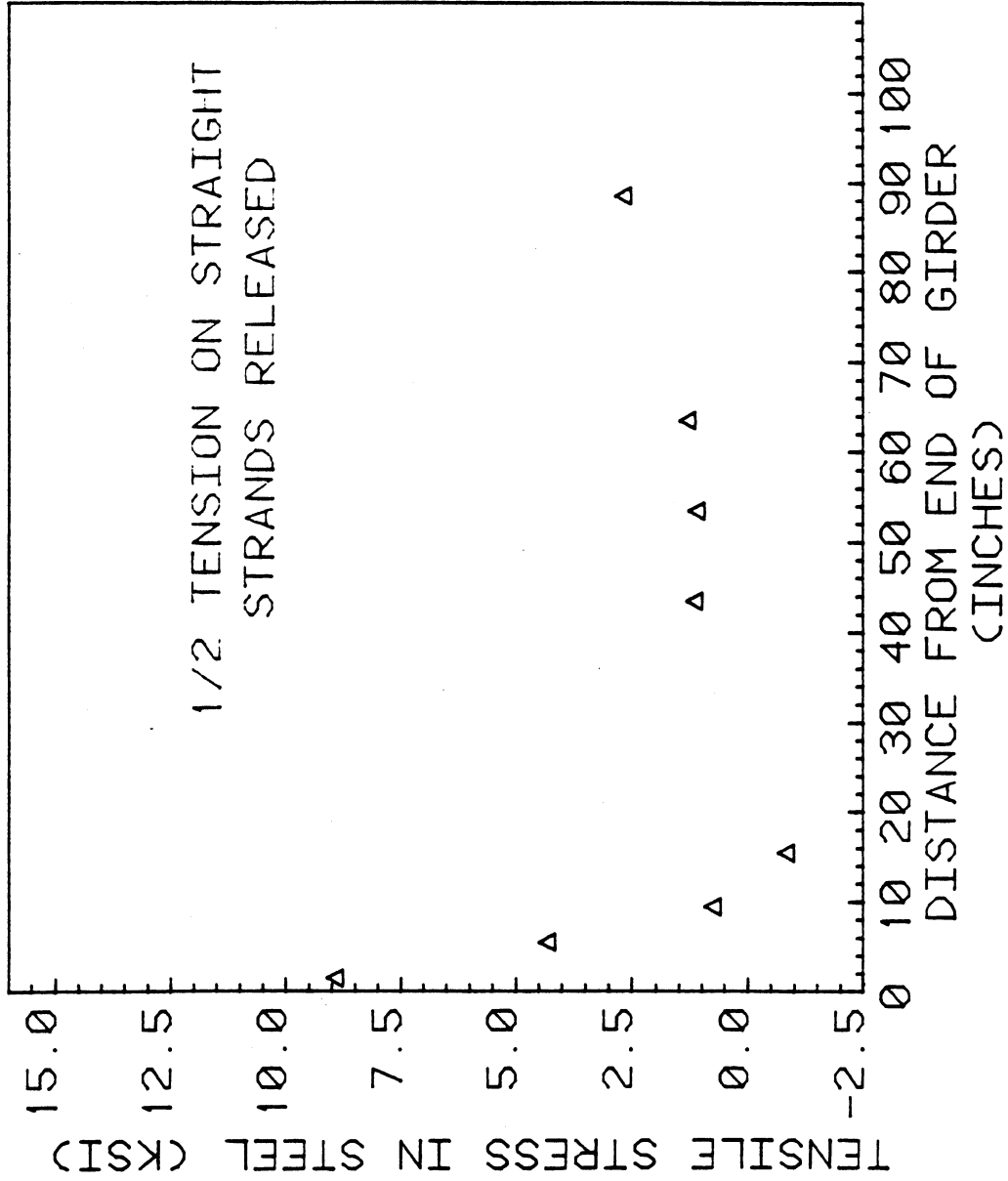


Figure 4.8c

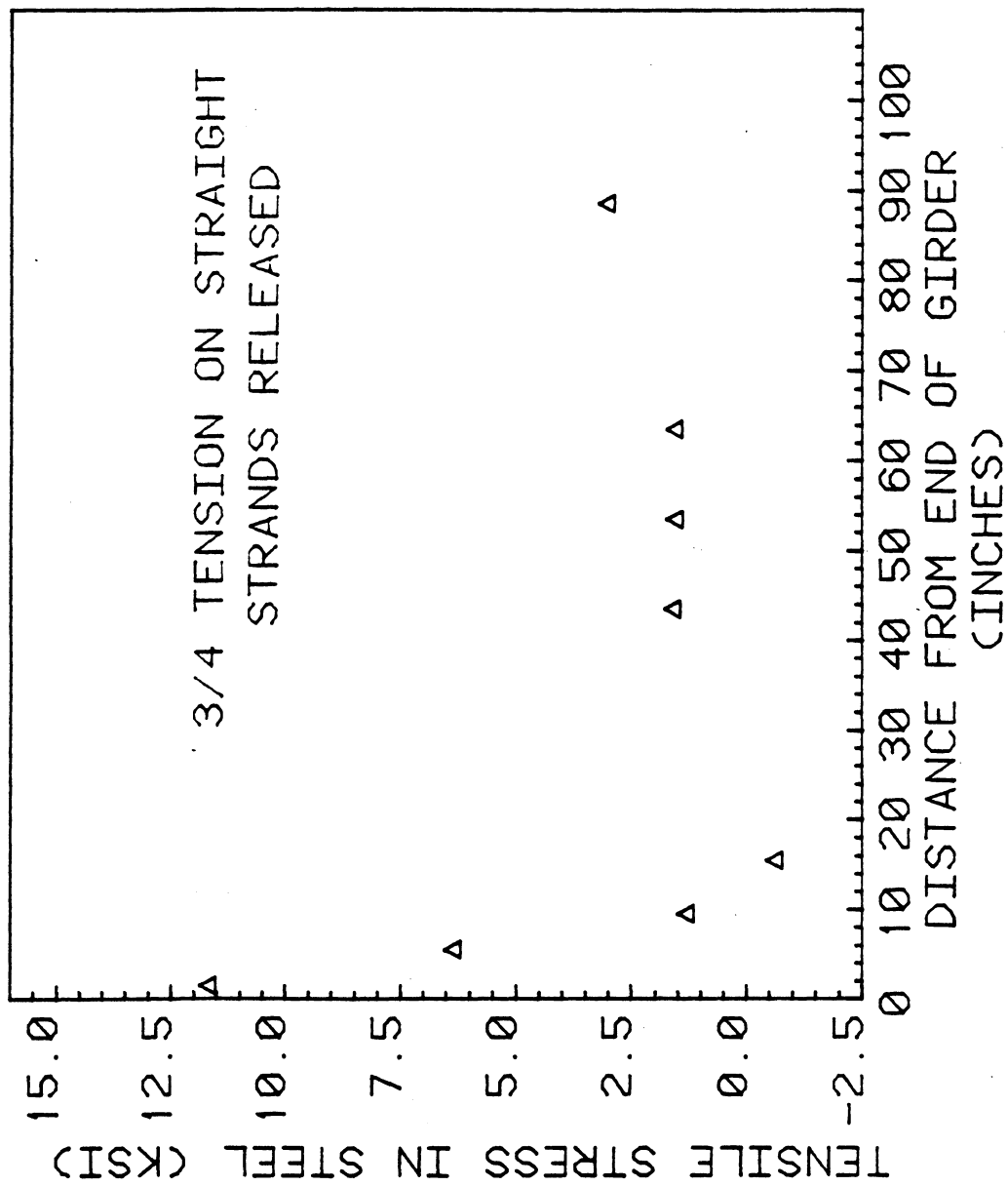


Figure 4.8d

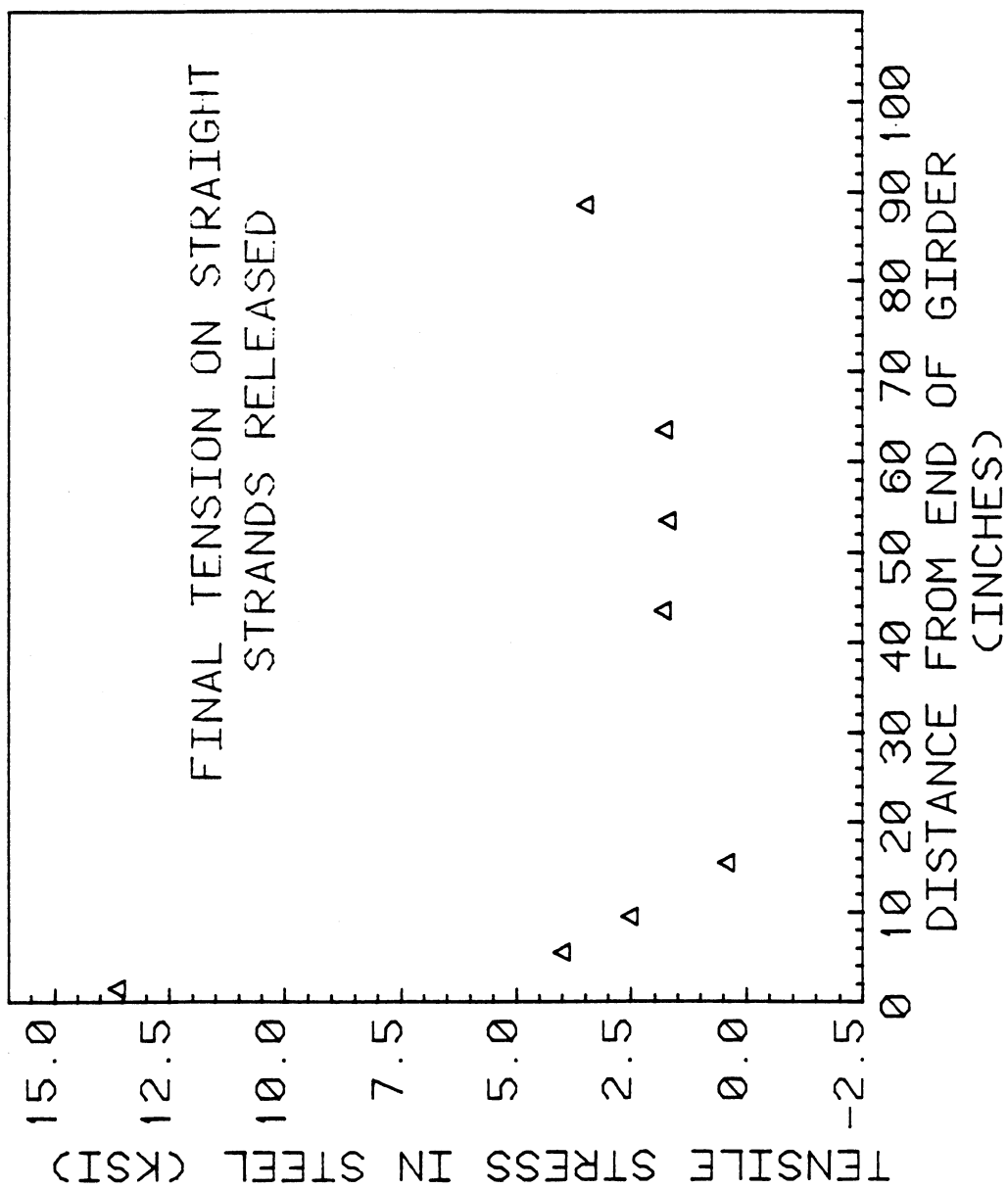


Figure 4.8e

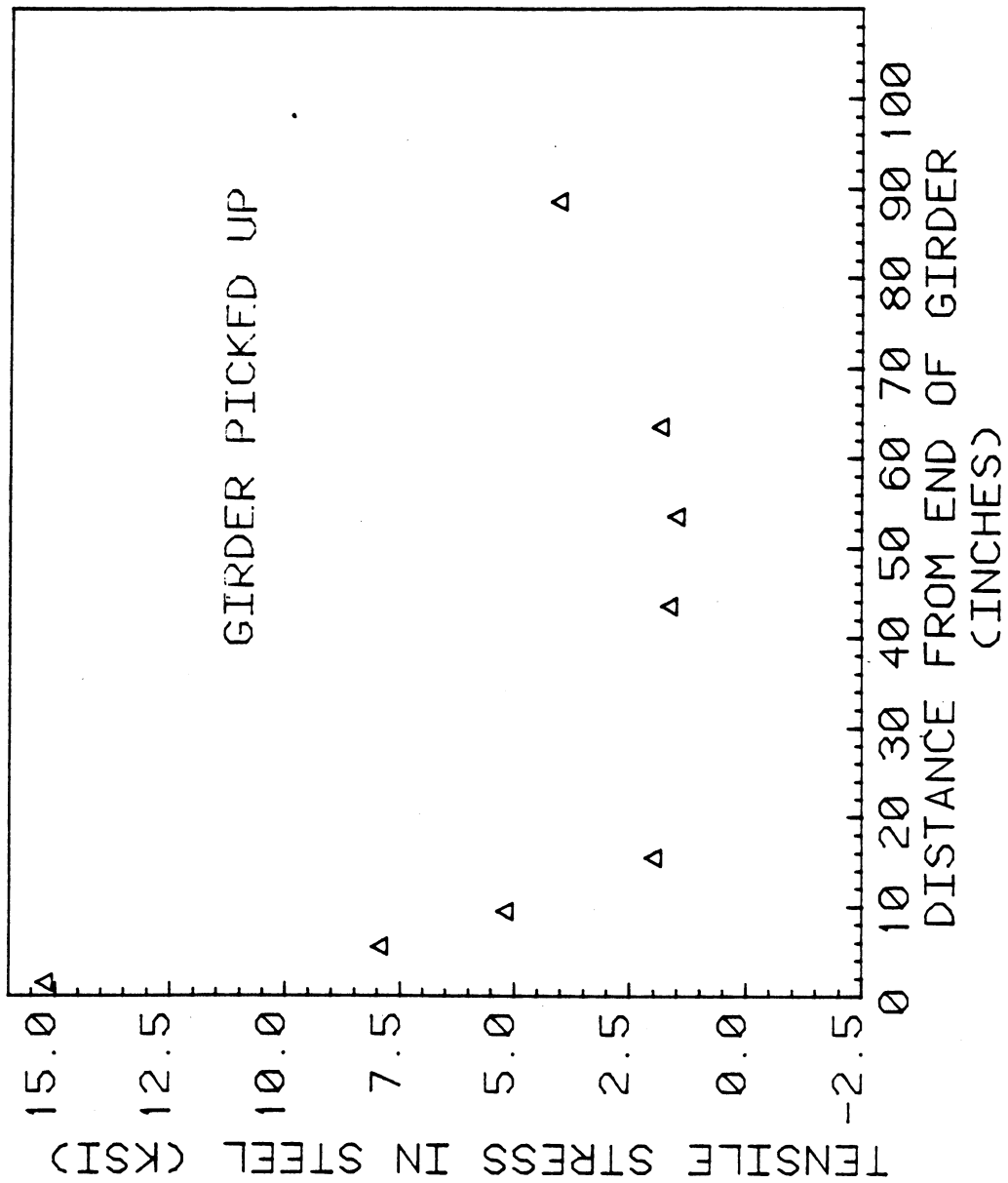


Figure 4.8f

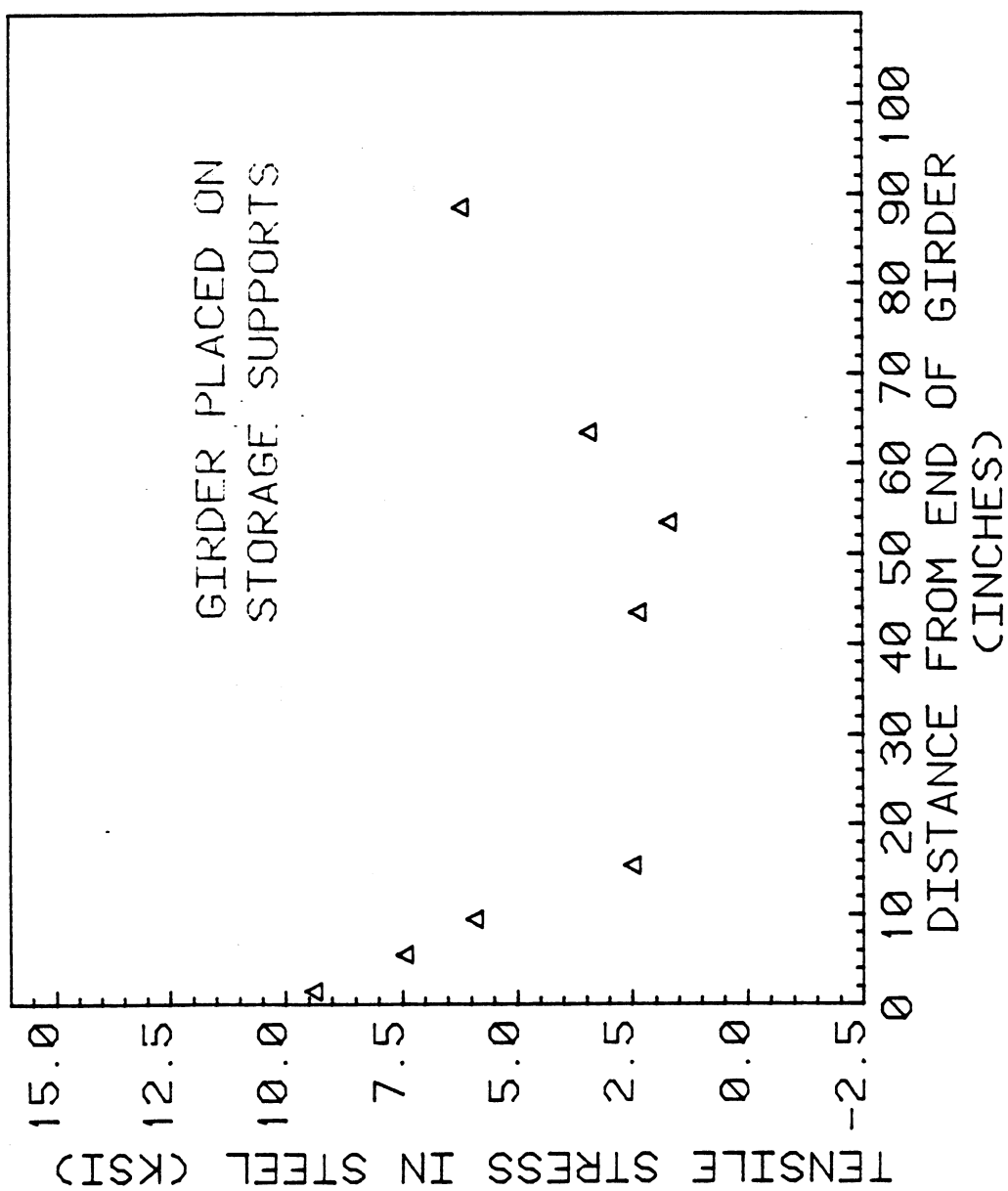


Figure 4.8g

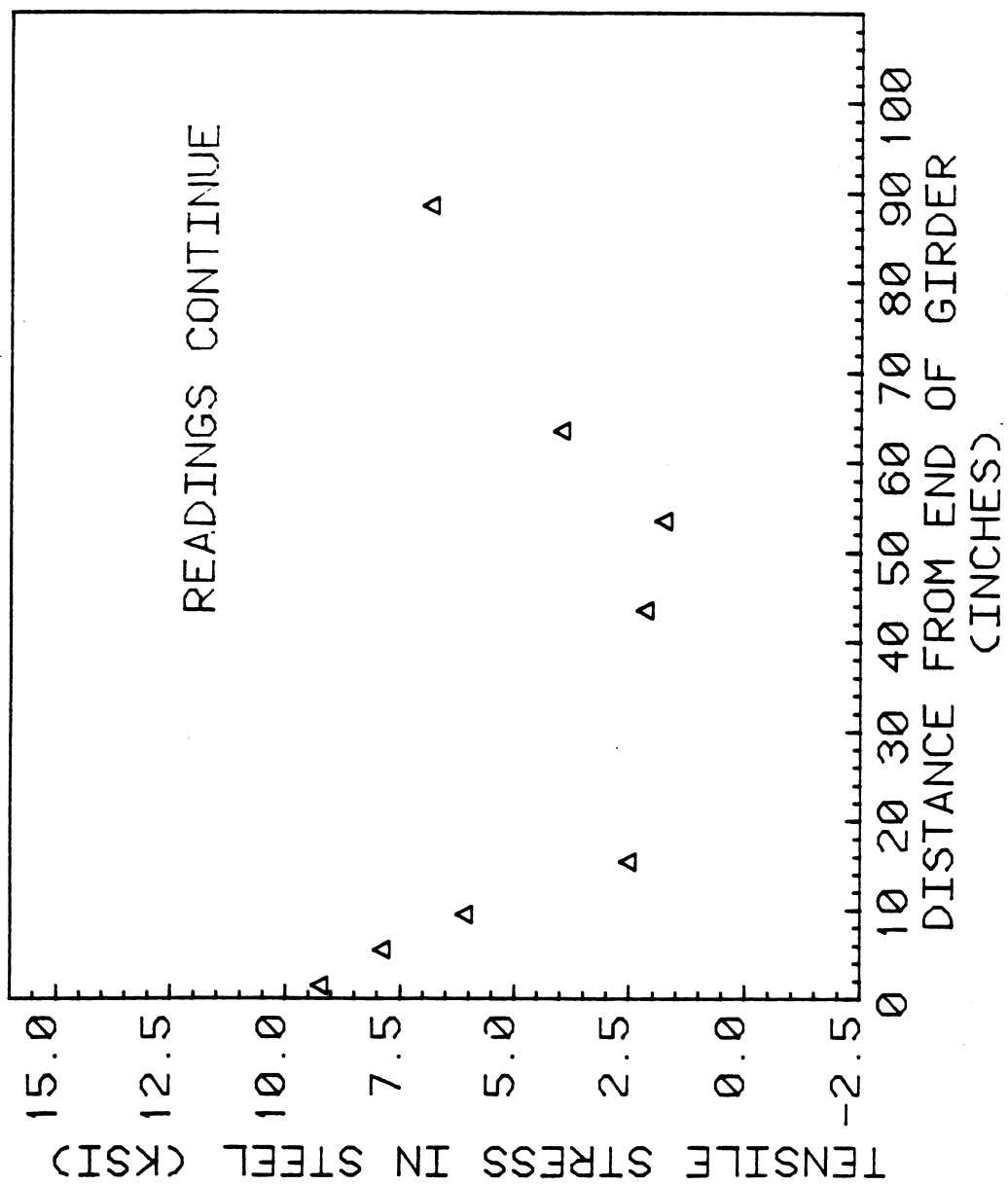


Figure 4.8h

end face of the girder and decreased to a minimum at a distance approximately equal to the transfer length from the end of the girder. A maximum stress of around 15,000 psi was recorded when the girder was picked up, however this is well within allowable limits and it also decreased when the girder was placed on supports.

The strains in the concrete were converted into principal stresses using the method as described in Chapter 3. The elastic modulus was estimated using the equation:

$$E_{ct} = 33w^{1.5} \sqrt{(f'_c)_t} \quad \text{Equation 4.1}$$

where w is the weight of the concrete, assumed to be 155 pcf, and $(f'_c)_t$ is the compressive strength of the concrete at the time of interest. For prestress transfer, cylinder tests indicated a compressive strength of around 4500 psi which corresponds to an elastic modulus of 4.27×10^6 psi. For Poisson's ratio, a value of 0.2 was assumed. The allowable stresses as calculated according to AASHTO specifications are 2700 psi ($0.6 f'_{ci}$) for compression and 503 psi ($7.5 \sqrt{f'_{ci}}$) for tension.

Figure 4.9 shows the principal stresses and their orientations on a diagram of the end of the girder. Many of the principal tensile stresses exceed the allowable value. This is the result of micro-cracks forming in the concrete. However, visual inspection of the end of the girder indicates that no visible cracks formed in these areas and therefore the tensile stresses are not of critical magnitude in the end region. The principal compressive stresses are well within the allowable limit indicating that the end of the girder is able to handle the transfer of prestress effectively, without the need for an end block.

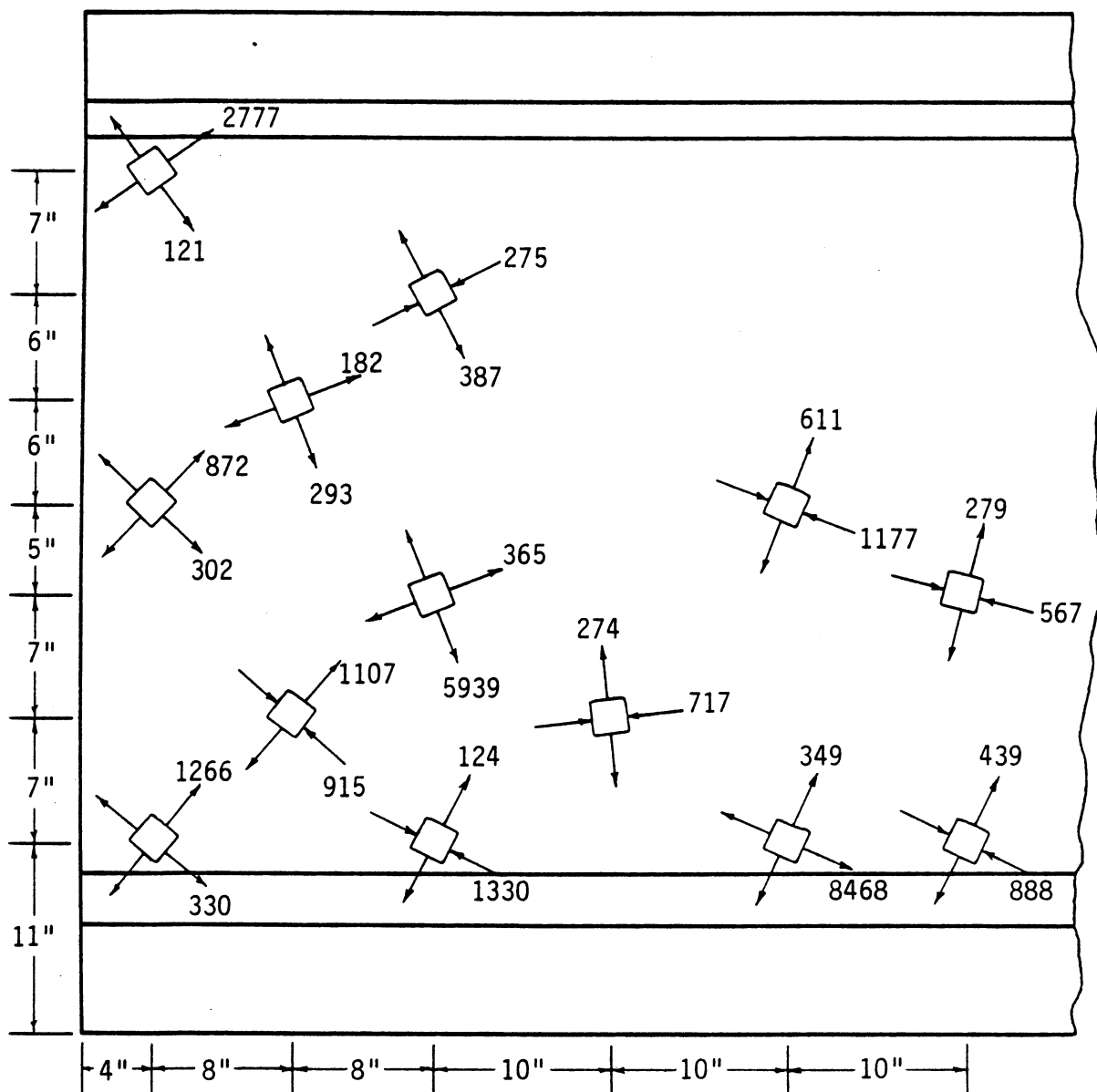


Figure 4.9 Principal stresses (psi) due to prestress transfer.

4.7 Addition of Concrete Slab

After approximately 28 days, the girder was transported and placed into the proper location on the piers of the SR 90/Sullivan Road interchange. It is an interior girder with the end without an end block located at the western end of the bridge (see Fig. 4.10) the other end is used in a continuous connection and therefore the end block is retained. The next load stage of interest was the addition of the $7\frac{1}{2}$ inch thick concrete roadway slab. The resulting stresses are most critical when the concrete is still wet because the concrete is heavier and also because the load is acting entirely on the girder section. After the slab cures, a composite section is formed and further loading acts on the new section. Therefore, it was important to measure the strains immediately after completing the placing of the slab.

4.8 Stresses Due to Addition of Concrete Slab

The strains in the steel reinforcement due to the addition of the concrete slab were converted to stresses and examined for any indication of problems. The magnitudes of the stresses were negligible, with only one of the gages indicating a tensile stress. As expected, the compression from the reaction tended to decrease or eliminate the transverse tensile stresses in the steel stirrups resulting from prestress transfer.

For determining the principal stresses in the concrete, the same procedure as described earlier was used. However, a new modulus of elasticity corresponding to the 28 day compressive strength of 7780 psi was calculated to be 5.62×10^6 psi. Also, the strains that were measured for the addition of the slab did not take into account the reinforcing



Figure 4.10 Girder without end block in place at bridge site.

steel because it was already in place when the initial reading was taken. To account for the weight of the steel, the strains were increased by a ratio of the total weight of the steel to the weight of the slab. This ratio was calculated to be 6 percent.

The principal stresses induced by the addition of the slab are rather small (see Figure 4.11), with the exception of three of the gages. The high compressive stresses are probably caused by the reaction of the bearing which is 13 inches wide with the centerline located 15 inches from the end of the girder. However, these stresses do not represent the actual condition. To get an idea of the actual stress condition, it is necessary to combine the stresses at prestress transfer with these stresses.

4.9 Superposition of Prestress Transfer and Slab Stresses

Using the same method as described in Chapter 3, the principal stresses due to prestress transfer and those due to the addition of the roadway slab were superimposed. The resulting principal stresses and orientations are shown in Figures 4.12a and 4.12b. The principal stresses in Fig. 4.12b take into account a 25 percent reduction in stresses at prestress transfer for losses due to creep and shrinkage of the concrete and relaxation of the prestressing steel. Comparing these with the AASHTO allowable stresses of 3112 psi compression and 529 psi tension reveals that a few of the stresses exceed the limits.

The tensile stresses that exceed the allowable value are not critical because upon cracking of the concrete, the tensile force is transferred to the stirrups.

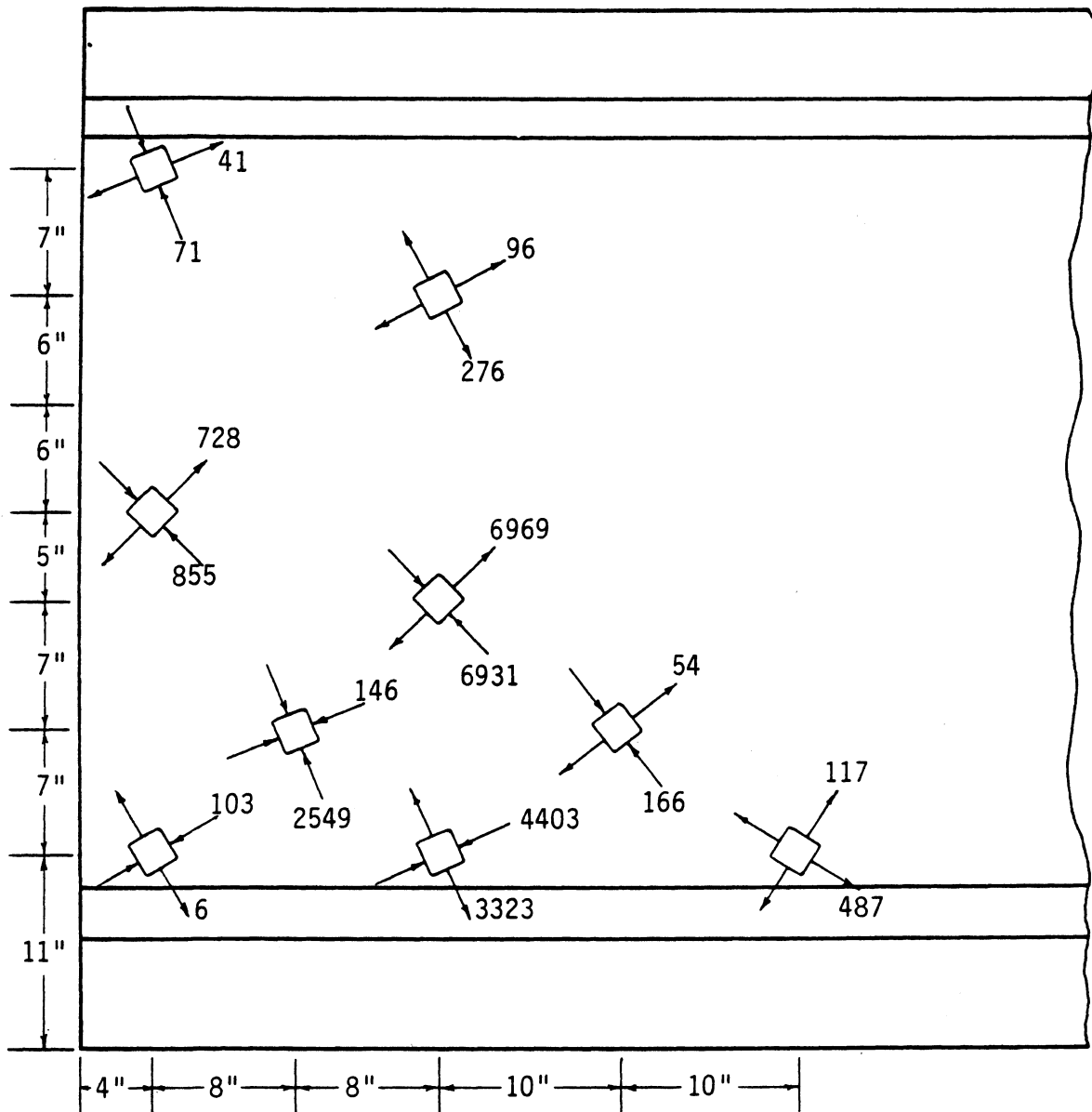


Figure 4.11 Principal stresses (psi) due to the addition of the concrete roadway slab.

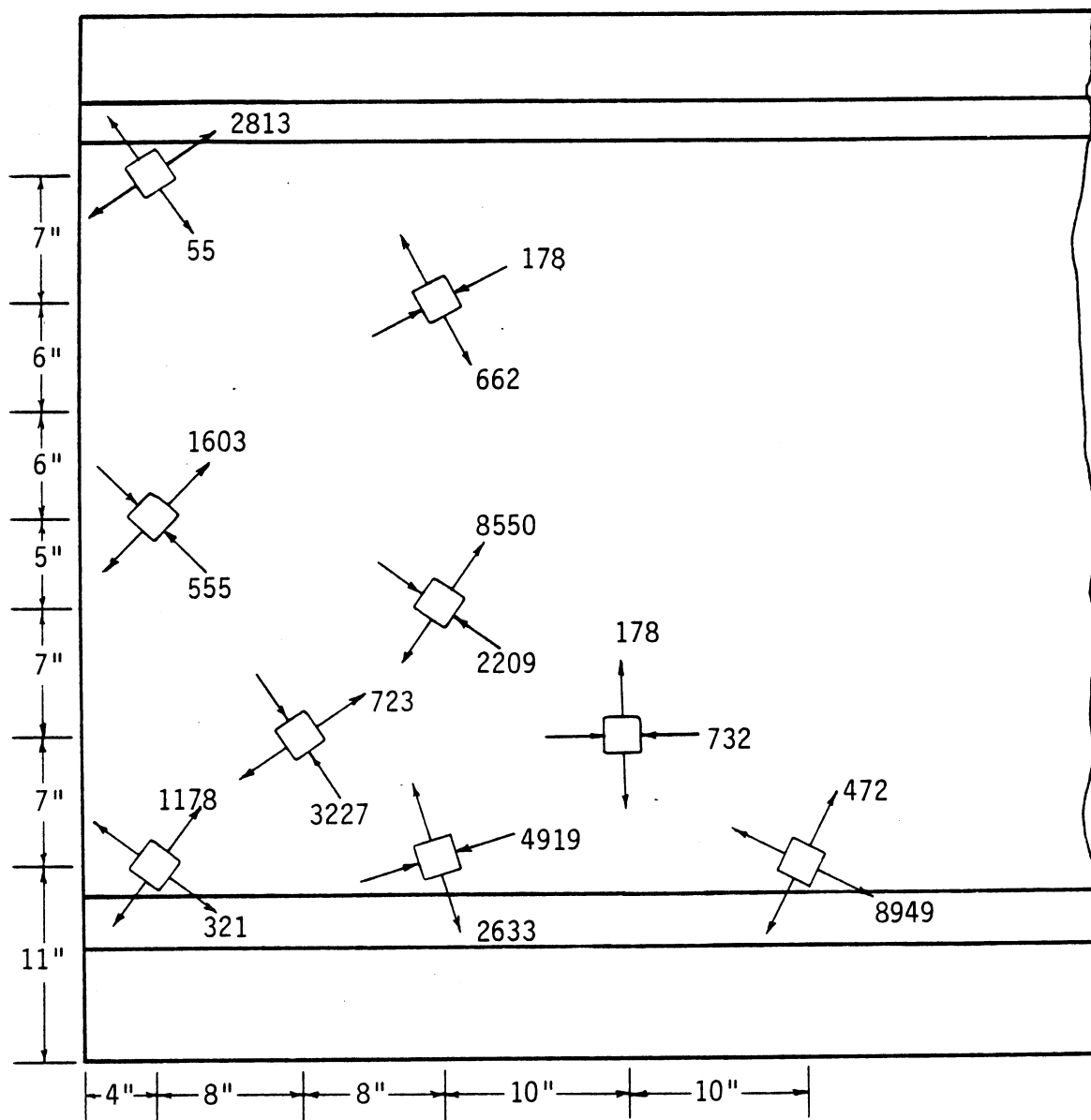


Figure 4.12a Principal stresses (psi) due to combination of prestress transfer and slab stresses.

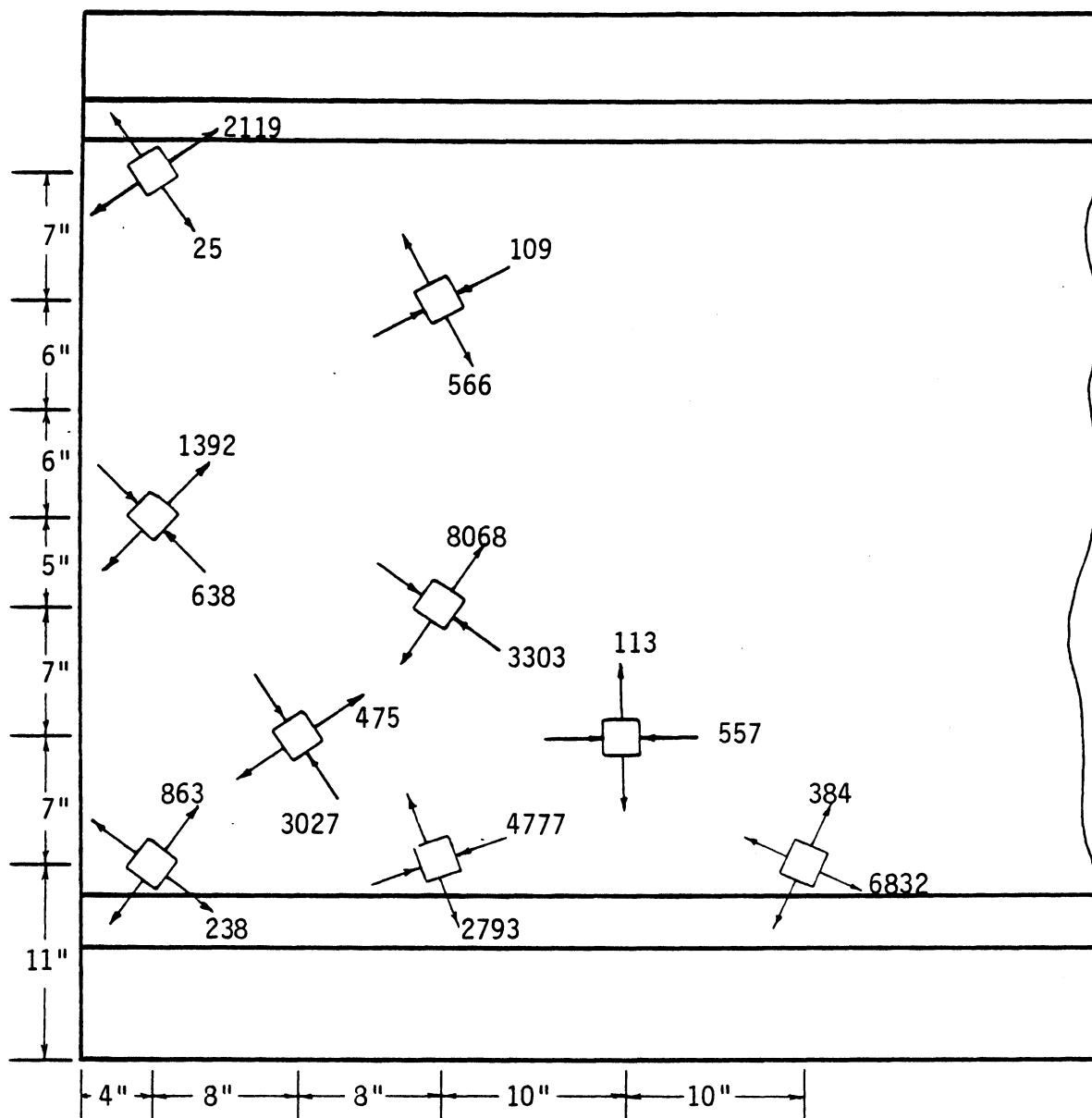


Figure 4.12b Principal stresses (psi) due to combination of prestress transfer and slab stresses, with reduction for losses.

The high compressive stresses resulting from the combined effect of the vertical reaction and the prestressing force are located above the position of the bearing pad. The highest stress of 4777 psi is approximately $0.6 f'_c$ which, although it exceeds the recommended allowable, should not be detrimental to the performance of the girder. In fact, according to T.Y. Lin (9), the compressive stresses upon which the girder design is based are fiber (horizontal) stresses, although the principal compressive stresses at that point are somewhat greater in magnitude.

4.10 Live Loading of Girder

On June 20th, 36 days after casting the slab, the final test was performed on the girder. This test involved the placement of a truck at preselected locations on the bridge, with the corresponding strain readings recorded. The vehicle used for this test consisted of a cab and trailer on five axles. One axle was located under the cab and two sets of two axles were under each end of the trailer, with the spacing between the axles shown in Figure 4.13. The width of the truck was approximately 8 feet with a space of about 4 feet between the two sets of tires.

The truck was weighed and the gross vehicle weight was determined to be 78.6 kips. By weighing the front and back axles separately, the concentrated axle loads were calculated to be 17.1 kips for each of the four axles under the trailer and 10.2 kips for the axle under the cab. For testing the girder, the tires on the right side of the truck were centered over the centerline of the girder, providing the direct girder loading shown in Figure 4.14.

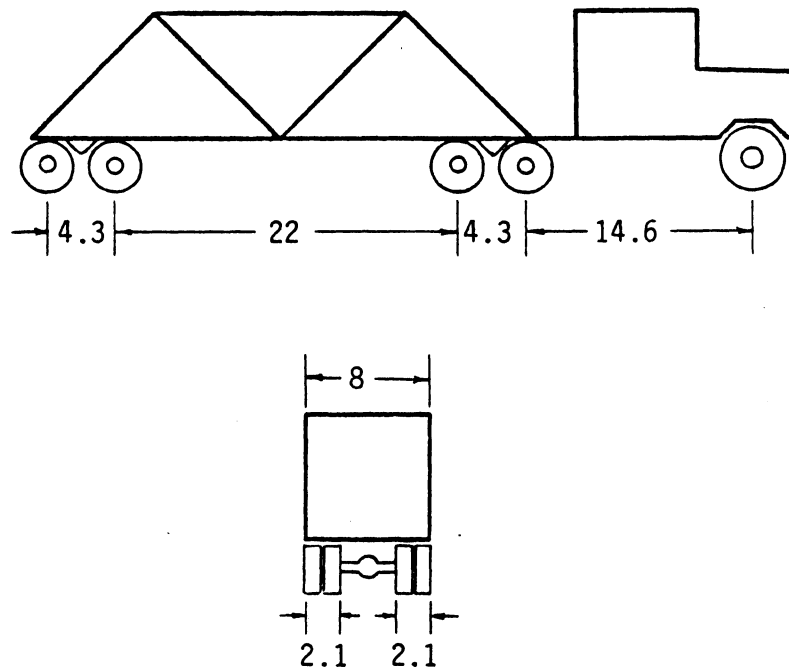


Figure 4.13 Dimensions (feet) of truck used for live load test.

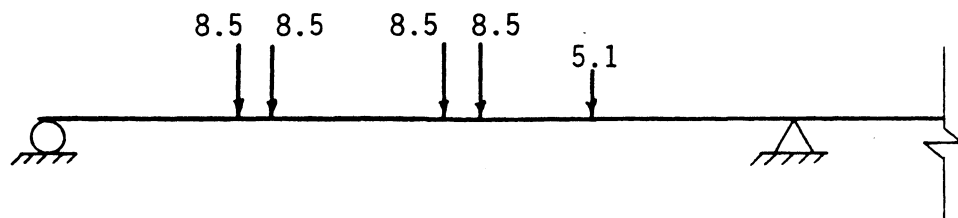


Figure 4.14 Direct concentrated loads on girders for live load test (kips).

The first strain reading was taken with the rear axle of the truck located directly over the end of the girder without an end block. This was followed by readings at 5, 10, 25 (span/4), 50 (span/2), and 75 (3 span/4) feet from the end. Strain readings were also taken with the rear axle of the truck located 10 and 5 feet from the opposite end of the girder, as well as at 5, 10 and 25 feet from the end of the adjacent, continuous span (see Figure 4.15).

4.11 Stresses Due to Live Loading

The strains recorded for the truck loading on the girder were rather small in magnitude. Strain gages mounted on the stirrups indicated strains in steel ranging from +10 microstrains to -35 microstrains, with the majority (around 70 percent) indicating compression (-). This converts to a range in stress from 290 psi tension to 1015 psi compression for the stirrups.

Similarly, the strains indicated by the rosettes on the concrete range from a maximum tensile strain of +20 microstrains to a maximum compressive strain of -12 microstrains. Converting the strains into principal stresses produced values ranging from 183.9 psi tension to 98.1 compression, with both extremes occurring with the rear axle of the truck located at or near the end of the girder. A sample of the principal stresses and their orientations is shown in Figures 4.16a and 4.16b.

A problem with strain readings of small magnitude such as those recorded for the truck loading is that they are greatly affected by errors inherent in strain measurement. During the live loading of the girder, there were several variables which could have affected the strain measurements. A gas generator was used as the power source for operating

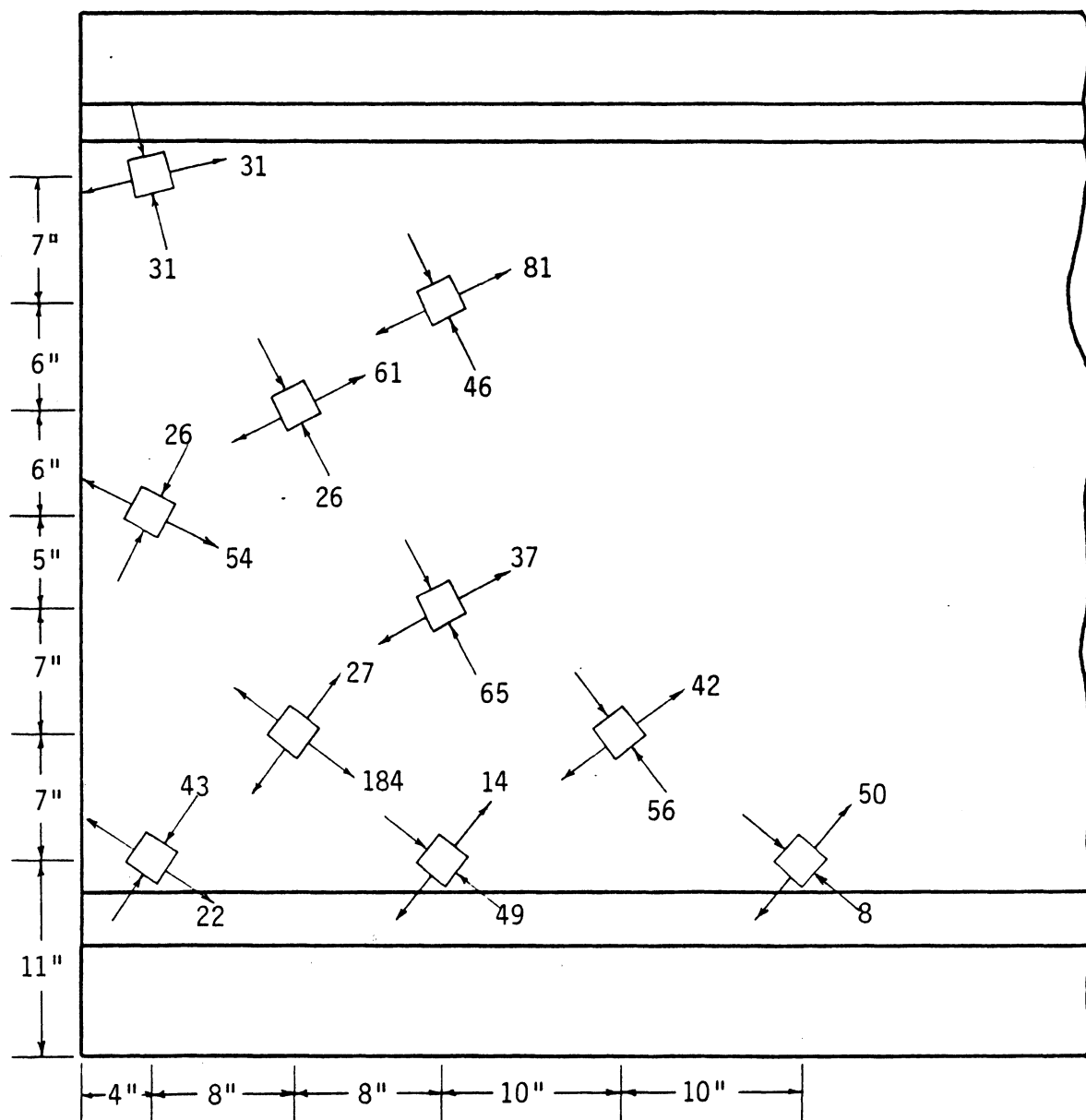


Figure 4.16a Principal stresses (psi) due to live loading with rear axle of truck located over end of girder.

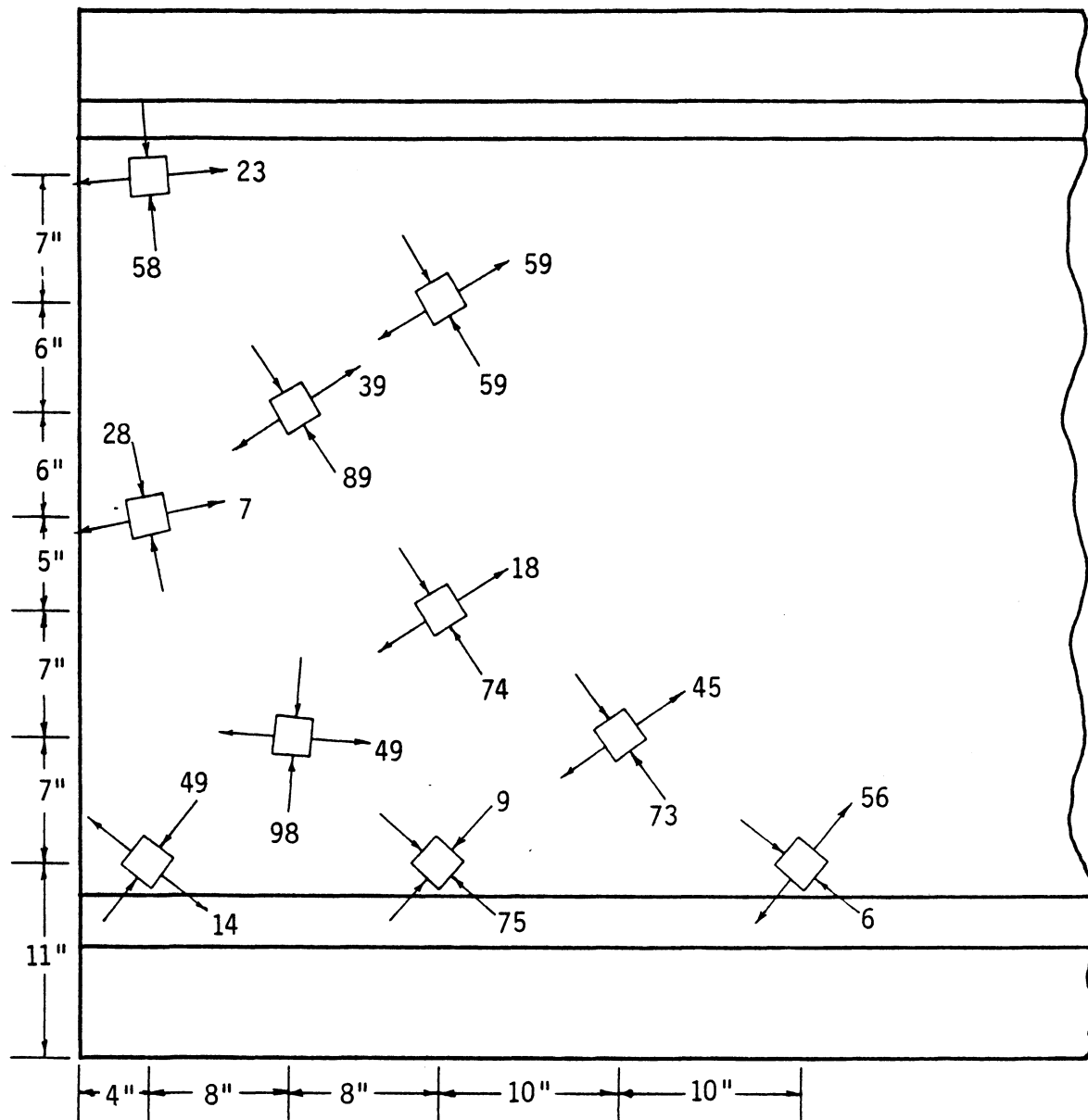


Figure 4.16b Principal stresses (psi) due to live loading with rear axle of truck located 5 feet from end of girder.

the data logger. Slight fluctuations in the current could cause a small distortion of the data. Also, the flow of traffic on the highway under the bridge causes vibrations in the superstructure and concrete girders. These vibrations tend to distort the strain readings. Finally, the amount of handling and weathering that the gages have undergone could also affect their ability to continuously provide accurate measurements.

Therefore, the treating of the stress values as the actual conditions present in the steel and concrete is questionable. Rather, the general magnitude of the stresses should be considered, with the specific values and the orientations of the principal stresses ignored. The magnitude of the stresses present in the steel and on the surface of the concrete due to the addition of the truck are reasonable and no where near a critical magnitude which would be dangerous to the safety of the girder.

4.12 Theoretical Comparison

As in Chapter 3, Krishnamurthy's method for determining the transverse stress distribution in the concrete of the end region was used to compare with the experimental distribution for the series 10 girder at prestress transfer. The plot in Figure 4.17 shows that Krishnamurthy's method tends to overestimate the actual stresses measured. Comparing the plot with the distributions of the series 14 girder in Figure 3.14 reveals that while the transverse stresses predicted using Krishnamurthy's equation are higher for the series 10 than those of the series 14, the actual measured stresses are lower. Therefore, it is concluded that Krishnamurthy's method is conservative when used for analyzing this type of girder.

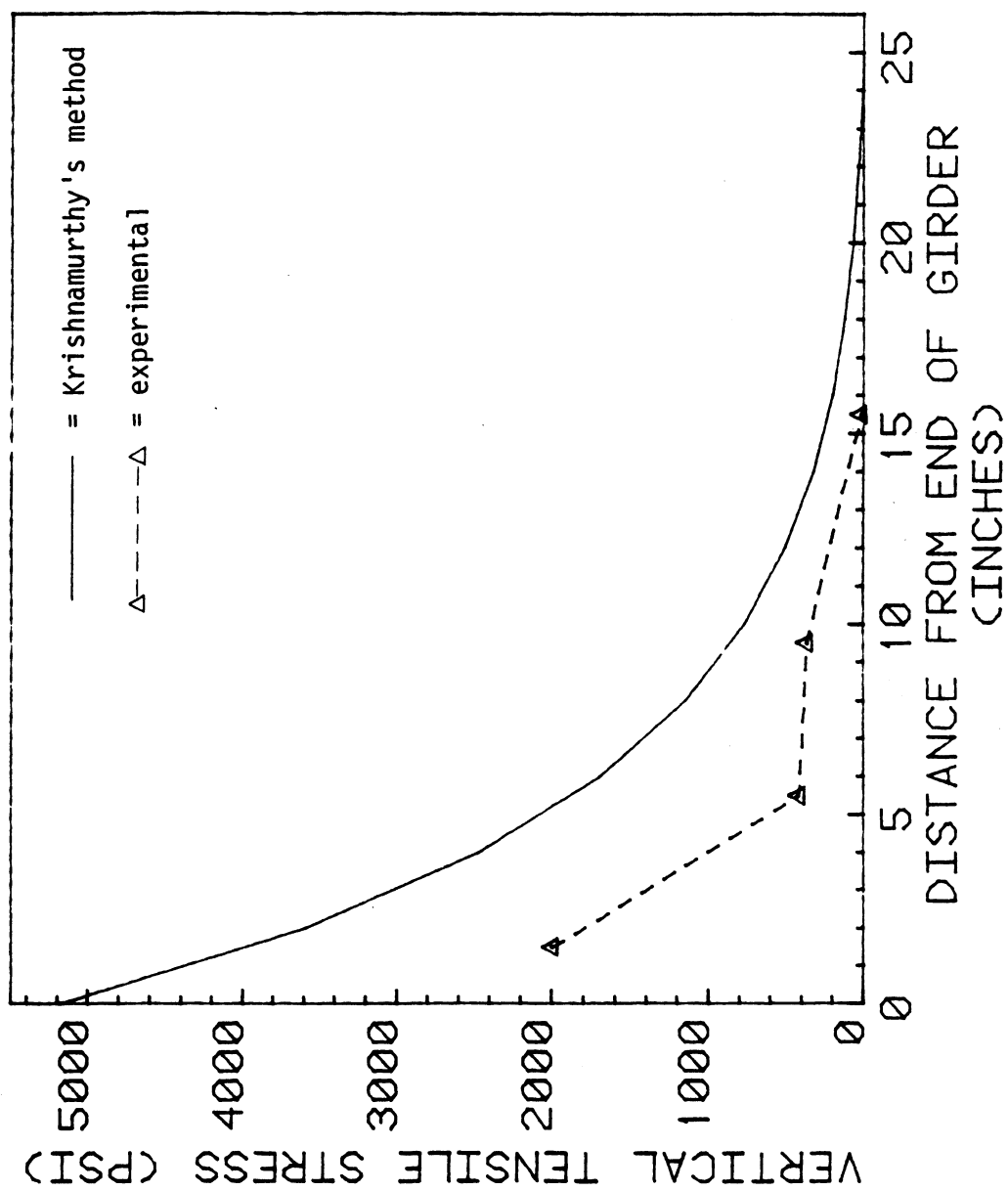


Figure 4.17 Transverse stress distribution.

4.13 Conclusion

The data obtained from monitoring the series 10 girder with the end block removed from one end again verified the effectiveness of the new design. Both experimental results, as well as visual inspection of the girder confirmed that the end blocks can be eliminated.

CHAPTER 5

CONCLUSIONS AND RECOMMENDATIONS

From the results of the ultimate load test performed at Concrete Technology Corporation, as well as the monitoring of the girder in the Sullivan Road overpass, it was determined that end blocks can be removed from the WSDOT pretensioned girders series, for the simply supported case. The analyses of the stresses in both the concrete and steel reinforcement of the end regions of the girders indicate that the modified ends perform effectively under both prestress transfer and service load conditions.

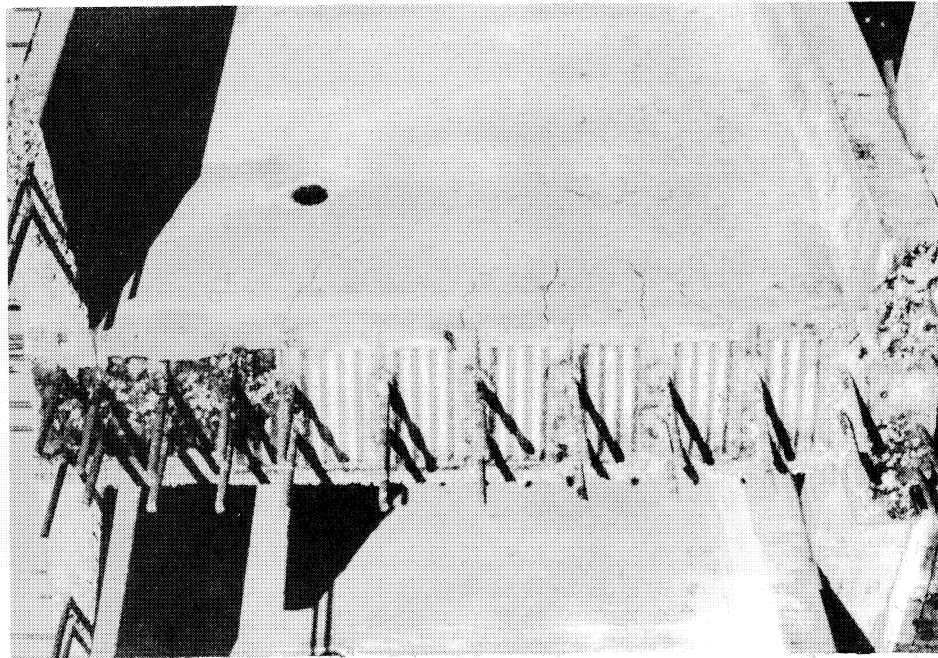
For removing the end blocks, the specifications of the 1983 AASHTO code were followed (see Appendix A for design summary as well as a sample calculation). Basically, the cross section of the girder with a web thickness of five inches is kept constant while providing adequate vertical reinforcement for the shear and anchorage zone requirements. The ties and longitudinal reinforcement are not affected by the change, and are therefore provided according to standard practice. This design will usually result in the placement of pairs of #4, 60 ksi stirrups spaced at 2 inches within a distance of $d/4$ from the end of the girder. It is recommended that this spacing be continued out to the face of the support and followed by a transition zone of gradual space increases up to the requirements for shear. In the case where the anchorage zone requirements are higher than can be provided by #4 stirrups at 2 inch spacing, it is recommended that bundled stirrups be used as necessary.

The production of the series 10 and series 14 girders for this project proved that the steel placement and compaction of concrete in the

end regions were possible with a five inch web. The transportation of the series 10 girder to the bridge site was also accomplished without any problems or damage to the girder due to vibrations. However, if any future difficulties with steel placement, concrete compaction or stability of the girder during transport arise, increasing the web thickness to a constant six inches across the girder may have to be considered.

The cost savings involved with removal of end blocks is not so much from a decrease in the amount of materials used, but rather in the decreased manufacturing and transportation costs. By providing a constant cross section, the formwork will no longer have to be altered for each girder or set of girders produced. Presently, the forms are cut and welded as the length of the girders vary, so that end blocks are provided within a certain tolerance. With the elimination of end blocks, the same pair of forms can be used for different lengths of girders by the simple placement of the form ends. This decreases both production costs and time significantly. Also, because end blocks constitute as much as 5 to 10 percent of the total weight of a girder, shipping costs should decrease upon their removal.

Of interest to this project is the investigation of horizontal cracking in the end regions of WSDOT series girders. It is perceived that the provision of end blocks is intended to reduce the horizontal cracking caused by detensioning of the prestressing strands. However, upon examining a random sample of approximately 15 series 10 and series 14 girders with end blocks, it was found that the end regions of all the girders contained as many as 2 to 5 cracks (see Fig. 5.1), with the widths ranging from 0.2 to 0.3 mm (0.008 to 0.012 in). The series 10 and

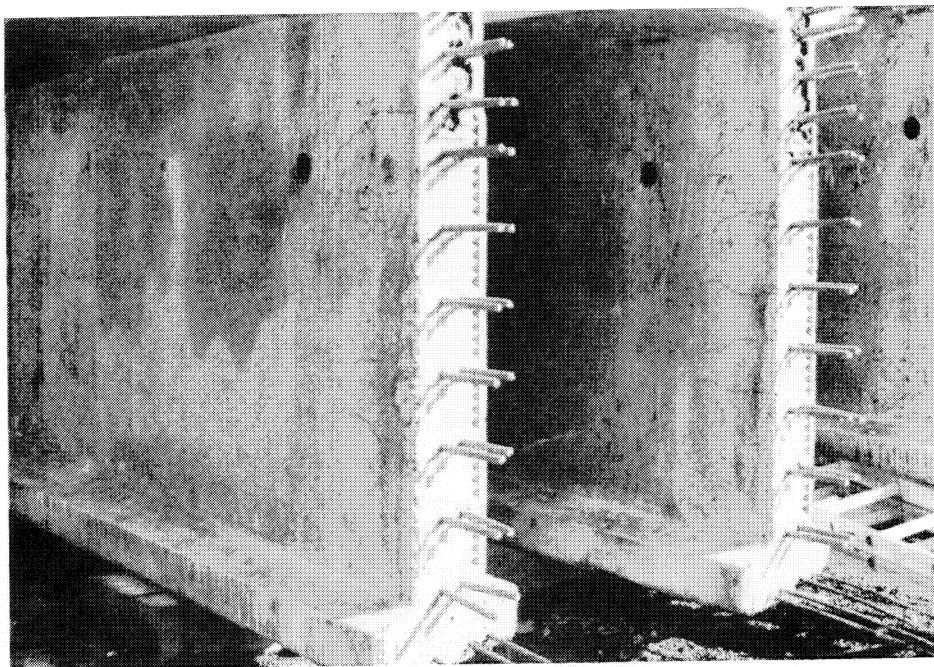


(a)

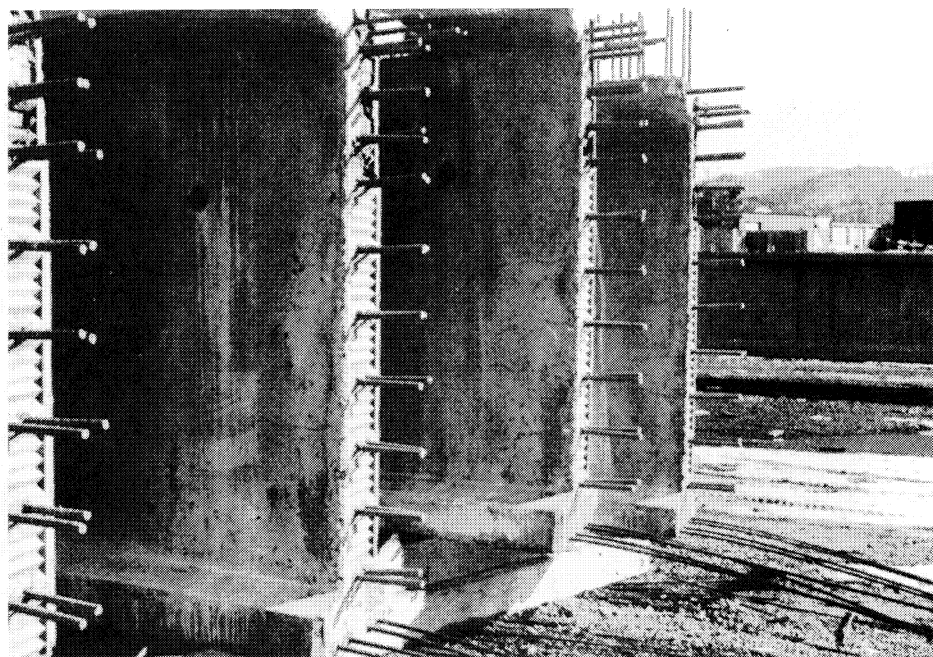


(b)

Figures 5.1a and b Cracks (outlined with black ink) in the ends of girders with end blocks.



(c)



(d)

Figures 5.1c and d More cracks in girders with end blocks.

series 14 girders without end blocks each only had one crack of width 0.1 mm (0.004 in) or less. Therefore, it is concluded that the modified design is effective at reducing the presence of cracks at prestress transfer.

Finally, it is concluded that the removal of end blocks from the WSDOT pretensioned concrete girder series is not only possible and desirable, but beneficial to Washington State and its taxpayers.

REFERENCES

1. Arthur, P.D., and Ganguli, S. "Tests on End-zone Stresses in Pretensioned Concrete I-beams," Magazine of Concrete Research, Vol. 17, No. 51, June 1965, pp. 85-96.
2. Ganguli, S., "Transmission Length in Pretensioned Prestressed Concrete," Indian Concrete Journal, Vol. 40, No. 1, January 1966, pp. 13-16.
3. Gergely, P., Sozen, M.A., and Seiss, C.P., "The Effect of Reinforcement on Anchorage Zone Cracks in Prestressed Concrete Members," Structural Research Series No. 271, University of Illinois, Urbana, July 1963.
4. Gergely, P. and Sozen, M.A., "Design of Anchorage Zone Reinforcement in Prestressed Concrete Beams," PCI Journal, Vol. 12, No. 2, April 1967, pp. 63-75.
5. Hawkins, N.M., "Behavior and Design of End Blocks for Prestressed Concrete Beams," Civil Engineering Transactions, Institution of Engineers, Australia, Vol CE8, No. 2, October 1966, pp. 193-202.
6. Kalyanasundaram, P., Krishnamoorthy, C.S., and Rao, P.S., "End-Zone Stresses in Pretensioned Prestressed Concrete Beams," Indian Concrete Journal, Vol. 50, No. 10, October 1976, pp. 303-307.
7. Krishnamurthy, D., "The Effect of the Method of Transfer on the End-Zone Stresses and Transmission Length in Pretensioned Concrete Members," Indian Concrete Journal, Vol. 44, March 1970, pp. 110-116 and 128.
8. Krishnamurthy, D., "A Method for Determining the Tensile Stresses in the End Zones of Pretensioned Beams," Indian Concrete Journal, Vol. 45, No. 7, July 1971, pp. 286-297 and 315.
9. Lin, T.Y., Design of Prestressed Concrete Structures, 2nd ed., John Wiley and Sons, Inc., New York, 1963, p. 213.
10. Marshall, W.T., and Mattock, A.H., "Control of Horizontal Cracking in the Ends of Pretensioned Prestressed Concrete Girders," PCI Journal, Vol. 7, No. 5, October 1962, pp. 56-74.
11. Marshall, W.T., "A Theory for End Zone Stresses in Pretensioned Concrete Beams," PCI Journal, Vol. 11, April 1966, pp. 45-51.
12. Nawy, E.G., and Potyondy, J.C., "Flexural Cracking Behavior of Pretensioned Prestressed Concrete I and T Beams," ACI Journal, Vol. 68, No. 5, May 1971, pp. 355-360.
13. Nilson, A.H., Design of Prestressed Concrete, Wiley, New York, 1978, pp. 159-161.

14. Rabbat, B.G., and Russell, H.G., "Proposed Replacement of AASHTO Girders with New Optimized Sections," Transportation Research Record 950: Second Bridge Engineering Conference Vol. 2, TRB, National Research Council, Washington, D.C., 1984, pp. 85-92.
15. Sarles, D., and Itani, R.Y., "Anchorage Zone Stresses in Prestressed Concrete Girders," PCI Journal, Vol. 29, No. 6, November/December 1984, pp. 100-114.
16. Zia, P., and Mostafa, T., "Development Length of Prestressing Strands," PCI Journal, Vol. 22, No. 5, September/October 1977, pp. 54-65.

APPENDIX A

DESIGN CONSIDERATIONS

For designing the end region of a girder without end blocks, the specifications of the 1983 AASHTO code pertaining to shear and anchorage zones were followed. Although these same specifications govern the current design, changes were necessary because of the modified geometry of the end region. The following is a summary of the design procedure used for the new girder cross section.

According to the code, steel reinforcement shall be provided for flexural prestressed concrete members subject to shear and diagonal tension stresses. The design of the cross section is based on the relation:

$$V_u \leq \phi (V_c + V_s)^* \quad \text{Equation A.1}$$

where, V_u = the factored shear force
 V_c = the nominal shear strength provided by concrete
 V_s = nominal shear strength provided by web reinforcement
 ϕ = strength capacity reduction factor (= 0.90 for shear)

With the first critical section at a distance of one-half the girder height ($h/2$) from the face of the support. Sections less than $h/2$ are designed for the same shear as that computed at $h/2$ because compression from the reaction tends to reduce the shear in the surrounding concrete.

* Note: Equations used in Appendix A, except Equations A.6, A.7 and A.9, are taken directly from the AASHTO'83 code. For consistency, units should be inches, lb, psi, and in-lb where applicable.

The nominal shear strength provided by concrete, V_c , is governed by the computed shear strengths for flexure shear cracking and web shear cracking, V_{ci} and V_{cw} respectively. The smaller of the two values controls in the design.

Flexure-shear cracking strength is calculated according to the equation:

$$V_{ci} = 0.6 \sqrt{f'_c} b' d + V_d + \frac{V_i M_{cr}}{M_{max}} \quad \text{Equation A.2}$$

where, V_{ci} = nominal shear strength provided by concrete when diagonal cracking results from combined shear and moment

f'_c = compressive strength of concrete at 28 days

b' = width of web

d = distance from extreme compressive fiber to centroid of the prestressing force (not less than $0.8h$)

V_d = shear force at section due to unfactored dead load

V_i = factored shear force at section due to externally applied loads occurring simultaneously with M_{max}

M_{max} = maximum factored moment at section due to externally applied loads

M_{cr} = moment causing flexural cracking at section due to externally applied loads

$$M_{cr} = \frac{I}{Y_t} (6\sqrt{f'_c} + f_{pe} - f_d) \quad \text{Equation A.2a}$$

where, I = moment of inertia about the centroid of the cross section

Y_t = distance from centroidal axis of gross section, neglecting reinforcement, to extreme fiber in tension

f_{pe} = compressive stress in concrete due to effective prestress forces only at extreme fiber of section where tensile stress is caused by externally applied loads

f_d = stress due to unfactored dead load at extreme fiber of section where tensile stress is caused by externally applied loads

The values of M_{max} and V_i are computed from the load causing the maximum moment at the section, and V_{ci} is limited by a minimum value of $1.7\sqrt{f'_c}b'd$.

Similarly, the web shear cracking strength is computed using the equation:

$$V_{cw} = (3.5\sqrt{f'_c} + 0.3f_{pc}) b'd + V_p \quad \text{Equation A.3}$$

where, f_{pc} = compressive stress in concrete (after allowing for all prestress losses) at centroid of cross section resisting externally applied loads or at junction of web and flange when centroid lies within flange

V_p = vertical component of effective prestress force at section

For the case where the section at a distance $h/2$ from the face of the support is closer than the transfer length to the end of the girder, V_{cw} is based on a reduced prestress force. The prestress force is assumed to be zero at the end of the strand and maximum at the prestress transfer length (50 diameters) from the end, varying linearly in between.

For computing the nominal shear strength provided by the shear reinforcement in the web, the code specifies the equation:

$$V_s = \frac{A_y f_{sy} d}{s} \quad \text{Equation A.4}$$

where, A_y = area of web reinforcement

f_{sy} = yield strength of nonprestressed conventional reinforcement in tension (not to exceed 60 ksi)

s = longitudinal spacing of web reinforcement

which is limited by a maximum value of $8\sqrt{f'_c}b'd$.

The required factored shear force at the section, V_u , can be determined using the known loading conditions and load factors and coefficients as specified by the code. This equation becomes:

$$V_u = \gamma[\beta_D(V_D) + \beta_L(V_{L+I})] \quad \text{Equation A.5}$$

where, γ = load factor (1.3 for this case)

β_D = coefficient = 1.0

β_L = coefficient = 1.67

V_D = dead load shear

V_{L+I} = live load plus impact shear

which simplifies to:

$$V_u = 1.3V_D + 2.17V_{L+I} \quad \text{Equation A.6}$$

Therefore, combining equations A.1 and A.4 and solving for the spacing, s , produces the relation:

$$s = \frac{\phi A_v f_{sy} d}{V_u - \phi V_c} \quad \text{Equation A.7}$$

which can be solved for the bar size used for the stirrups. The code specifies a maximum spacing of $0.75h$ or 24 inches, which is reduced by 50 percent for the case where V_s is greater than $4\sqrt{f'_c}b'd$. The area of web reinforcement is also given a minimum value of:

$$A_v = \frac{50b's}{f_{sy}} \quad \text{Equation A.8}$$

As well as the shear reinforcement requirements, the code specifies anchorage zone reinforcement for the end region of the girder. This reinforcement consists of vertical stirrups designed to control the longitudinal cracking caused by vertical tensile stresses. These stresses are maximum at the time of prestress transfer, and are the result of the highly concentrated forces of the prestressing strands.

For their design, the code specifies that ". . . vertical stirrups acting at a unit stress of 20,000 psi to resist at least 4 percent of the total prestressing force shall be placed within the distance of $d/4$ of the end of the beam, the end stirrups to be as close to the end of the beam as practicable."

Converting this specification into the form of an equation for the amount of steel required provides the following relationship:

$$A_s = \frac{0.04 P_i}{20,000} \quad \text{Equation A.9}$$

where, A_s = amount of steel in the form of stirrups required within a distance $d/4$ from the end of the girder

P_i = initial prestress force before losses (psi)

This does not add to the steel requirements for shear because it is only necessary to control cracking at the time of detensioning. Under loading conditions when shear stresses become important, the prestressing force has decreased from losses due to creep and shrinkage of the concrete and relaxation of the prestressing steel causing a proportionate decrease in the vertical tensile stress. Furthermore, compression from the reaction introduces further reduction in the transverse tensile stress with even a zone of transverse compression in the end region. Therefore, it is felt that the requirements for shear and anchorage are not additive in the end region, but rather that they tend to compliment each other.

DESIGN EXAMPLE

The following is an example of the procedure used for designing the vertical steel reinforcement for the end region of a WSDOT series 14 pretensioned girder without end blocks.

The girder is to have a span length of 142 feet (assumed simply supported) with 5.75 feet spacing between girders. A total of 50, grade 270, $\frac{1}{2}$ inch diameter strands are to be used for prestressing. Twenty of the strands are to be harped with an initial force of 578 kips, with the remaining 30 straight strands jacked to an initial force of 868 kips. The design is to be based on an HS20-44 loading, with a 7.5 inch thick concrete roadway slab acting compositely with the girder.

The dead loads acting on the girder are

$$\text{girder dead load} = 750 \text{ lb/ft (62.5 lb/in)}$$

$$\text{slab + diaphragm dead load} = 761 \text{ lb/ft (63.42 lb/in)}$$

$$\text{curb + asphalt dead load} = 143 \text{ lb/ft (11.92 lb/in)}$$

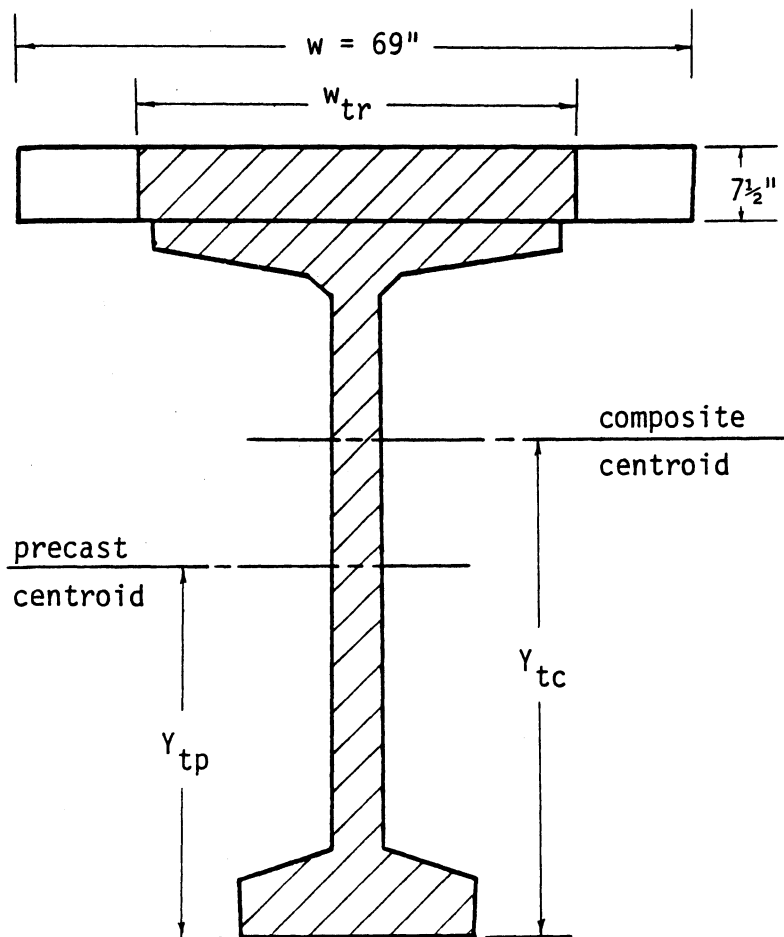
and the compressive strengths of the concrete are assumed to be

$$f'_{ci} = 6000 \text{ psi}$$

$$f'_c = 7000 \text{ psi}$$

$$f'_{cslab} = 3300 \text{ psi}$$

Composite cross section



Calculation of transformed section

$$W_{tr} = nw$$

$$n = \frac{E_{slab}}{E_{girder}}$$

$$E_{slab} = 33w^{1.5} \sqrt{f'_c} = 33(150)^{1.5} \sqrt{3300}$$

$$E_{slab} = 3.483 \times 10^6 \text{ psi}$$

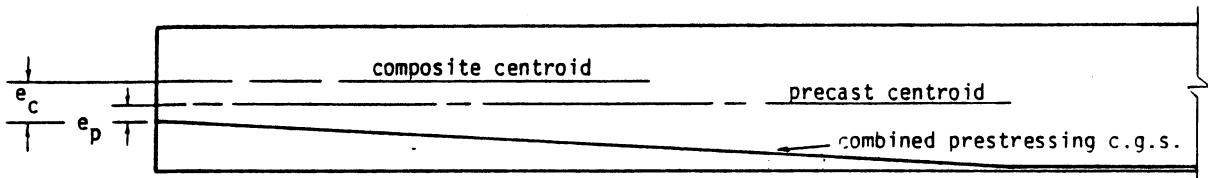
$$E_{girder} = 5.328 \times 10^6 \text{ psi}$$

$$W_{tr} = \frac{3.483}{5.328} (69'') = 45.11''$$

Section properties

	Precast	Composite (Transformed)
Concrete area	$A_p = 673.2 \text{ in}^2$	$A_c = 1013 \text{ in}^2$
Moment of inertia	$I_p = 512878 \text{ in}^4$	$I_c = 860000 \text{ in}^4$
Distance to extreme fiber in tension	$Y_{tp} = 38.22 \text{ in}$	$Y_{tc} = 51.23 \text{ in}$

Eccentricity of prestressing strands:



$$\text{precast } e_p = 10.595 + 0.03484x$$

$$\text{composite } e_c = 23.605 + 0.03484x$$

First, the flexure-shear cracking strength is calculated using Equation A.2

$$V_{ci} = 0.6 \sqrt{f'_c} b' d + V_d + \frac{V_i M_{cr}}{M_{max}}$$

where, $f'_c = 7000 \text{ psi}$

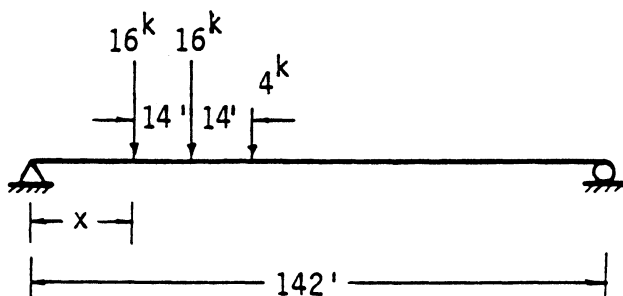
$$b' = 5 \text{ in}$$

$$d = 0.8(73.5 + 7.5) = 64.8 \text{ in}$$

$$V_d = (w_{\text{girder}} + w_{\text{slab}}) \left(\frac{L}{2} - x \right) = 125.92 \left(\frac{1704}{2} - x \right)$$

$$V_d = 107284 - 125.92x \quad \text{where } x \text{ is the distance from the end of the girder to the section of interest}$$

For computing V_i and M_{\max} for sections near the end of the girder, the maximum moment due to externally applied loads is assumed to occur with the rear axle located directly over the section being designed.



$$\begin{aligned}
 V_i &= 1.3(V_{\text{curb d.l.}}) + 2.17(V_{\text{live load}}) \\
 &= 1.3(11.92)\left(\frac{1704}{2} - x\right) + 2.17\left(\frac{1}{1704}\right) \\
 &\quad [16000(1704 - x) + 16000(1536 - x) + 4000(1368 - x)]
 \end{aligned}$$

$$V_i = 86188 - 61.34x$$

$$\begin{aligned}
 M_{\max} &= 1.3(M_{\text{curb}}) + 2.17(M_{\text{live load}}) \\
 &= 1.3(11.92)\left(\frac{x}{2}\right)(1704 - x) + 2.17\left(\frac{x}{1704}\right) \\
 &\quad [16000(1704 - x) + 16000(1536 - x) + 4000(1368 - x)]
 \end{aligned}$$

$$M_{\max} = 86188x - 53.59x^2$$

$$M_{\text{cr}} = \frac{I_p}{Y_{\text{tp}}} (6\sqrt{f'_c} + f_{\text{pe}} - f_d)$$

where,
$$f_{\text{pe}} = \frac{P_e}{A_c} + \frac{P_e e_c Y_{\text{tc}}}{I_c}$$

assuming losses = 45 ksi

$$P_e = 50(.153)[.7(270000) - 45000]$$

$$P_e = 1101600 \text{ lb}$$

$$f_{pe} = \frac{1101600}{1013} + \frac{1101600(23.605 + 0.03484x)(51.23)}{860000}$$

$$f_{pe} = 2636 + 2.286x$$

$$f_d = \frac{M_{girder} Y_{tp}}{I_p} + \frac{M_{slab} Y_{tc}}{I_c}$$

$$= \frac{62.5(\frac{x}{2})(1704 - x)(38.22)}{512878}$$

$$+ \frac{63.42(\frac{x}{2})(1704 - x)(51.23)}{860000}$$

$$f_d = 7.187x - 0.00422x^2$$

$$M_{cr} = \frac{860000}{51.23} (6\sqrt{7000} + 2636 + 2.286x - 7.187x + 0.00422x^2)$$

$$M_{cr} = 52677660 - 82273x + 70.84x^2$$

$$V_{ci} = 0.6\sqrt{7000}(5)(64.8) + 107284 - 125.92x$$

$$+ \frac{(86188 - 61.34x)(52677660 - 82273x + 70.84x^2)}{(86188x - 53.59x^2)}$$

therefore,

$$V_{ci} = 123549 - 125.92x$$

$$+ \frac{(86188 - 61.34x)(52677660 - 82273x + 70.84x^2)}{(86188x - 53.59x^2)}$$

V_{ci} is limited by a minimum value of $1.7\sqrt{f'_c}b'd$

$$V_{ci,min} = 1.7\sqrt{7000}(5)(64.8)$$

$$V_{ci,min} = 46083 \text{ lb}$$

Next, the web shear cracking strength is calculated using Equation A.3

$$V_{cw} = (3.5\sqrt{f_c} + 0.3f_{pc})b'd + V_p$$

where,
$$f_{pc} = \frac{P_e}{A_p} - \frac{P_e e_p c}{I_p} + \frac{M_{girder+slab c}}{I_p}$$

$$f_{pc} = \frac{1101600}{673.2} - \frac{1101600(10.595 + .03484x)(13.01)}{512878} + \frac{128.62(\frac{x}{2})(1704 - x)(13.01)}{512878}$$

$$f_{pc} = 1340.3 + 1.81x - 0.00163x^2$$

$$V_p = P_{e, harped} \sin \theta$$

$$P_{e, harped} = 20(.153)[.7(270000) - 450000] = 440640 \text{ lb}$$

$$\theta = \tan^{-1} \frac{59.375}{681.6} = 4.98^\circ$$

$$V_p = 440640 \sin 4.98^\circ$$

$$V_p = 38250 \text{ lb}$$

$$V_{cw} = [3.5\sqrt{7000} + 0.3(1340.3 + 1.81x - 0.00163x^2)](5)(64.8) + 38250$$

therefore,

$$V_{cw} = 263400 + 175.93x - 0.528x^2$$

The total shear force at factored loads is computed using Equation A.6

$$V_u = 1.3V_D + 2.17V_{L+I}$$

where,
$$V_D = w(\frac{L}{2} - x) = 137.84(\frac{1704}{2} - x)$$

$$V_D = 117440 - 137.84x$$

Fraction of wheel load distributed to girder (AASHTO'83 3.23.2.3.1.5)

$$\frac{S}{5.5} = \frac{5.75}{5.5} = 1.045$$

Amount of impact allowance (AASHTO'83 3.8.2.1)

$$I = \frac{50}{L+125} = \frac{50}{142+125} = 0.187$$

$$V_{L+I} = 1.045(1 + 0.187)(33634 - 21.13x)$$

$$V_{L+I} = 41720 - 26.21x$$

$$V_u = 1.3(117440 - 137.84x) + 2.17(41720 - 26.21x)$$

$$V_u = 243204 - 236.07x$$

Now, the reinforcement required for shear can be determined for different sections of the end region. Assuming the stirrups consist of pairs of No. 4 bars ($A_v = 0.20 \text{ in}^2$) with a yield strength of 60,000 psi. The spacing is computed using Equation A.7. The first section to consider is at a distance $\frac{h}{2}$ from the face of the support = 63 in.

$$s = \frac{\phi A_v f_{sy} d}{V_u - \phi V_c}$$

$$V_{ci} = 828280 \text{ lb}$$

$$V_{ci,min} = 46080 \text{ lb}$$

$$V_{cw} = 273860 \text{ lb} \leftarrow \text{controls } V_c$$

$$V_u = 228330 \text{ lb}$$

$$s = \frac{0.9(2)(.2)(60000)(64.8)}{228330 - 0.9(273860)}$$

$$s = -77.1 \text{ in}$$

The negative value for spacing indicates that no reinforcement is required and that maximum spacing of 24 inches governs the design. However, in keeping with WSDOT practice, a maximum stirrup spacing of 18 inches will be used.

The other section considered for shear design is at the former end of the transition zone for a girder with end blocks = 132 inches

$$V_{ci} = 482610 \text{ lb}$$

$$V_{ci,min} = 46080 \text{ lb}$$

$$\begin{aligned}
 V_{cw} &= 283870 \text{ lb} \quad \longleftarrow \text{controls } V_c \\
 V_u &= 212040 \text{ lb}
 \end{aligned}$$

$$s = \frac{0.9(2)(.2)(60000)(64.8)}{212040 - 0.9(283870)}$$

$$s = -32.2 \text{ (use 18 inch spacing)}$$

Finally, the anchorage requirements are computed using Equation A.9

$$\begin{aligned}
 A_s &= \frac{0.04 P_i}{20,000} = \frac{0.04(1446000)}{20,000} \\
 A_s &= 2.892 \text{ in}^2
 \end{aligned}$$

This requirement is satisfied by placing 8 pairs of No. 4 stirrups ($A_s = 3.2 \text{ in}^2$) starting at $1\frac{1}{2}$ inches from the end of the girder with 2 inch spacing between stirrups.

As a method of practice, it is suggested that the 2 inch spacing be continued out to the face of the support. Following this, provide a transition zone of 4 inch and 8 inch spacings up to $\frac{h}{2}$ where the 18 inch spacing is used. The following spacing is suggested for the vertical steel reinforcement of this girder:

Using pairs of No. 4, 60 ksi stirrups, provide the first pair at $1\frac{1}{2}$ inches from the end followed by 11 pairs at 2 inches, 4 pairs at 4 inches, 3 pairs at 8 inches followed by the maximum spacing of 18 inches.

624.1834
ITANI
1986
c.2